NOLTR 70-243

COMPARISON OF METHODS USED FOR SHOCK AND FOURIER SPECTRA COMPUTATIONS

By
Robert S. Reed, Jr.

24 NOVEMBER 1970

NOL

NAVAL ORDNANCE LABORATORY, WHITE OAK, SILVER SPRING, MARYLAND

NOLTR 70-243

Unclassified
Security Classification

DOCUMENT CONTROL DATA - R & D

(Security classification of title, body of abstract and indexing annotation must be entered when the overall report is classified)

1 ORIGINATING ACTIVITY (Corporate author) Naval Ordnance Laboratory White Oak, Silver Spring, Maryland	2a. REPORT SECURITY CLASSIFICATION Unclassified 2b. GROUP

3 REPORT TITLE

Comparison of Methods Used for Shock and Fourier Spectra Computations

4 DESCRIPTIVE NOTES (Type of report and inclusive dates)

5 AUTHOR(S) (First name, middle initial, last name)

Robert S. Reed, Jr.

6 REPORT DATE	7a. TOTAL NO. OF PAGES	7b. NO. OF REFS
24 November 1970	144	34

8a. CONTRACT OR GRANT NO	9a. ORIGINATOR'S REPORT NUMBER(S)
b. PROJECT NO.	NOL-TR 70-243
c.	9b. OTHER REPORT NO(S) (Any other numbers that may be assigned this report)
d.	

10 DISTRIBUTION STATEMENT

Distribution of this document is unlimited.

11. SUPPLEMENTARY NOTES	12 SPONSORING MILITARY ACTIVITY

13 ABSTRACT

Analog and digital techniques used in the computation of the shock and Fourier spectra are presented and compared on the bases of speed, accuracy and ease of usage. Analog computers with active and passive elements are considered, and it is concluded that active RC networks make accurate and simple-to-use computers for the analog determination of the spectra. The digital techniques studied included the impulse-invariant Fast Fourier transform, z-transform, and the O'Hara method which uses a parabolic interpolation formula. It was determined that the z-transform technique had a five to one timing advantage over the O'Hara technique for the simultaneous computation of shock and Fourier spectra and that the FFT had a dramatic timing advantage over both methods for the computation of only Fourier spectra. It was also shown that the O'Hara technique could maintain less than 5% error when the transient was sampled with a Nyquist rate which was approximately five times the frequency of dominant Fourier spectrum values. It was also shown that for functions which roll off at $1/\omega^2$, the impulse-invariant technique required four times the sampling rate required by the O'Hara technique in order to achieve equivalent accuracies. In addition to the above comparisons an equation was derived which gives the minimum sampling requirements for the computation of damped shock spectra. The damped shock spectra have previously been sampled with little or no justification for the sampling scheme.

DD FORM 1 NOV 68 1473 (PAGE 1)

S/N 0101-807-6801

Unclassified
Security Classification

14 KEY WORDS	LINK A		LINK B		LINK C	
	ROLE	WT	ROLE	WT	ROLE	WT
Fourier Spectra						
Shock Spectra						
Computation						

NOLTR 70-243

COMPARISON OF METHODS USED FOR SHOCK AND FOURIER SPECTRA COMPUTATIONS

Prepared by:
Robert S. Reed, Jr.

ABSTRACT: Analog and digital techniques used in the computation of the shock and Fourier spectra are presented and compared on the bases of speed, accuracy and ease of usage. Analog computers with active and passive elements are considered, and it is concluded that active RC networks make accurate and simple-to-use computers for the analog determination of the spectra. The digital techniques studied included the impulse-invariant Fast Fourier transform, z-transform, and the O'Hara method which uses a parabolic interpolation formula. It was determined that the z-transform technique had a five to one timing advantage over the O'Hara technique for the simultaneous computation of shock and Fourier spectra and that the FFT had a dramatic timing advantage over both methods for the computation of only Fourier spectra. It was also shown that the O'Hara technique could maintain less than 5% error when the transient was sampled with a Nyquist rate which was approximately five times the frequency of dominant Fourier spectrum values. It was also shown that for functions which roll off at $1/\omega^2$, the impulse-invariant technique required four times the sampling rate required by the O'Hara technique in order to achieve equivalent accuracies. In addition to the above comparisons an equation was derived which gives the minimum sampling requirements for the computation of damped shock spectra. The damped shock spectra have previously been sampled with little or no justification for the sampling scheme.

NAVAL ORDNANCE LABORATORY
WHITE OAK, MARYLAND

NOLTR 70-243 24 November 1970

Comparison of Methods Used for Shock and Fourier Spectra Computations

The material in this report was submitted as a thesis to the Faculty of the Graduate School of the University of Maryland in partial fulfillment of the requirements for the degree of Master of Science in Mechanical Engineering. Most of the analysis techniques studied are in use at NOL. Some improvements have been made in the analysis capability of the Environmental Evaluation Department as a result of this study.

Thanks are extended to Mr. G. J. O'Hara of the Naval Research Laboratory, Washington, D. C., for his excellent documentation of some of the techniques investigated and for his consultation at the outset of the study. Thanks are also extended to Dr. P. F. Cunniff of the University of Maryland for his assistance and review of this work.

GEORGE G. BALL
Captain, USN
Commander

V. M. KORTZ
By direction

CONTENTS

CONTENTS

ILLUSTRATIONS

ILLUSTRATIONS

ILLUSTRATIONS

ILLUSTRATIONS

TABLES

LIST OF SYMBOLS

$f(t)$	Arbitrary function of time
$F(\omega)$	Fourier integral of $f(t)$
m	Mass, lb sec/in^2
k	Spring constant, lb/in
c	Damping constant, lb sec/in
F	Force, lb
$x(t)$	Base motion
$y(t)$	Absolute motion of mass
$r(t)$	Relative motion of mass
$e(t)$	Time dependent voltage
R	Resistance, ohms
L	Inductance, henry
C	Capacitance, farads
$a(t)$	Base acceleration = $\ddot{x}(t)$
$v(t)$	Base velocity = $\dot{x}(t)$
ω_n	Natural frequency, radians/sec
ζ	Fraction of critical damping
ω_d	Damped natural frequency = $\omega_n \sqrt{1-\zeta^2}$
$A(\omega)$	Fourier integral of base acceleration
$V(\omega)$	Fourier integral of base velocity
$A(\omega)_i$	Imaginary part of $A(\omega)$
$A(\omega)_r$	Real part of $A(\omega)$
s	Laplace operator
$R(s)$	Laplace transform of relative response
$A(s)$	Laplace transform of base acceleration

K_i	Weights for decoupled response
θ_A	Fourier integral phase angle
$H(\omega)$	Transfer function
$h(t)$	Impulse response
$G(\omega)$	Power transfer function
$\Delta\omega$	Frequency increment
T	Duration of transient
c_k	Complex Fourier series coefficients
$\delta(t)$	Delta function
$p(t)$	Periodic representation of a transient
$b(t)$	Square pulse
$P(\omega)$	Fourier integral of period representation
$B(\omega)$	Fourier integral of square pulse
K	Frequency distribution constant
$s(t)$	Infinite pulse train, sampling function
f_i	Discrete samples of f(t)
F_k	Discrete samples of F(ω)
h	Time increment
b_k	Input coefficients for recursive filter
d_j	Output coefficients for recursive filter
$R(z)$	z-transform of sampled r(t)
$A(z)$	z-transform of sampled a(t)
a_i^0, a_i^1, a_i^2	Coefficients of parabolic approximation to acceleration a(t)
V_i^0, V_i^1, V_i^2	Coefficients of parabolic approximation to velocity V(t)
N	Sampled data length T/h

T_t	Total computation time
T_i	Iteration time
T_{oh}	Overhead time
$F_t(\omega)$	Reference Fourier spectrum value
$S_t(\omega)$	Reference shock spectrum value
$\mathcal{L}[\ ], \mathcal{L}^{-1}[\ ]$,	Laplace transform and inverse transform
$\lvert\ \rvert$	Absolute value or complex magnitude
$(\ )^*$	Complex conjugate
$\bar{F}(t)$	Sampled time function
t	Independent variable time
t_p	Time of peak response relative to the end of the transient

BLANK PAGE

CHAPTER I

INTRODUCTION

Objectives

The Fourier spectrum and shock spectrum are widely used as methods for determining the effects of transients on mechanical as well as electrical systems. The available literature on the computation of the two spectra is widely diverse as to which techniques are best suited for determination of the spectra. This is particularly true in the digital computation of spectra where a variety of "rules of thumb" appear which are not usually consistent between different authors.

The object of this paper is to compare and contrast the various methods which are available and to establish which methods are best suited to a particular application. A second objective is to establish realistic guidelines for the computation of the Fourier and shock spectra of transients.

Definitions of the Shock and Fourier Spectra

Both the shock spectrum and Fourier spectrum definitions vary in the references. They will be defined here as they are used throughout the paper.

Shock Spectra

"A shock spectrum is the plot of the maximum absolute values of the relative displacements multiplied by appropriate scaling factors, of a set of either damped or undamped single-degree-of-freedom oscillators with negligible mass, which have been subjected to a base shock motion, the values being plotted as a function of the natural frequency of the simple oscillators. These graphs can be constructed with units of displacement, velocity or equivalent static acceleration by the choice of the scaling factors of unity, ω or ω^2/g respectively, where ω is the angular frequency of the oscillator."[1] Some additional terms are used in describing the shock spectrum. They will be defined here for later reference. The residual shock spectrum is the maximum absolute value occurring after the transient stops. The positive shock spectrum is the largest positive relative displacement of the oscillator and the negative shock spectrum is the greatest negative displacement. These can also be multiplied by scale factors and put in units of displacement, velocity or equivalent static acceleration.

Fourier Spectra

The Fourier spectrum is most easily defined as the magnitude of the complex Fourier integral. The Fourier spectrum is also defined differently in the references

so it will be defined here as it will be used throughout this paper. The Fourier transform pair is given [2] as

$$F(\omega) = \int_{-\infty}^{\infty} f(t) \exp(-j\omega t)\, dt \qquad (1)$$

$$f(t) = \frac{1}{2\pi} \int_{-\infty}^{\infty} F(\omega) \exp(j\omega t)\, d\omega \qquad (2)$$

The Fourier integral is, in general, complex having both a real and imaginary part. The vector sum of the two parts is called the Fourier spectrum.

Background Information

Among the first authors of papers concerning shock spectra is Dr. J. M. Frankland. His work on what he termed dynamic load factors was published in 1942. [3] The same concept, under the name of amplification factor, was used by R. D. Mindlin [4] and published in 1945. The fundamental concepts of shock spectra were used by Biot [5] in his 1943 paper on Analytical and Experimental Methods in Engineering Seismology. Since the publication of these original works, a tremendous amount of literature has appeared on the interpretation, computation, and application of shock spectra.

Gardner and Barns [6] summarizes the development of the Fourier and Laplace transform techniques. The names associated with these developments are too numerous to

mention in total. But certain of these are associated with theory and technique which will be used throughout this presentation. Briefly some of the names and techniques follow: Laplace, Cauchy, Heaviside, Dirichlet, Riemann, Mellin, Parseval and Duhamel.

Formulation of the Shock Spectra

The single-degree-of-freedom oscillator required for the shock spectrum analysis is shown in Figure 1 along with an equivalent RLC series two-port network. The equation of motion will be formulated here for the spring mass oscillator with the assumption that there is no static deflection caused by gravitational forces. The summation of forces on the mass using D'Alembert's principle yields

$$\sum F = m\ddot{y} = k(x-y) + c(\dot{x}-\dot{y}) \qquad (3)$$

This can be rewritten substituting the relative displacement $r = y - x$ in the form

$$\ddot{r} + {}^{c}/_{m}\,\dot{r} + {}^{k}/_{m}\,r = -\ddot{x} \qquad (4)$$

The equation shows that neglecting initial conditions, the shock spectrum is only a function of the base acceleration. This means that regardless of which form the transient is measured in, displacement, velocity, or acceleration, the shock spectrum is a function of only acceleration. The

analogous formulation for the RLC series two-port network is as follows

$$\ddot{e}_o + \frac{R}{L}\dot{e}_o + \frac{1}{LC}e_o = \frac{1}{LC}e_1(t) \qquad (5)$$

The solution of these equations with no input is shown in several references. Using the solutions, the equations can be written in terms of the undamped resonance frequency (ω_n) and the damping ratio (ζ) as

$$\ddot{r} + 2\zeta\omega_n\dot{r} + \omega_n^2 r = -\ddot{x} \qquad (6)$$

and

$$\ddot{e}_o + 2\zeta\omega_n\dot{e}_o + \omega_n^2 e_o = \omega_n^2 e_1(t) \qquad (7)$$

respectively. The RLC series two-port network differs only because of the ω_n^2 scale factor. The discussion that follows uses the spring-mass oscillator primarily, but the small difference is easily compensated for if further discussion of the electrical network is desired. The Laplace transform technique will be used to solve the differential equation. The Laplace transform of equation (4) can be written with initial conditions $\dot{r}(o)$ and $r(o)$ representing the initial conditions as

$$R(s) = \frac{-\mathcal{L}\left[\ddot{x}(t)\right] + \dot{r}(o) + (2\zeta\omega_n + s)\, r(o)}{s^2 + 2\zeta\omega_n s + \omega_n^2} \qquad (8)$$

The system is linear and can therefore be solved for

response to initial conditions and input separately and then the two responses can be added to get the total response. This is a convenient approach here since the solution is going to be determined for the two cases of velocity v(t) and acceleration a(t) input. Using a table of Laplace transforms, the transform, in the absence of an input motion, and its inverse are:

$$R(s) = \frac{\dot{r}(o) + \zeta\omega_n r(o)}{(s + \zeta\omega_n)^2 + \omega_d^2} + \frac{r(o)\ (s + \zeta\omega_n)}{(s + \zeta\omega_n)^2 + \omega_d^2} \qquad (9)$$

where $\omega_d = \omega_n \sqrt{1 - \zeta^2}$, and

$$r(t) = \frac{1}{\omega_d} (\dot{r}(o) + \zeta\omega_n r(o)) \exp(-\zeta\omega_n t) \sin(\omega_d t)$$

$$+ r(o) \exp(-\zeta\omega_n t) \cos(\omega_d t) \qquad (10)$$

The forced solution in terms of the input base motion will now be determined for the two cases of velocity and acceleration input. The base acceleration input $\ddot{X}(t)$ will now be written as a(t) and its Laplace transform as

$$\mathcal{L}\left[a(t)\right] = A(s) \qquad (11)$$

The Laplace transform of the response to base acceleration is therefore

$$r(t) = \mathcal{L}^{-1}\left[\frac{A(s)}{((s+\zeta\omega_n)^2 + \omega_d^2)}\right] \tag{12}$$

Using the convolution theorem [2] the response can be written in terms of the oscillator impulse response h(t) and the base acceleration as

$$r(t) = -\int_0^t h(\tau) \cdot a(t-\tau)d\tau \tag{13}$$

$$h(t) = \frac{1}{\omega_d} \exp(-\zeta\omega_n t) \sin(\omega_d t) \tag{14}$$

Combination of these two equations and the response to initial conditions yields the total response of the oscillator to base acceleration as

$$r(t) = \left(\frac{\dot{r}(o)}{\omega_d} + \frac{\zeta r(o)}{\sqrt{1-\zeta^2}}\right) \exp(-\zeta\omega_n t) \sin(\omega_d t)$$

$$+ r(o) \exp(-\zeta\omega_n t) \cos(\omega_d t)$$

$$- \frac{1}{\omega_d}\int_0^t a(\tau) \exp(-\zeta\omega_n(t-\tau)) \sin(\omega_d(t-\tau))\, d\tau \tag{15}$$

The other possible form of input is the velocity v(t). The Laplace transform of the base acceleration in terms of the velocity is

$$\mathcal{L}\left[\dot{v}(t)\right] = sV(s) - v(o) \tag{16}$$

The response to base velocity is therefore given by

$$r(t) = -\mathcal{L}^{-1}\left[\frac{sV(s) - v(o)}{((s + \xi\omega_n)^2 + \omega_d^2)}\right] \qquad (17)$$

Solution, again using the convolution theorem, yields the response to base velocity with no initial conditions as

$$r(t) = \frac{v(o)}{\omega_d} \exp(-\xi\omega_n t) \sin(\omega_d t)$$

$$- \int_o^t v(\tau) \exp(-\xi\omega_n (t-\tau)) \cos(\omega_d (t-\tau))\, d\tau$$

$$+ \frac{\xi}{\sqrt{1-\xi^2}} \int_o^t v(\tau) \exp(-\xi\omega_n (t-\tau)) \sin(\omega_d (t-\tau))\, d\tau \qquad (18)$$

The total solution to a base velocity with initial conditions is therefore

$$r(t) = \left(\frac{\dot{r}(o) + v(o)}{\omega_d} + \frac{\xi r(o)}{\sqrt{1-\xi^2}}\right) \exp(-\xi\omega_n t) \sin(\omega_d t)$$

$$+ r(o) \exp(-\xi\omega_n t) \cos(\omega_d t)$$

$$- \int_o^t v(\tau) \exp(-\xi\omega_n (t-\tau)) \cos(\omega_d (t-\tau))\, d\tau$$

$$+ \frac{\xi}{\sqrt{1-\xi^2}} \int_o^t v(\tau) \exp(-\xi\omega_n (t-\tau)) \sin(\omega_d (t-\tau))\, d\tau \qquad (19)$$

Equations (15) and (19) can be considerably simplified if only the undamped oscillators are considered. The undamped equations will be presented here for later

reference. The equations, when written with $\zeta = 0$, become

$$r(t) = \frac{\dot{r}(o)}{\omega_n} \sin(\omega_n t) + r(o) \cos(\omega_n t) - \frac{1}{\omega_n} \int_o^t a(\tau) \sin(\omega_n(t-\tau))\, d\tau \qquad (20)$$

$$r(t) = \frac{\dot{r}(o) + v(o)}{\omega_n} \sin(\omega_n t) + r(o) \cos(\omega_n t) - \int_o^t v(\tau) \cos(\omega_n(t-\tau))\, d\tau \qquad (21)$$

for the cases of acceleration and velocity input, respectively.

Formulation of the Fourier Spectra

The Fourier integral as defined in equations (1) and (2) can be somewhat simplified for this application by noting some of the properties of the transient being analyzed. Again assume that the motion is given in one of two forms, base acceleration a(t) or base velocity v(t). If now it is assumed that the shock is causal and therefore does not exist for $t<0$, and assuming that the transforms exist, the expression for the Fourier integrals can then be written as

$$A(\omega) = \int_o^\infty a(t) \exp(-j\omega t)\, dt \qquad (22)$$

$$V(\omega) = \int_o^\infty v(t) \exp(-j\omega t)\, dt \qquad (23)$$

The Fourier spectrum for the acceleration is therefore $|A(\omega)|$ and the Fourier spectrum for the velocity is $|V(\omega)|$. The inverse transform relationships for equations (22) and (23) are given by

$$a\ t) = \frac{1}{2\pi} \int_{-\infty}^{\infty} A(\omega) \exp\ (j\omega t)\ d\omega \qquad (24)$$

$$v(t) = \frac{1}{2\pi} \int_{-\infty}^{\infty} V(\omega) \exp\ (j\omega t)\ d\omega \qquad (25)$$

Differentiating equation (25) with respect to t yields a second expression for acceleration,

$$\frac{d\dot{v}(t)}{dt} = a(t) = \frac{1}{2\pi} \int_{-\infty}^{\infty} j\omega V(\omega) \exp\ (j\omega t)\ d\omega \qquad (26)$$

Comparison of equation (24) with equation (26) shows that the Fourier integral of the acceleration is equal to jω times the Fourier integral of the velocity, that is,

$$A(\omega) = j\omega V(\omega) \qquad (27)$$

and therefore the spectra are related by

$$|A(\omega)| = |j\omega V(\omega)| = \omega |V(\omega)| \qquad (28)$$

Equations (27) and (28) are valid when the transforms exist.[2]

The existence of the Fourier spectrum has not as yet been established. Papoulis [2] gives a sufficient condition for the existence as follows:

If f(t) is absolutely integrable in the sense

$$\int_{-\infty}^{\infty} |f(t)|\,dt < \infty \tag{29}$$

then its Fourier integral $F(\omega)$ exists and satisfies equation (2), i.e.,

$$f(t) = \frac{1}{2\pi} \int_{-\infty}^{\infty} F(\omega) \exp(j\omega t)\, d\omega \tag{30}$$

This is as rigorous a test for existence as is necessary for most applications to be considered here. The acceleration and velocity transients discussed here will begin at time zero and will be of finite length T which means they will always be absolutely integrable even in the presence of discontinuities.

Application

Although the primary objective is the computation of shock and Fourier spectra, some discussion of applications seems in order. The shock and Fourier spectra have been used extensively for two purposes. One is the specification and evaluation of laboratory simulations of shock measured in the field. [7] [8] The other is the analysis of complex structures to shock motions. [9] [10]

The use of shock spectra as a means for specifying laboratory test has been a matter of some controversy and will not be discussed here. The use of shock spectra for the prediction of the response of complex structures is more applicable to this treatment.

It is very obvious that if a structure can be accurately modeled using the single-degree-of-freedom oscillator, and if the presence of the oscillator has no effect on the base motion, the shock spectrum is directly applicable to the peak response calculation. It can be shown that the equations of motion for both continuous and lumped parameter linear elastic systems can be, in general, decoupled so that the resulting response can be written as a summation of simple oscillator responses with appropriate weighing factors.[9] [10] The derivation of the technique will be shown here and demonstrated with an example in Appendix A. Assume that the transfer characteristics between the base and some point on a structure can be written as the ratio of two polynomials in s as follows,

$$\frac{R(s)}{A(s)} = \prod_{k=1}^{N} \frac{(s-s_k)}{(s-s_j)} \prod_{j=1}^{M} \qquad N < M \tag{31}$$

where the s_k's represent the zeros and the s_j's represent the poles of the transfer function. Assuming now that the

poles occur as M/2 complex conjugate pairs, the transform can be decoupled and rewritten as

$$\frac{R(s)}{A(s)} = \sum_{i=1}^{M/2} \frac{K_i}{s^2 + 2\xi\omega_i s + \omega_i^2} \tag{32}$$

Where the, in general complex, weighting factor K_i is determined from the residue at the poles of the denominator. The total response r(t) due to a(t) can then be written using the convolution theorem and superposition as

$$r(t) = \sum_{i=1}^{M/2} \frac{K_i}{\omega_{di}} \int_0^t a(\tau) \exp\left\{-\xi\omega_i(t-\tau)\right\} \sin\left\{\omega_{di}(t-\tau)\right\} d\tau \tag{33}$$

A conservative estimate of the peak response can be written as

$$r(t) \leq \sum_{i=1}^{M/2} \frac{K_i}{\omega_{di}} \left| \int_0^t a(\tau) \exp\left\{-\xi\omega_i(t-\tau)\right\} \sin\left\{\omega_{di}(t-\tau)\right\} d\tau \right|_{max} \tag{34}$$

where the term in the absolute value bracket is the velocity shock spectrum value at ω_i. If the input acceleration is time limited: a(t) = 0, t ≥ T and there is no damping present, a conservative estimate of the residual response can be written as

$$t \geq T \qquad r(t) \leq \sum_{i=1}^{M/2} \frac{K_i}{\omega_i} \left| \int_0^T a(\tau) \sin\left\{\omega_i(t-\tau)\right\} d\tau \right|_{max} \tag{35}$$

The term in brackets will be shown later as the Fourier spectra value at ω_i. Techniques for determining the K_i values for mechanical systems are shown in references [9] [10] and [11] and demonstrated in Appendix A.

The shock spectrum approach has been shown to have several shortcomings. The greatest problem is in the neglect of loading effects or structural feedback. The driving point impedance or resistance to motion of the base of a structure is greatest at its natural frequencies (see Appendix A). Or in terms of the Laplace transform, the natural frequencies of the structure or simple oscillator become zeros of the base motion when the structure and base are both considered in the response calculation. The effect of this is to reduce the Fourier and shock spectrum values at the natural frequency of the structure when it is put in place. This problem has been investigated by several authors [12] [1].

CHAPTER II

COMPARISON OF THE SHOCK AND FOURIER SPECTRA VALUES

Fourier Spectra and the Undamped Residual Shock Spectra

There is a fairly well known [13] [14] relationship between the residual velocity shock spectrum and the Fourier spectrum which will be shown here and used in later discussions. The expression for the residual velocity undamped shock spectrum can be written from equation (20) as the maximum value of the integral

$$\omega_n r(t) = -\int_0^T a(\tau) \sin(\omega_n(t-\tau))\, d\tau \qquad (36)$$

evaluated for $t \geq T$, where T represents the total duration of the transient. The "n" subscript can be dropped to simplify notation. Here ω implies ω_n. The integral can be expanded using the identity

$$\sin(\omega t - \omega\tau) = \sin(\omega t)\cos(\omega\tau) - \cos(\omega t)\sin(\omega\tau)$$

which results in

$$\omega r(t) = -\sin(\omega t)\int_0^T a(\tau)\cos(\omega\tau)\, d\tau + \cos(\omega t)\int_0^T a(\tau)\sin(\omega\tau)\, d\tau \qquad (37)$$

The Fourier integral definition can be expanded by writing the exponential in terms of its real and imaginary parts to yield

$$A(\omega) = \int_0^T a(t) \cos(\omega t)\, dt - j \int_0^T a(t) \sin(\omega t)\, dt \quad (38)$$

$$A(\omega) = A(\omega)_r + jA(\omega)_i = |A(\omega)| \exp(j\theta_A) \quad (39)$$

where the subscripts r and i indicate the real and imaginary parts of the Fourier integral and θ_A represent the phase angle of the integral value in polar form. Comparison of the equations shows that the residual velocity shock spectrum can be written in terms of the real and imaginary parts of the Fourier integral as

$$\omega r(t) = - A(\omega)_r \sin(\omega t) - A(\omega)_i \cos(\omega t) \quad (40)$$

which after some manipulation yields

$$\omega r(t) = |A(\omega)| \cos(\omega t + \theta_A + \pi/2) \quad (41)$$

The residual velocity shock spectrum value is the peak value and is seen to be identical to the Fourier spectrum value.

Another relationship which O'Hara has shown to be useful is the relation between the maximum residual response and the relative velocity $\dot{r}(T)$ and displacement $r(T)$ at the

end of the transient. The displacement and velocity at the end of the transient can be written from equation (40) and its derivative as

$$r(t) = \frac{-A(\omega)_r}{\omega} \sin(\omega t) + \frac{A(\omega)_i}{\omega} \cos(\omega t) \qquad (42)$$

$$\dot{r}(t) = -A(\omega)_r \cos(\omega t) + A(\omega)_i \sin(\omega t) \qquad (43)$$

The simultaneous solution at t = T then yields an expression for the Fourier integral values and therefore, the residual velocity shock spectrum as

$$A(\omega)_r = -\omega r(T) \sin(\omega T) - \dot{r}(T) \cos(\omega T) \qquad (44)$$

$$A(\omega)_i = \omega r(T) \cos(\omega T) - \dot{r}(T) \sin(\omega T)$$

$$\omega r_{max} = \sqrt{A^2(\omega)_r + A^2(\omega)_i} = \sqrt{\omega^2 r^2(T) + \dot{r}^2(T)} \qquad (45)$$

Residual Response of the Damped Oscillator

A similar expression can be developed for the residual response of the damped oscillator although it is not simply related to the Fourier integral. To avoid integration beyond the end of the transient the peak response can be written again in terms of the velocity and displacements at the end of the transient as follows. The damped residual response from equation (10) is given by

$$r(t) = \frac{1}{\omega_d}\left(\dot{r}(T) + \zeta\omega_n r(T)\right) \exp\left(-\zeta\omega_n t\right) \sin\left(\omega_d t\right)$$

$$+ r(T) \exp\left(-\zeta\omega_n t\right) \cos\left(\omega_d t\right) \qquad (46)$$

where t = 0 in equation (14) translates to t = T in this case. The true residual velocity response can be obtained by differentiating equation (46) with respect to time. The time of peak response relative to the end of the transient for equation (46) can be found by setting the residual velocity response equal to zero and solving for t. This results in the following expression:

$$t_p = \frac{1}{\omega_d} \arctan\left(\frac{+\dot{r}(T)\sqrt{1-\zeta^2}}{\dot{r}(T)\zeta + r(T)\omega_n}\right), \qquad (47)$$

where the principal value of the arc tangent is used. Substitution into equation (46) yields the first positive or negative peak residual damped response without needless integration beyond the end of the transient.

Characteristics of the Damped Oscillator When Viewed as a Simple Filter

In the chapter which follows it will be shown that there are considerable advantages to computing the damped shock spectrum as opposed to the undamped. For purposes of aiding that discussion the characteristics of the oscillator when viewed as a filter will be determined here. The steady state response to a sinusoidal base acceleration input can be expressed by substitution of $s = j\omega$ into equation (8) with no initial conditions which yields

$$H(\omega) = \frac{R(\omega)}{A(\omega)} = \frac{1}{\omega_n^2} \frac{1}{\left((1 - \frac{\omega^2}{\omega_n^2}) + j2\zeta \frac{\omega}{\omega_n} \right)} \tag{48}$$

where $H(\omega)$ will be used to denote the transfer characteristics. The power-transfer function $G(\omega)$ can be written as $H(\omega)$ times its complex conjugate which yields

$$G(\omega) = H(\omega)H^*(\omega) = \frac{1}{\omega_n^4 \left\{ (1 - \frac{\omega^2}{\omega_n^2})^2 + 4\zeta^2 \frac{\omega^2}{\omega_n^2} \right\}} \tag{49}$$

Differentiation of the denominator with respect to ω and setting it equal to zero yields the frequency ω_p for which the power-transfer function peaks. The result is

$$\omega_p = \omega_n \sqrt{1 - 2\zeta^2} \tag{50}$$

The peak value of the power transfer function is therefore

$$|G(\omega)|_{max} = \frac{1}{4\zeta^2 \omega_n^4 (1 - \zeta^2)}, \tag{51}$$

and the corresponding peak magnitude in the complex transfer function is

$$|H(\omega)|_{max} = \frac{1}{2\zeta\omega_n^2 \sqrt{1 - \zeta^2}} \tag{52}$$

The half power points of the filter are those for which the power transfer function is given by

$$\left|G(\omega_{h.p.})\right| = \frac{1}{8\zeta^2\omega_n^4(1-\zeta^2)} \tag{53}$$

The solution of equation (53) for $\omega_{h.p.}$ yields as the four (two negative and two positive) half power points

$$\omega_{h.p.} = \pm\,\omega_n\left\{1 \pm 2\zeta\,(1-\zeta^2)^{1/2} - 2\zeta^2\right\}^{1/2} \tag{54}$$

By using the Taylor's expansion in terms of ζ about zero, twice the half power points can be approximated by

$$\omega_{h.p.} \approx \pm\,\omega_n\left\{1 \pm \zeta - \frac{3}{2}\zeta^2 \pm \zeta^3 \mp \frac{17}{8}\zeta^4\,,\ldots\right\},$$

and for small damping ratios

$$\omega_{h.p.} \approx \pm\,\omega_n\,(1 \pm \zeta) \tag{55}$$

The normalized bandwidth of the filter is then given to a reasonable approximation for small damping ratios by

$$\frac{\Delta\omega}{\omega_n} = \frac{\omega_n\,(1+\zeta) - \omega_n\,(1-\zeta)}{\omega_n} = 2\zeta \tag{56}$$

If Q is defined as $1/2\zeta$, the transfer characteristic can be written in terms of Q as follows

$$H(j\omega) = \frac{1}{\left(1 - \frac{\omega^2}{\omega_n^2}\right) + \frac{j\omega}{Q\omega_n}} \qquad (57)$$

From equation (57), it is seen that Q can be used to denote the sharpness of the resonant peak of the filter.

CHAPTER III

COMPUTATION OF THE SHOCK AND FOURIER SPECTRA

General Discussion of Computation

Before considering specific methods for determining the shock and Fourier spectra, there are several aspects which must be considered regardless of the method used. These are presented in the forms of questions. What is the minimum sampling required to define or display the spectrum adequately? In the case of digital computation, how often must the transient be sampled to define or analyze it adequately? Is the measured or apparent transient an accurate representation of the true transient or has it been influenced by the measurement-system phase shifts, drifts, calibration errors, etc?

For the last consideration, a great amount of judgment is required. Often instrumentation with little or no frequency response at $\omega = 0$, such as piezoelectric accelerometers, will drift when subjected to a transient of sufficient duration. In some cases it is possible to note the existence of drift and remove it prior to performing the analysis. Often it is possible to detect the presence of such problems by using tests for reasonableness. For example, if an acceleration transient is measured on a structure which is seen to be stationary before and after the transient, the integral of the acceleration transient, or equivalent, the low frequency value

of the Fourier and velocity shock spectrum, should be zero. If the structure is seen to be in the same place and assuming that no yielding has taken place, the second integral of the input acceleration should also be zero. If on the other hand the structure has displaced a finite amount, then the second integral should equal this value. These errors for the most part are dealt with on the basis of technical judgment and, therefore, will receive no further discussion here.

Sampling the Continuous Spectra and Transient

Both the shock and Fourier spectra are continuous and have values for all frequencies; however, it is impractical to determine the values at all frequencies. Therefore it becomes necessary to use a finite number of samples to define and display the spectra. The question of how frequently must the spectrum be sampled is answered by the sampling theorem [2]. The theorem for purposes of discussion here can be stated as follows: If a function f(t) equals zero outside the range $-T/2 \leq t \leq T/2$ the Fourier integral can be uniquely determined from its values $F(2\frac{\pi}{T}k)$, $k = 0,1,2,\ldots$ which are samples taken at frequencies $\frac{2\pi}{T}$ radians/sec apart.

The proof of the sampling theorem is presented below.

For a function f(t) which is zero outside the range $-T/2 \leq t \leq T/2$, the Fourier integral equation (1) can be expressed as

$$F(\omega) = \int_{-T/2}^{T/2} f(t) \exp(-j\omega t)\, dt \qquad (58)$$

The function could also be defined in the interval by a Fourier series which would repeat outside the interval with a period of T. The periodic function, p(t), is defined as follows:

$$p(t) = \sum_{k=-\infty}^{\infty} c_k \exp\left(\frac{j2\pi kt}{T}\right), \qquad (59)$$

and

$$f(t) = p(t), \quad -T/2 \leq t \leq T/2$$

The coefficients c_k of the Fourier series are given by

$$c_k = \frac{1}{T} \int_{-T/2}^{T/2} f(t) \exp\left(\frac{-j2\pi kt}{T}\right) dt \qquad (60)$$

The Fourier integral of a periodic function can be expressed in terms of the delta function $\delta(\omega)$ as [2]

$$\int_{-\infty}^{\infty} \exp\left(\frac{j2\pi kt}{T}\right) \exp(-j\omega t)\, dt = 2\pi\delta\left(\omega - \frac{2\pi k}{T}\right) \qquad (61)$$

Therefore, the Fourier integral of the periodic representation p(t) is given by,

$$P(\omega) = \int_{-\infty}^{\infty} \sum_{k=-\infty}^{\infty} c_k \exp\left(\frac{j2\pi kt}{T}\right) \exp(-j\omega t)\, dt \qquad (62)$$

$$P(\omega) = 2\pi \sum_{k=-\infty}^{\infty} c_k \, \delta\left(\omega - \frac{2\pi k}{T}\right)$$

The Fourier integral values of the time limited function f(t), evaluated at frequencies $\frac{2\pi}{T}$ apart, are given by

$$F_k = F\left(\frac{2\pi k}{T}\right) = \int_{-T/2}^{T/2} f(t) \exp\left(\frac{-j2\pi kt}{T}\right) dt = TC_k \qquad (63)$$

Therefore, the Fourier integral of the periodic representation of the function can be expressed in terms of the F_k samples of the Fourier integral of the time limited function as

$$P(\omega) = \frac{2\pi}{T} \sum_{k=-\infty}^{\infty} F_k \, \delta\left(\omega - \frac{2\pi k}{T}\right) \qquad (64)$$

The F_k values are those indicated by the sampling theorem as being the minimum required to define the Fourier integral of the time-limited function. Therefore, if the continuous Fourier integral can be found from these sampled values, the theorem is proven. The time-limited function can be determined from the periodic function by multiplying by a pulse or boxcar function b(t), where b(t) = 1 for $-T/2 \leq t \leq T/2$ and b(t) = 0 everywhere else.

$$f(t) = p(t)b(t) \qquad (65)$$

Reference [2] gives the transform pair for convolution using the Fourier integral as

$$p(t)\, b(t) \Leftrightarrow \frac{1}{2\pi} \int_{-\infty}^{\infty} P(\bar{\omega})\, B(\omega-\bar{\omega})\, d\bar{\omega} \qquad (66)$$

This can be evaluated using the Fourier integral of the square pulse from Appendix B as follows

$$F(\omega) = \int_{-\infty}^{\infty} \sum_{k=-\infty}^{\infty} F_k\, \delta\left(\bar{\omega} - \frac{2\pi k}{T}\right) \frac{\sin\left(\frac{\omega T}{2} - \frac{\bar{\omega} T}{2}\right)}{\left(\frac{\omega T}{2} - \frac{\bar{\omega} T}{2}\right)}\, d\bar{\omega} \qquad (67)$$

Therefore the continuous Fourier spectrum is given in terms of its sampled values F_k, $k = 0,1,2,\ldots\infty$ as

$$F(\omega) = \sum_{k=-\infty}^{\infty} F_k \frac{\sin\left(\frac{\omega T}{2} - \pi k\right)}{\left(\frac{\omega T}{2} - \pi k\right)} \qquad (68)$$

There is an equivalent sampling theorem for the sampling of frequency-limited signals in the time domain. This is a useful theorem for the discussion of digital spectrum analysis techniques and will be presented here without proof.

It states that "if the Fourier transform of a function f(t) is zero above a certain frequency ω_c, called the Nyquist frequency

$$F(\omega) = 0 \text{ for } |\omega| \geq \omega_c$$

then f(t) can be uniquely determined from its values

$$f_i = f\left(\frac{i\pi}{\omega_c}\right) \quad i = 0,1,2,\ldots\infty$$

which is a series or equidistant points, distant $\frac{\pi}{\omega_c}$ apart.[2] In fact, the continuous function f(t) is given in terms of the sampled function f_i by

$$f(t) = \sum_{i=-\infty}^{\infty} f_i \frac{\sin(\omega_c t - i\pi)}{(\omega_c t - i\pi)} \qquad (69)$$

This is the function performed by an ideal digital-to-analog converter.[5] Both sampling theorems can be treated as ideal interpolators for the time and frequency limited functions, respectively. The two sampling theorems are exclusive. Continuous functions cannot be both time and frequency limited.[16] The author further states that

> "Evidently, the mathematical model should not be pushed too far in applying it to the real world; the mathematical model of a band limited function is a useful mathematical approximation of, but does not necessarily correspond exactly to, the physical world." [16]

How far the band-limited, time-limited model can be pushed for certain well known transients is discussed in the next chapter and Appendix B. Although the sampling theorem discussed here is not directly applicable to the shock spectrum, it seems reasonable to assume that it can be used as a guideline. The Fourier and shock spectra shown and discussed in this report show that the shock

spectrum is at least as smooth a function as the Fourier spectrum.

Sampling the Damped Shock Spectra

In practice, the shock spectrum is often computed using damped oscillators with constant ζ's, and the Fourier spectrum, or a semblance of it, is determined using constant percentage, constant-Q filters. There are several justifications for this approach. Often electrical and mechanical systems in the real world behave in a fashion which is modeled more accurately by the constant-Q oscillator than by the constant-bandwidth oscillator. The computation is also improved by the added damping. The damping increases the stability of the oscillator, and as will be shown here, reduces the sampling requirements for the spectrum.

Consider now using the damped oscillator having a bandwidth which is always a constant percentage of the natural frequency. Since the range of sensitivity or bandwidth of the oscillator is increasing in proportion to the natural frequency, it seems reasonable that the natural frequencies could be distributed logarithmically as follows

$$\omega_k = \omega_o K^k \qquad k = 0,1,2,3,\ldots \tag{70}$$

If it is required that the half-power points of a particular filter correspond to the natural frequencies of the

filters to either side, the bandwidth of the kth filter must be

$$\Delta\omega_k = \omega_o \left(K^{k+1} - K^{k-1}\right) = \omega_k \left(\frac{K^2-1}{K}\right) \qquad (71)$$

This equation used in conjunction with equation (56) (the filter bandwidth approximation equation) yield as an approximate value for K

$$K \approx (1 + \zeta) \qquad (72)$$

If now it is assumed that the initial frequency is that indicated by the sampling theorem, the distribution of natural frequencies becomes

$$\omega_k = \frac{2\pi}{T} (1 + \zeta)^k \qquad k = 0,1,2,3,\ldots \qquad (73)$$

The value of this equation will be demonstrated in the next chapter using examples.

There are a variety of analog, digital, and most recently hybrid, partly digital partly analog, techniques [17] which can be used for the computation of the shock and Fourier spectra. Transients which can be described by a reasonable expression in closed form can be handled by evaluation of the definitions. This technique will only be used to aid in discussions such as Appendix B. The primary concern here is the determination of shock and Fourier spectra of transients which are measured in the

field and laboratory. Only in extreme cases will they be easily expressed in closed form. The most common form of the measured transient is the frequency modulated (FM) tape recording. It is possible in some cases to perform analysis on data which are in graphic form such as oscillographic records or photographic prints taken from, for example, an oscilloscope with a camera attached. This is demonstrated in reference [7] and is actually a specific type of digital analysis and will therefore be applicable to the following discussions.

Analog Computation of the Spectra

Analog techniques have been used for some time to compute shock and Fourier spectra of transient data. With the present availability of digital techniques, the role of the analog methods seems to be that of making timely "quick look" analyses. The analog Fourier or shock spectra computers can[1] can be made small and portable [18] [19], which makes them ideally suited to shock-spectrum and Fourier-spectrum computations at the measurement site. The analog-computer equipment used for these analyses are of two types: general purpose and special purpose computers. The general purpose computer can be programmed by writing equation (6) in terms of its highest derivative as follows:

---

[1]Reference [2] reserves the term analyzer for devices which compute density functions, computer is more applicable to devices which determine specific values of $F(\omega)$.

$$\ddot{r} = -\ddot{x} - 2\zeta\omega_n\dot{r} - \omega_n^2 r \qquad (74)$$

For the case of acceleration inputs, this equation can be easily solved on general purpose computer by implementing the program shown in Figure 2.

For the case of velocity inputs the relative displacement y-x has to be substituted for r in equation (74). This yields the required differential equation shown below:

$$\ddot{y} = 2\zeta\omega_n(\dot{x} - \dot{y}) + \omega_n^2(x - y) \qquad (75)$$

The block diagram for the required program is shown in Figure 3.

The advantage to this technique comes from the fact that the analogous electrical system behaves in a fashion which is identical to the oscillator being modeled. The displacement, true velocity, and true acceleration can all be generated with some reprogramming. This is particularly advantageous for developing a full understanding of the oscillator behavior. The displacement can be displayed and the peak value picked off or with some additional circuitry, the peak values can be automatically stored for read-out. The program for the acceleration input requires two integrators, one sign inverting summing amplifier. The program for velocity inputs requires one additional summing amplifier. These requirements

restrict the number of oscillators which can be programmed simultaneously. The programs require that two potentiometer settings be changed for each change in frequency for constant-Q analysis, and only one potentiometer change for constant bandwidth analysis.

The special purpose Fourier spectra and shock spectra analog computers have several advantages over the use of general purpose computers. They can be designed to minimize the complexity of the operation so that less time is required to set up and there is a smaller probability of error involved. With good design they can be made small and portable. As a first attempt in designing a special purpose shock or Fourier spectrum computer, passive networks such as the two-port RLC network of Figure 1 might seem usable. A method similar to this was employed in the design of a passive computer [20]. The author admits to several problems which were unsolvable. Consider first the requirements for setting the natural frequency. Equation (5) and (7) shows that the natural frequency of the passive two-port network was given by $\omega = \frac{1}{\sqrt{LC}}$. Thus, for example, a 1 radian/second oscillator requires an LC product of 1. This requirement can be met by a 1 henry inductor and a 1 farad capacitor. Capacitors and inductors of this size are not readily available or readily movable. Of course, decreasing the size of either one results in an increase in the size of the other. The passive spectra computer [20] had a lower frequency limit of 100 Hz and required that the data be played

back at greater than the real time rate to determine low frequency values. Another problem was the inability to limit or control the damping ratio. Because of these problems the active RC network was used in the design of a shock spectra computer [19]. The required networks for the active RC network Fourier and shock spectra computers can be most easily designed using the transfer functions of Chapter 1. The transfer function required to compute the equivalent static acceleration from the acceleration input with no initial conditions using equation (8) and the definition of the shock spectra is given by

$$H_1(s) = \frac{-\omega_n^2}{s^2 + 2\zeta\omega_n s + \omega_n^2} \tag{76}$$

The equation for computing the velocity shock spectra or Fourier spectra of the acceleration from the velocity input with no initial condition is given by

$$H_2(s) = \frac{-\omega_n s}{s^2 + 2\zeta\omega_n + \omega_n^2} \tag{77}$$

Active RC networks requiring a single high gain amplifier and having the required transfer function can be found in tables such as those in references [21]. The only remaining problem is to determine the correspondence between the elements of the circuit and the ω_n and ζ characteristics of the oscillator. The required circuit diagrams appear

in Figures 4 and 5. The verification of the transfer function and correspondence for the two transfer functions appear in Appendix C. The initial conditions can be included if necessary. For example the acceleration transient can be preceded by an impulse of appropriate weight if an initial velocity is required with the first circuit.

Digital Computation of the Spectra

Digital techniques are used widely for the computation of shock and Fourier spectra[7] [14] [22] [23]. The primary application has been for the computation of detailed spectra for purposes of reporting the results of laboratory and field tests usually after some passage of time. There are some facilities, however, which are doing on-line computation of the shock and Fourier spectra successfully[23]. The reference describes a system which has the capability of analyzing field data on-line. The concern here is primarily with the algorithms used to determine the spectra and not so much the hardware or the actual computer used.

The Digital Model of the Transient

Before discussing specific means of computing the spectra, it is considered instructive to discuss the sampling process and the digital model of the continuous transient. References [15] [24] use multiplication by a pulse train as the mathematical model of the sampling process.

Consider the sampling function s(t) which is an indefinitely long train of equally spaced impulses which can be expressed as

$$s(t) = \sum_{i=-\infty}^{\infty} \delta(t - ih) \tag{78}$$

The sampling of a function f(t) then appears as

$$\bar{f}(t) = \sum_{i=-\infty}^{\infty} f_i = s(t)f(t) = f(t) \sum_{i=-\infty}^{\infty} \delta(t - ih) \tag{79}$$

If the function is causal and time-limited to T, f(t) = 0 for $t \geq T$. Equation (79) reduces to

$$\bar{f}(t) = f(t) \sum_{i=0}^{N-1} \delta(t - ih) \tag{80}$$

where

$$N = \frac{T}{h}$$

The above is a frequency-limited representation of a time-limited transient. (The sampling has implied that the transient is frequency-limited.) As was stated previously, the validity of any of the following analysis is dependent on the accuracy of this model.

The Finite Discrete Fourier Transform

Consider now the Fourier transform of this model

$$F(\omega) = \int_{-\infty}^{\infty} \sum_{i=0}^{N-1} f(t)\delta(t - ih) \exp(-j\omega t)\, dt$$

$$= \sum_{i=0}^{N-1} f_i \exp(-j\omega hi) \qquad (81)$$

The transform appears to be valued for all frequencies, and could be evaluated as such. This would be somewhat inefficient as will be discussed in Chapter IV. By sampling the function with the interval h, it was implied that the Fourier transform of the function was limited to the range of frequencies $-\omega_c \leq \omega \leq \omega_c$, $\omega_c = \frac{\pi}{h}$. Also since the function is time-limited, the spectrum need only be sampled at the interval $\frac{2\pi}{T}$. Placing these restrictions on the transform, and using F_k as the sampled spectrum the Fourier transform of the time-limited, frequency-limited, model becomes

$$F_k = F\left(\frac{2\pi k}{Nh}\right) = h \sum_{i=0}^{N-1} f_i \exp\left(\frac{-j2\pi ki}{N}\right) \qquad (82)$$

$$k = 0,1,2,3,\ldots, N-1$$

The inverse transform by similar reasoning is

$$f_i = f(ih) = \frac{1}{T} \sum_{k=0}^{N-1} F_k \exp\left(\frac{j2\pi ki}{N}\right) \qquad (83)$$

$$i = 0,1,2,3,\ldots, N-1$$

The range of k is from 0 to N-1 instead of $-\frac{N}{2} < K \leq \frac{N}{2}$ as substitution would have indicated. The exponential has

the same values in the ranges $\frac{N}{2}$ to N-1 and $\frac{-N}{2}$ to -1 which allows for the convenient notation.

This is the finite discrete Fourier transform. This form of the Fourier transform has been implemented on the digital computer in a variety of ways. Most recently and most efficiently the technique used is credited to Cooley and Tukey [25] and is known as the Fast Fourier Transform (FFT). This technique, as will be shown in the next chapter when timing is discussed, represents a major contribution to the use of digital computers for spectra analysis. The actual method used in the FFT is fairly complex and will not be covered here. References [25] [26] [27] give detailed discussions of the implementation of the algorithm. Some discussions of the limitations of the technique will be useful. The technique uses binary arithmetic extensively which results in the fact that it is most efficient when applied to sampled data having a sample length which is an even power of two, $N = 2^m$. The data are shifted continually during the execution of the routine; therefore, the value of the summation (equation (82)) cannot be given for each instant in time as would be the case with direct evaluation of the summation. This restriction seems to eliminate the possibility of a fast shock spectrum routine similar to the FFT. An FFT routine taken from SHARE [28], the IBM computer users group, is shown in Appendix D. The FFT is an impulse invariant technique. The transform pair, equations (82) and (83), is exact, within the accuracy

of the computer. This does not imply that the Fourier integral is exact since the impulsive data are only a model of the continuous transient. Several of the techniques for computing the shock and Fourier spectra discussed here will be impulse-invariant.

The Shock and Fourier Spectra by the Direct Method

There are shortcut methods available for the determination of impulse-invariant simultaneous solutions for the shock and Fourier spectra. These shortcut solutions will be presented later in this chapter. In order to demonstrate the actual meaning of the impulse-invariant solutions, they will be derived first by direct application of the general solution, equations (15) and (19). Let the inputs for acceleration and velocity be impulsive. The sampling function equation (78) can be applied to the convolution integral in equation (15) which yields

$$r(t) = \frac{-h}{\omega_d} \int_0^t a(\tau) \sum_{i=-\infty}^{\infty} \delta(\tau - ih) \exp\left[-\zeta\omega_n(t-\tau)\right] \sin\left[\omega_d(t-\tau)\right] d\tau \tag{84}$$

The h is a necessary weighting factor which gives the transient model a more accurate integral. This equation reduces to

$$r(t) = \frac{-h}{\omega_d} \sum_{i=0}^{N-1} a_i \exp\left[-\zeta\omega_n(t-ih)\right] \sin\left[\omega_d(t-ih)\right], \tag{85}$$

where $N = \frac{T}{h}$

If the response is considered to be in a particular interval between $t = ih$ and $t = ih + \bar{t}$, $\bar{t} \leq h$, the total response becomes

$$r(ih+\bar{t}) = \frac{\dot{r}_i}{\omega_d} \exp(-\zeta\omega_n\bar{t}) \sin(\omega_d\bar{t}) + r_i \exp(-\zeta\omega_n\bar{t}) \left\{\cos(\omega_d\bar{t}) + \frac{\zeta}{\sqrt{1-\zeta}} \sin(\omega_d\bar{t})\right\} - \frac{ha_i}{\omega_d} \exp(-\zeta\omega_n\bar{t}) \sin(\omega_d\bar{t}) \quad (86)$$

The velocity in the interval is given by differentiation of equation (86) as

$$\dot{r}(ih+\bar{t}) = \dot{r}_i \exp(-\zeta\omega_n\bar{t}) \left\{\cos(\omega_d\bar{t}) - \frac{\zeta}{\sqrt{1-\zeta^2}} \sin(\omega_d\bar{t})\right\} - \frac{r_i\omega_n}{\sqrt{1-\zeta^2}} \exp(-\zeta\omega_n\bar{t}) \sin(\omega_d\bar{t}) - a_i h \exp(-\zeta\omega_n\bar{t}) \left\{\cos(\omega_d\bar{t}) - \frac{\zeta}{\sqrt{1-\zeta^2}} \sin(\omega_d\bar{t})\right\} \quad (87)$$

These equations can be simplified if the velocity $\dot{r}_i$ is assumed to be evaluated at $ih +$ or slightly after the acceleration impulse. If the values of the response are viewed at the end of the interval $\bar{t} = h$, the equations become

$$r_i = \frac{\dot{r}_{i-1}}{\omega_d} \exp(-\zeta\omega_n h) \sin(\omega_d h)$$

$$+ r_{i-1} \exp(-\zeta\omega_n h) \left\{\cos(\omega_d h) + \frac{\zeta}{\sqrt{1-\zeta^2}} \sin(\omega_d h)\right\} \quad (88)$$

$$\dot{r}_i = \dot{r}_{i-1} \exp(-\zeta\omega_n h) \left\{\cos(\omega_d h) - \frac{\zeta}{\sqrt{1-\zeta^2}} \sin(\omega_d h)\right\}$$

$$- r_i \frac{\omega_n}{\sqrt{1-\zeta^2}} \exp(-\zeta\omega_n h) \sin(\omega_d h) - a_i h \quad (89)$$

An equivalent approach for velocity inputs using the sampling function on equation (19) yields as the impulse-invariant solution for velocity input as

$$r_{i+1} = \frac{(\dot{r}_i + V_i)}{\omega_d} \exp(-\zeta\omega_n h) \sin(\omega_d h)$$

$$+ (r_i - V_i h) \exp(-\zeta\omega_n h) \left\{\cos(\omega_d h) + \frac{\zeta}{\sqrt{1-\zeta^2}} \sin(\omega_d h)\right\} \quad (90)$$

and

$$\dot{r}_{i+1} = (\dot{r}_i + V_i) \exp(-\zeta\omega_n h) \left\{\cos(\omega_d h) - \frac{\zeta}{\sqrt{1-\zeta^2}} \sin(\omega_d h)\right\}$$

$$- \frac{(r_i - V_i)}{\sqrt{1-\zeta^2}} \omega_n \exp(-\zeta\omega_n h) \sin(\omega_d h) \quad (91)$$

The assumption of an impulsive velocity is unrealistic. A more realistic approach would be to maintain the assumption of an impulsive acceleration which implies that the velocity

is constant in the interval. The acceleration at the ith velocity sample then becomes

$$a_i h = v_i - v_{i-1} \tag{92}$$

The response to velocity inputs using the equations (88) and (89) becomes

$$r_i = \frac{\dot{r}_{i-1}}{\omega_d} \exp(-\zeta\omega_n h) \sin(\omega_d h) + r_{i-1} \exp(-\zeta\omega_n h) \left(\cos(\omega_d h) + \frac{\zeta}{\sqrt{1-\zeta^2}} \sin(\omega_d h)\right) \tag{93}$$

$$\dot{r}_i = \dot{r}_{i-1} \exp(-\zeta\omega_n h) \left(\cos(\omega_d h) - \frac{\zeta}{\sqrt{1-\zeta^2}} \sin(\omega_d h)\right) - r_i \frac{\omega_n}{\sqrt{1-\zeta^2}} \exp(-\zeta\omega_n h) \sin(\omega_d h) - v_i + v_{i-1} \tag{94}$$

Fortran IV programs which were implemented using equations (88), (89), (93), and (94) are shown in Appendix D.

The Shock and Fourier Spectra by the Z-Transform Method

The method employed by Lane [29] is a simplified method for finding the impulse-invariant responses. This method is discussed in references [15] and [27], and only an outline of it is presented here. It is known as the z-transform technique.

A general expression for discrete convolution can be written as [27]

$$r_i = -\sum_{j=1}^{J} d_j r_{i-j} + \sum_{k=0}^{K} b_k a_{i-k} \qquad (95)$$

Where this is known as the general expression for recursive digital filters. The equation can be expanded to yield

$$r_i + d_1 r_{i-1} \cdots + d_j r_{i-j} = b_o a_i + b_1 a_{i-1} \cdots + b_k a_{i-k} \qquad (96)$$

In order to determine the transfer function for the recursive filter both sides of equation will be Laplace transformed. With $z = \exp(sh)$, the discrete Laplace transform or z-transform of the a_i input and the r_i output can be written as

$$\mathcal{L}\left[r_i\right] = R(z)$$
$$\mathcal{L}\left[a_i\right] = A(z) \qquad (97)$$

If now the shifting theorem [16] is applied and it is noted that

$$\mathcal{L}\left[r_{i-1}\right] = R(z)\, z^{-1}$$
$$\mathcal{L}\left[a_{i-1}\right] = A(z)\, z^{-1} \qquad (98)$$

The total transfer function for the recursive relationship becomes

$$\frac{R(z)}{A(z)} = \frac{b_0 + b_1 z^{-1} + b_2 z^{-2}, \ldots\ b_k z^{-k}}{1 + d_1 z^{-1} + d_2 z^{-2}, \ldots\ d_J z^{-J}} \qquad (99)$$

The problem is to find the coefficients which correspond to the desired transfer function. This will be done for

the cases of the acceleration and velocity inputs. The transfer function for the acceleration input and relative displacement output is again from equation (12) given by

$$\frac{R(s)}{A(s)} = \frac{-1}{(s + \zeta\omega_n)^2 + \omega_d^2} \tag{100}$$

The z-transform can be determined using the methods shown in reference [24]. In the case of this fairly common transfer function the z-transform can be taken from tables in the same reference as

$$\frac{R(z)}{A(z)} = \frac{-h}{\omega_d} \frac{z^{-1} \exp(-\zeta\omega_n h) \sin(\omega_d h)}{1 - z^{-1}(2 \exp(-\zeta\omega_n h) \cos \omega_d h) + z^{-2} \exp(-2\zeta\omega_n h)} \tag{101}$$

The coefficients from a comparison of equations (99) and (100) are given by

$$b_0 = 0, \quad b_1 = \frac{-h}{\omega_d} \exp(-\zeta\omega_n h) \sin(\omega_d h),$$

$$d_1 = -2 \exp(-\zeta\omega_n h) \cos \omega_d h, \text{ and}$$

$$d_2 = \exp(-2\zeta\omega_n h) \tag{102}$$

Therefore the use of the coefficients with equation (95) yields an impulse-invariant oscillator response to an acceleration input. The required transfer function for the case of velocity inputs with no initial condition is, from equation (17), given by

$$\frac{R(s)}{V(s)} = \frac{-s}{(s+\zeta\omega_n)^2 + \omega_d^2} \tag{103}$$

Using techniques from reference [24] the z-transform is

$$\frac{R(z)}{V(z)} = -h \frac{1+z^{-1}\left[\zeta/\sqrt{1-\zeta}\,\sin\,\omega_d h - \cos\,\omega_d h\right]\,\exp\,(-\zeta\omega_n h)}{1 - 2z^{-1}\exp(-\zeta\omega_n h)\cos\,(\omega_d h) + z^{-2}\exp\,(-2\zeta\omega_n h)} \tag{104}$$

The required coefficients from equation (99) and (104) are therefore

$$b_0 = -h$$

$$b_1 = -h\left[\frac{\zeta}{\sqrt{1-\zeta}}\sin\,(\omega_d h) - \cos\,(\omega_d h)\right]\exp\,(-\zeta\omega_n h)$$

$$d_1 = -2\exp\,(-\zeta\omega_n h)\cos\,(\omega_d h)$$

$$d_2 = \exp\,(-2\zeta\omega_n h) \tag{105}$$

One problem with the z-transform techniques is that the velocity is not given at the end of the transient as it is with the direct method. This problem can be overcome by noting the relationship between the responses r_{N-1} and r_N as given by equation (88). Solving for $\dot{r}_{N-1}$ yields the value of the velocity at the last sample in terms of the last displacement sample and one residual sample as

$$\dot{r}_{N-1} = \frac{\omega_d\left(r_N - r_{N-1}\exp\,(-\zeta\omega_n h)\left\{\cos\,(\omega_d h) + \frac{\zeta}{\sqrt{1-\zeta^2}}\sin\,(\omega_d h)\right\}\right)}{\exp\,(-\zeta\omega_n h)\,\sin\,(\omega_d h)} \tag{106}$$

The peak residual response and Fourier spectrum can then be determined using equations (45) or (47). The FFT, the direct method, and the z-transform method all yield an impulse invariant solutions for the spectra.

The Shock and Fourier Spectra by the O'Hara Method

One obvious error in the techniques discussed previously is the lack of consideration for the behavior of the transient in the interval between samples. There are a variety of means which could be used to interpolate between the samples to improve the model. The ideal digital-to-analog conversion formula might be used under the assumption that the data are ideally frequency limited. A less difficult approach is to assume the transient can be represented by a polynomial in the interval. This technique was used by O'Hara [14] with the assumption being that the transient could be approximated by a parabola in the interval.

Using a parabolic assumption, the acceleration can be written in terms of the first and second forward differences in the interval (i-1)h to ih as

$$a(t) = \bar{a}_i^0 + \bar{a}_i^1 \frac{t}{h} + \frac{\bar{a}_i^2}{2}\left(\frac{t^2}{h^2} - \frac{t}{h}\right) \quad 0 \leq t \leq h \tag{107}$$

for i > 1 the parabola is determined using rearward points as

$$\bar{a}_i^0 = a_{i-1}$$

$$\bar{a}_i^1 = a_i - a_{i-1}$$

$$\bar{a}_i^2 = \bar{a}_i^1 - \bar{a}_{i-1}^1 = a_i - 2a_{i-1} + a_{i-2} \tag{108}$$

for i = 1 the parabola is determine using forward points as

$$\bar{a}_1^0 = a_0$$

$$\bar{a}_1^1 = a_1 - a_0$$

$$\bar{a}_1^2 = a_2 - 2a_1 + a_0 \tag{109}$$

The response is determined by substitution of equation (107) into equation (15) and its derivative. From reference [14] the result in the undamped case is

$$r_i = r_{i-1} \cos(\omega h) + \frac{\dot{r}_{i-1}}{\omega} \sin(\omega h) - \frac{\bar{a}_i^0}{\omega^2}(1 - \cos(\omega h)) - \frac{\bar{a}_i^1}{\omega^2}\left(1 - \frac{\sin(\omega h)}{\omega h}\right) + \frac{\bar{a}_i^2}{\omega^2}\left[\frac{(1 - \cos(\omega h))}{\omega^2 h^2} - \frac{\sin(\omega h)}{2\omega h}\right] \tag{110}$$

$$\frac{\dot{r}_i}{\omega} = -r_{i-1} \sin(\omega h) + \frac{\dot{r}_{i-1}}{\omega} \cos(\omega h) - \frac{\bar{a}_i^0}{\omega^2} \sin(\omega h) - \frac{\bar{a}_i^1}{\omega^2}\left(\frac{1 - \cos(\omega h)}{\omega h}\right) + \frac{\bar{a}_i^2}{\omega^2}\left[\frac{\sin(\omega h)}{\omega^2 h^2} - \frac{(1 + \cos(\omega h))}{2\omega h}\right] \tag{111}$$

When the base velocity is given, the velocity can be approximated in the interval h(i-1) to hi by a parabola as follows

$$V(t) = \bar{V}_i^0 + \bar{V}_i^1 \frac{t}{h} + \frac{\bar{V}_i^2}{2}\left(\frac{t^2}{h^2} - \frac{t}{h}\right) \tag{112}$$

For i > 1 the parabola is determined using rearward points as

$$\bar{V}_i^0 = V_{i-1}$$

$$\bar{V}_i^1 = V_i - V_{i-1}$$

$$\bar{V}_i^2 = \bar{V}_i^1 - \bar{V}_{i-1}^1 = V_i - 2V_{i-1} + V_{i-2} \tag{113}$$

For i = 1 the parabola is determined using forward points

$$\bar{V}_1^0 = V_1$$

$$\bar{V}_1^1 = V_2 - V_1$$

$$\bar{V}_1^2 = V_2 - 2V_1 + V_0 \tag{114}$$

Since the shock spectrum is dependent only on acceleration, equation (112) can be differentiated to obtain the acceleration

$$A(t) = \frac{\bar{V}_i^1}{h} + \frac{\bar{V}_i^2}{2}\left(\frac{2t}{h^2} - \frac{1}{h}\right) \tag{115}$$

Thus it is seen that the assumption of parabolic velocity is equivalent to assuming linear acceleration. From reference [14] the result in the undamped case is

$$r_i = r_{i-1} \cos(\omega h) + \frac{\dot{r}_{i-1}}{\omega} \sin(\omega h) - \nabla_i^1 \left(\frac{1 - \cos(\omega h)}{\omega^2 h} \right) - \nabla_i^2 \left(\frac{1 + \cos(\omega h)}{2\omega^2 h} - \frac{\sin(\omega h)}{\omega^3 h^2} \right) \quad (116)$$

$$\dot{r}_1 = -r_{i-1}\, \omega \sin(\omega h) + \dot{r}_{i-1} \cos(\omega h) - \nabla_i^1 \frac{\sin(\omega h)}{\omega h} - \nabla_i^2 \left(\frac{1 - \cos(\omega h)}{\omega^2 h^2} - \frac{\sin(\omega h)}{2\omega h} \right) \quad (117)$$

FORTRAN IV programs which employ each of the methods discussed here are included in Appendix B. The damped and undamped solutions were programmed separately because the coefficients, and in some cases the computation, are considerably simplified when no damping is present. The programs included are the damped and undamped direct method solutions for acceleration and velocity inputs; the damped and undamped z-transform solutions for acceleration and velocity inputs; the damped and undamped O'Hara solutions for the acceleration and velocity inputs; and the FFT routine from the IBM users group SHARE [28].

Inverse Transformation

The primary concern has been with the computation of the shock and Fourier spectra. Problems similar to

those discussed occur when equations (82) and (83) are used to compute the transfer function and the correlation function, and to evaluate the convolution integral using transient data. These relationships have been used for compensating for structural feedback using mechanical impedance techniques [30], synthesis of shock on vibration test equipment [31], and the evaluation of the convolution integral [32]. The problems and errors associated with these techniques are closely related to those problems and errors discussed in this report. The primary difference being that the convolution has been computed in this report with one of the input functions equal to the impulse response of the simple oscillator.

It will now be shown that the operation of inverse transforming is equivalent to taking the complex conjugate of the transform of the complex conjugate. By taking the conjugate of both sides of equation (1) and treating f(t) as complex for the moment, it can be seen that

$$F^*(\omega) = \int_{-\infty}^{\infty} f^*(t) \exp(j\omega t)\, dt \qquad (118)$$

Equation (2) can be rewritten as

$$f(t) = \int_{-\infty}^{\infty} F(\omega) \exp(j\omega t)\, df \qquad (119)$$

It can be seen that the operation of transform and inverse transform can be accomplished by a single routine which is capable of computing a complex transform. Consider now the

sampling theorem as applied to the transform and inverse transform as they might be used for correlation or convolution of two time-limited signals.

Consider the convolution problem. Given the system response h(t) to an impulsive input $\delta(0)$ and a generalized input f(t), the response x(t) can be computed as

$$x(t) = \int_0^\infty h(t)\, f(t-\tau)\, d\tau \tag{120}$$

Transforming both sides

$$X(\omega) = \int_0^\infty \int_0^\infty h(\tau) f(t-\tau)\, d\tau \exp(-j\omega t)\, dt \tag{121}$$

By changing the order of integration

$$X(\omega) = \int_0^\infty h(\tau) \int_0^\infty f(t-\tau) \exp(-j\omega t)\, dt\, d\tau, \tag{122}$$

and using the shifting theorem

$$f(t-\tau) = f(t) \exp(-j\omega\tau) \tag{123}$$

The following relations develop:

$$X(\omega) = F(\omega) \int_0^\infty h(\tau) \exp(-j\omega\tau)\, d\tau \tag{124}$$

$$X(\omega) = F(\omega)\, H(\omega) \tag{125}$$

$$x(t) = \frac{1}{2\pi} \int_0^{\infty} F(\omega)\ H(\omega)\ \exp\ (-j\omega t)\ d\omega \qquad (126)$$

The sampling theorem states that $X(\omega)$ must be sampled at a interval no less than $2\pi/T_x$ where T_x is the response duration and is equal to the duration of the input and impulse response combined. Therefore to perform convolution, using for example the FFT routine, between $h(t)$ which is of duration T_h and $f(t)$ which is of duration T_f the two functions must be extended with zeros to a length T_x or greater where $T_x = T_h + T_f$.

CHAPTER IV

EVALUATION OF METHODS FOR DETERMINING THE SHOCK AND FOURIER SPECTRA

In order to determine which of the methods discussed is best suited to a particular application they will be compared and contrasted on the basis of speed and accuracy.

Analog Computer Techniques

The time required to compute the spectra using both the special purpose and general purpose analog computer is dependent on how well the computer is programmed. If considerable effort is made to automate the process and several oscillators are available simultaneously, the spectra can be computed in reasonable amounts of time. As indicated before, very often only a "quick look" analysis is desired from the analog analysis, and the digital techniques are used later to determine the spectra in greater detail. The accuracy with analog techniques is also dependent on how well the oscillator is programmed. In the case of the general purpose computer, the potentiometer settings are most critical. The accuracies of the special purpose analog computers are dependent primarily on the accuracies of the selected components. One percent components are readily available. Higher accuracy components are available but are usually

costly. An alternate method was employed in the construction of the shock-spectrum computer (reference [20]) in that the components were selected using an impedance bridge. The shock-spectrum computer achieved accuracies which were better than 5% for half-sine, saw-tooth, isosceles-triangle inputs. The author indicates that the actual computing error is close to 1% and that the greatest error comes from the scaling of peaks on the oscillograph used to display the oscillator responses. This computer displays three responses simultaneously and can compute a total of 24 spectrum points with a 1/3 octave distribution, $K = 2^{1/3}$ in equation (70), by simply selecting the range using a switch on the front panel. The range can be extended by playing data through the computer at reduced speeds using FM tape recorders.

Computation Time Using Digital Techniques

The computation time for shock and Fourier spectra using the digital computer is more easily formulated. As stated before, the execution of the shock and Fourier spectra FORTRAN IV subroutines of Appendix D will yield one spectrum point. Therefore, if the time for the subroutine is established, it can be multiplied by the number of spectrum points (m) to compute the total time for the overall spectrum. The time for the subroutines of Appendix D, with the exception of the FFT routine, can be approximated by two parts. Each time the routine is executed it computes a series of coefficients. It then uses the coefficients on the data,

and using the final velocity and displacement values computes the Fourier spectrum value or damped residual response. The computation of coefficients and the Fourier or residual response value can be put together and termed the overhead time (T_{oh}). The time required to use the coefficients on the data can be termed the iteration time (T_i). Therefore, the total time (T_t) required to compute an m-point spectrum from N data is

$$T_t = m\ (T_{oh} + NT_i) \tag{127}$$

The FFT routine has its advantage in timing. The time for the FFT algorithm is given by [25] as

$$T_t = KN \log_2 N \tag{128}$$

Here the time is dependent on only N because execution of the program always yields the complete N-point spectrum.

In order to determine the required constants, the subroutines were timed on an IBM 7090 computer with FORTRAN IV and the IBSYS operating system. For the first case (equation (27)), two spectra were computed using different numbers of data and spectra points. The timings on the two runs were used to compute the required two constants. The FFT routine was also used on two examples, although one should be sufficient to determine the single constant. The results of both examples were in agreement using equation (128).

Only the undamped spectra routines were used for timing purposes. The results can be modified and applied to the damped case as will be discussed later. The values of overhead and iteration time are shown in Table 1 along with three examples. The examples used to determine the time were similar to example 1 and not example 3 because of the time required as seen in Table 1. The table shows the undamped z-transform routine is approximately five times as fast as O'Hara's method for acceleration inputs and approximately three times as fast for velocity inputs. The direct method is in between the two in both cases. The table also shows why the FFT routine represents such a significant break-through in spectrum computation on digital computers. One disadvantage of the FFT is that the total spectrum, from $-w_c$ to w_c, must always be computed. In some situations where partial spectra are desired it is possible that the O'Hara and z-transform routines would be faster.

Computation Time for Digital Computation of Damped Spectra

As previously mentioned, the damped routines were not timed. Inspection of the damped and undamped routines of Appendix D will give some insight into the computation time required for these routines. In the case of the O'Hara and the direct method, the iteration time is unchanged, and since the overhead time is insignificant for a large number of data, the time will be only slightly affected in those

cases. In the case of the z-transform with acceleration inputs the iteration time increases approximately by two since the damped computation requires two multiplications per data and the undamped computation requires only one. This results in approximately two to one timing advantage for the computation of damped spectra for the z-transform over the O'Hara method when large numbers of data are involved.

The value of the damped spectrum sampling formula, equation (73), can now be demonstrated with the aid of example 3 from Table 1. Given a one second record (T = 1.0 second) of $8192 = 2^{13}$ data, the time increment h is

$$h = \frac{T}{8192} = 1.221 \times 10^{-4} \text{ sec} \tag{129}$$

Assuming that the minimum total spectrum is to be computed, the frequency increment and Nyquist frequency become

$$\Delta f = \frac{1}{T} = 1 \text{ Hz} = 2\pi \text{ Rad/Sec},$$

$$f_c = \frac{1}{2h} = 4096 \text{ Hz} = 8192\pi \text{ Rad/Sec} \tag{130}$$

The total number of frequencies is therefore

$$m = \frac{f_c}{\Delta f} = 4096 \tag{131}$$

This would require five hours and one hour on a 7090 respectively using the O'Hara and z-transform techniques.

Consider now taking advantage of the sampling benefits for the damped spectrum. For this example the spectrum

will be computed using a damping ratio $\zeta = .05$. Equation (73) indicates that the shock spectrum values should be computed at frequencies given by

$$\omega_k = 2\pi\,(1+\zeta)^k \qquad k = 0,1,2,3,\ldots,m$$
$$\omega_m = 8192\pi \text{ Rad/Sec} \tag{132}$$

The total number of spectrum samples m is therefore given by

$$m = \frac{\log\left(\frac{\omega_m}{\Delta\omega}\right)}{\log(1+\zeta)} = 87 \tag{133}$$

The time required using values from Table 1 is therefore

$$\text{O'Hara } T_t = \frac{87}{4096}\ (318) = 6.75 \text{ min.}$$
$$\text{z-transform } T_t = \frac{2(87)\ (67)}{4096} = 2.85 \text{ min.} \tag{134}$$

The factor 2 was included in the z-transform equation for reasons previously discussed. Since cost is directly proportional to time on digital computers the amount of savings is quite evident. It is often desirable to use a smaller frequency increment than is required by the sampling theorem particularly at the low frequencies since the lower frequencies contain insights into the nature of the transient. If the initial increment is quartered, the number of spectrum values and time required for constant increment computation is increased by a factor of four. The result would be computation times of twenty and four hours for the O'Hara and z-transform method for the complete spectrum. It is unlikely

that anyone would compute a complete spectrum with that much time required.

Now the increment will be quartered and the damped sampling formula will be applied. The required number of points in the spectrum are given by

$$m = \frac{\log\left(\frac{4\omega_m}{\Delta\omega}\right)}{\log\,(1+\zeta)} = 102 \qquad (135)$$

The timing now becomes

O'Hara	T_t = 7.9 min	
z-transform	T_t = 3.3 min	(136)

Or an increase of approximately 15% which is easily tolerated.

Table 2 shows the reduction or, in some cases, increase in number of spectrum samples as indicated by the damped sampling formula for a variety of examples.

Computation of Spectra for Typical Transients

In order to demonstrate and test the techniques presented here, six typical acceleration records were chosen for analysis. The transients chosen and their analyses are presented in Figures 6 through 20. They are as follows:

a. The half-sine as shown in Figure 6

$$a(t) = \sin(\pi t)\ L/sec^2 \qquad 0 \le t \le 1 \qquad (137)$$

b. The full-sine as shown in Figure 9

$$a(t) = \sin(2\pi t)\ L/sec^2 \qquad 0 \le t \le 1 \qquad (138)$$

c. Combined sinusoids not shown in any of the figures

$$a(t) = \sin(2\pi t) + \sin(10\pi t) + \sin(40\pi t) + \sin(200\pi t) \text{ L/sec}^2 \qquad 0 \le t \le 1 \tag{139}$$

d. Inverted parabola as shown in Figure 12

$$a(t) = 4t(1-t) \text{ L/sec}^2 \qquad 0 \le t \le 1 \tag{140}$$

e. Decaying sinusoid as shown in Figure 14

$$a(t) = \exp(-4.605t) \sin(20\pi t) \text{ L/sec} \qquad 0 \le t \le 1 \tag{141}$$

f. The combined decaying sinusoids as shown in Figure 18

$$a(t) = 100 \left\{ \exp(-129t) \sin(200\pi t) + \exp(-208t) \sin(600\pi t) \right\} \qquad 0 \le t \le .06 \tag{142}$$

The combined decaying sinusoid was used by references [7] and [33] as a typical pulse for evaluation of the shock and Fourier spectra. The undamped velocity shock spectra and Fourier spectra of the functions, excluding the combined sinusoids, are shown in Figures 7, 10, 13, 15, 16, and 19. The spectrum for the decaying sinusoid is shown in Figure 15 with linear axes and in Figure 16 with logarithmic axes. It is apparent that the logarithmic display offers a better low frequency resolution.

The undamped shock spectra and Fourier spectra were computed using the O'Hara technique and 1000 samples in the

period of the function. Later error analysis verified the use of these as accurate estimates of the spectra. Spectra computed with lower Nyquist rates converged on these values well before reaching this 1000-point representation. The undamped shock spectra, computed with constant frequency sampling, and the damped shock spectra computed using the damped sampling formula, equation (73), are shown in Figures 8, 11, 17, and 20. The damped spectra samples are shown with x's. The spectra for the combined sinusoid are shown in Figure 11. This function was chosen, because of the sharp resonant peaks, as a test for the damped sampling formula. In this case and all others shown, the damped spectrum seems well represented by the constant percentage samples. The damped sampling formula causes a higher density of points at the lower frequency and, therefore, better represents the spectrum at these frequencies, as can be seen in the figures.

Accuracy of the Digital Techniques

Having established the relative speeds of the various digital techniques, the accuracies will be investigated. The error associated with the digital techniques can be, in general, classified in three categories. They are aliasing errors, integrating errors, and, in the case of shock spectrum, errors from sampling the response. Other sources of errors such as quantitation errors associated with the analog-to-digital conversion of transients and round-off errors during computation are dependent on resolution of the

ADC and accuracies of the computer. These errors are discussed in some detail in reference [22] but are considered insignificant here when compared to those errors sighted above.

Aliasing Errors

Aliasing errors occur because the sampling process, as a result of the sampling theorem, implies that the sampled function is band-limited. In the case of transients considered here, the sampling process implies that the spectrum is limited to the range $-\omega_c \leq \omega \leq \omega_c$ where ω_c is the Nyquist or corner frequency and is equal to $\frac{\pi}{h}$. When aliasing occurs, the spectrum which is outside the specified limits is folded about the corner frequency and even multiples of it, and added algebraically to the spectrum value in the above range [16]. Once this occurs it is impossible to reconstruct the transient exactly from the samples as indicated by the sampling theorem as sufficient for the purpose. Since aliasing errors are always present in the discrete model of the transient, they can only be minimized. If the true spectrum for all frequencies is known, the aliasing can be predicted. This is done for half-sine and square pulse functions in Appendix B.

A problem closely related to aliasing occurs if the undamped shock spectrum or Fourier spectum is computed using the impulse-invariant techniques above the Nyquist rate. The cyclic sine and cosine coefficients repeat in

magnitude in the range $\omega_c \leq \omega \leq 2\omega_c$. They repeat in magnitude and sign in the next range $2\omega_c \leq \omega \leq 3\omega_c$ and so on. This is demonstrated in Figure 21 where the Nyquist frequency is 2 Hz and the analysis was done in the range $0 \leq f \leq 4$ Hz.

Integration Error

Integration error occurs in both the impulse-invariant and O'Hara techniques. The error in the impulse-invariant solution is a result of the lack of consideration for the oscillator and data behavior between samples. The integration error in the O'Hara method is a result of the inaccuracy of the parabola as an approximation to the transient values between samples. Since the Fourier spectrum values are taken at the end of the transient only the integration and aliasing errors are present. Figure 22 shows the Fourier spectrum and velocity shock spectrum for a half-sine acceleration input which was modeled by two samples taken at t = 0, and 1/2. The figure shows that the undamped velocity shock spectrum and Fourier spectrum for the impulse-invariant technique was equal to h or 0.5, as would be expected. The spectra computed, using the O'Hara technique, are already converging on the correct spectra with only the one sample. The half-sine and inverted parabola are very much alike, Figures 6 and 12, which accounts for this effect.

Sampling Errors

In addition to the integration errors, the shock

spectra have errors which result from the fact that testing for peak value is done only at the sample times. Both O'Hara and Lane were aware of the sampling error, and suggested, or in Lane's case implemented, a technique for eliminating them. Lane used a 5th degree polynomial derived using the Lagrange method [16] to interpolate between the sampled outputs for purposes of peak detection. O'Hara's technique was implemented in reference [33]. Peak detection is done in O'Hara's technique by using coefficients which are functions of the fraction of interval time $\bar{t}$ as was used in equations (86) and (87) for the direct method. The interval containing the peak is determined and using the continuous expression for response in the interval, the peak is found. In the case of the impulse-invariant z-transform method, this same computation can be performed using modified z-transform [15] [24]. With this form of z-transform the continuous response can be evaluated. The response is still impulse-invariant and the continuous and sampled responses coincide at the end points of the interval.

In order to determine the amount of error associated with the impulse-invariant and O'Hara techniques, the undamped shock and Fourier spectra were computed for the typical acceleration inputs, excluding the combined sinusoids, using various Nyquist frequencies. The error was defined for the Fourier spectrum as

$$\% \text{ error} = 100 \frac{|F_e(\omega) - F_t(\omega)|}{|F_t(\omega)|} \tag{143}$$

and for the shock spectra as

$$\% \text{ error} = 100 \frac{|S_e(\omega) - S_t(\omega)|}{|S_t(\omega)|} \tag{144}$$

When $F_t(\omega)$ and $S_t(\omega)$ are the values determined using 1000 samples in the period of the transient and the O'Hara technique, Figures 7, 10, 13, and 15. This sampling corresponds to a Nyquist rate of 500 Hz for the one-second transients and 8333.3 Hz for the .06-second transient.

The impulse-invariant Fourier spectrum error for the half-sine acceleration input is shown in Figure 23 for Nyquist rates of 5, 10, and 20 Hz. These rates are equivalent to 10, 20, and 40 samples in the one second interval. For the Nyquist frequency of 5 Hz, the error is nearly 75% at 4 Hz or 80% of the corner frequency.

Figure 24 shows the shock spectrum error for the impulse-invariant technique for the same Nyquist rates. A surprising result has occurred, the shock spectrum error is less than or equal to the Fourier spectrum error for each of the rates. The reduction which results from poor sampling of the output has compensated for some of the aliasing error. Therefore improving the peak detection using the modified z-transform or interpolation formula actually reduces the accuracy of the result for this function.

The Fourier spectrum error for the half-sine pulse using O'Hara's technique is shown in Figure 25. The error is not as well behaved as it is with the impulse-invariant method, but the error is considerably less than with impulse-invariant methods. The error for the Nyquist rate of 5 Hz, using O'Hara's technique, Figure 25, is very nearly equal to the error in the impulse-invariant technique, Figure 23, for a Nyquist rate of 20 Hz. This would indicate that the O'Hara method can achieve equivalent results with one fourth as many samples. The O'Hara method appears more accurate by several orders of magnitude near the Nyquist rate.

The shock spectrum error for the O'Hara method with the half-sine acceleration input is shown in Figure 26. The error appears to oscillate around the Fourier spectrum error for the same Nyquist rates. This would imply that the accuracy can be improved or made more nearly equal to the Fourier spectrum error by use of interpolation. The error analysis for the full-sine input is shown in Figures 27, 28, 29, and 30. The results are comparable to those of the half-sine case when intuitively it might be expected that the error would be greater than that of the half-sine because the sampling rate is effectively half that of the half-sine. The inverted parabola input was chosen in order to separate the integration and sampling errors. The Fourier-spectrum error using the O'Hara technique gave less than 0.01% error for this function as might be expected. The Fourier-spectrum error using the impulse-invariant technique is shown

in Figure 31 and the shock-spectrum error with this same technique is shown in Figure 32. The shock-spectrum error for this input and the O'Hara technique is shown in Figure 33. The errors associated with the decaying sinusoid are shown in Figures 34, 35, 36, and 37. The errors for the combined decaying sinusoids are shown in Figures 38, 39, 40, and 41.

Inspection of the error analysis figure yields an interesting result. The errors for all of the acceleration inputs are nearly equal. This is because the inputs selected have Fourier spectra which roll-off at the $1/\omega^2$ rate. The derivation of Appendix B indicates that the error at some frequency in the spectrum is a function of the roll-off rate of the true spectrum and the Nyquist rate. If the transient has been sampled above the dominant frequencies of the Fourier spectrum the error is predictable, based on the roll-off rate. For greater roll-off rates, the error would be reduced (Appendix B). This is intuitively correct since the band-limited model becomes more accurate with higher roll-off rates.

CHAPTER V

CONCLUSIONS AND FUTURE WORK

It has been shown that both general purpose and special purpose analog computers can be used to compute the shock and Fourier spectra. References have indicated that the active RC network has several advantages of passive RLC network in the construction of special purpose computers.

The constant percentage or logarithmically distributed spectrum samples, as indicated by the damped sampling formula, can effectively reduce the computation time required for damped shock spectrum computed using either analog or digital techniques.

The z-transform technique for computing shock and Fourier spectra simultaneously proved to be faster than the O'Hara technique by factors of 5 to 1 for large numbers of data. The FFT routine which only generates the impulse-invariant Fourier spectrum proved to be many times faster than either the z-transform or the O'Hara techniques.

The results have indicated that for transients which roll-off at the $1/\omega^2$ rate, the O'Hara method can achieve accuracies which are comparable to an impulse-invariant technique with four times the sampling rate. The O'Hara method had errors in order of 5% near the corner frequency while the impulse-invariant technique had this accuracy

to only one-quarter of the corner frequency. The results have indicated that the accuracy of shock spectra computed using the O'Hara method could be improved using interpolation between the sampled response values. This was not, in general, true for the impulse-invariant techniques.

If the available sampling rate and storage is not a factor and only the Fourier spectrum is desired, the FFT appears to be the best method even if it requires sampling with a Nyquist frequency which is four times the frequency of interest to achieve accuracies of the same order of magnitude as the O'Hara method.

When both the Fourier and shock spectra are desired, the accuracy of the O'Hara method appears to make this the most favorable approach of the methods tested.

The study of digital techniques has been limited to the commonly accepted techniques of the impulse-invariant, z-transform and FFT, and the parabolic interpolation method of O'Hara. There are several other possible approaches to the problem of computing shock and Fourier spectra rapidly and accurately on digital computers. For example, higher order polynomials might increase accuracy to a greater extent than they increase computation time. The use of compensation or smoothing techniques in conjunction with the impulse-invariant techniques might make a considerable improvement in accuracy with a very small increase in the time required for computation. The accuracy of the impulse-invariant technique is a function of the roll-off

rate of the transient. This relationship could be studied further and possibly could lead to optimum compensation for various roll-off rates.

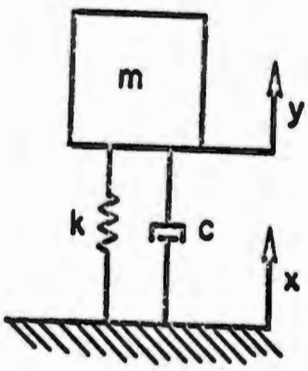

FIGURE 1A.

SINGLE-DEGREE-OF-FREEDOM SPRING MASS SYSTEM

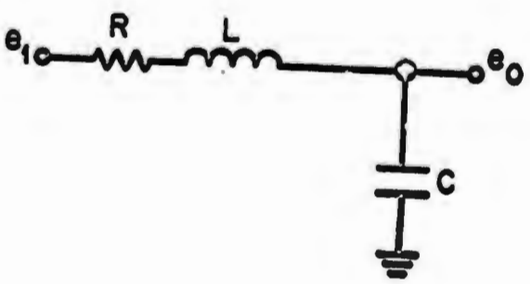

FIGURE 1B.

PASSIVE TWO-PORT RLC NETWORK

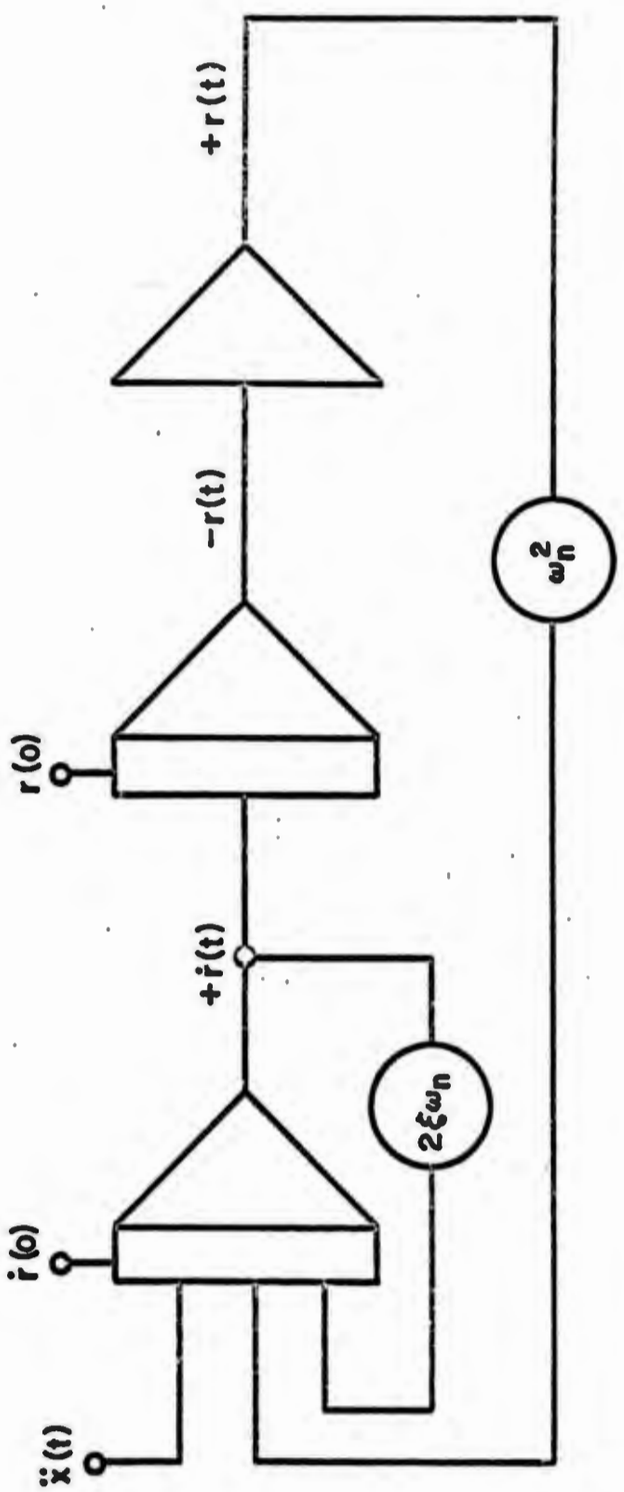

FIGURE 2.

ANALOG COMPUTER BLOCK DIAGRAM FOR COMPUTATION OF SHOCK AND FOURIER SPECTRA FROM ACCELERATION INPUTS

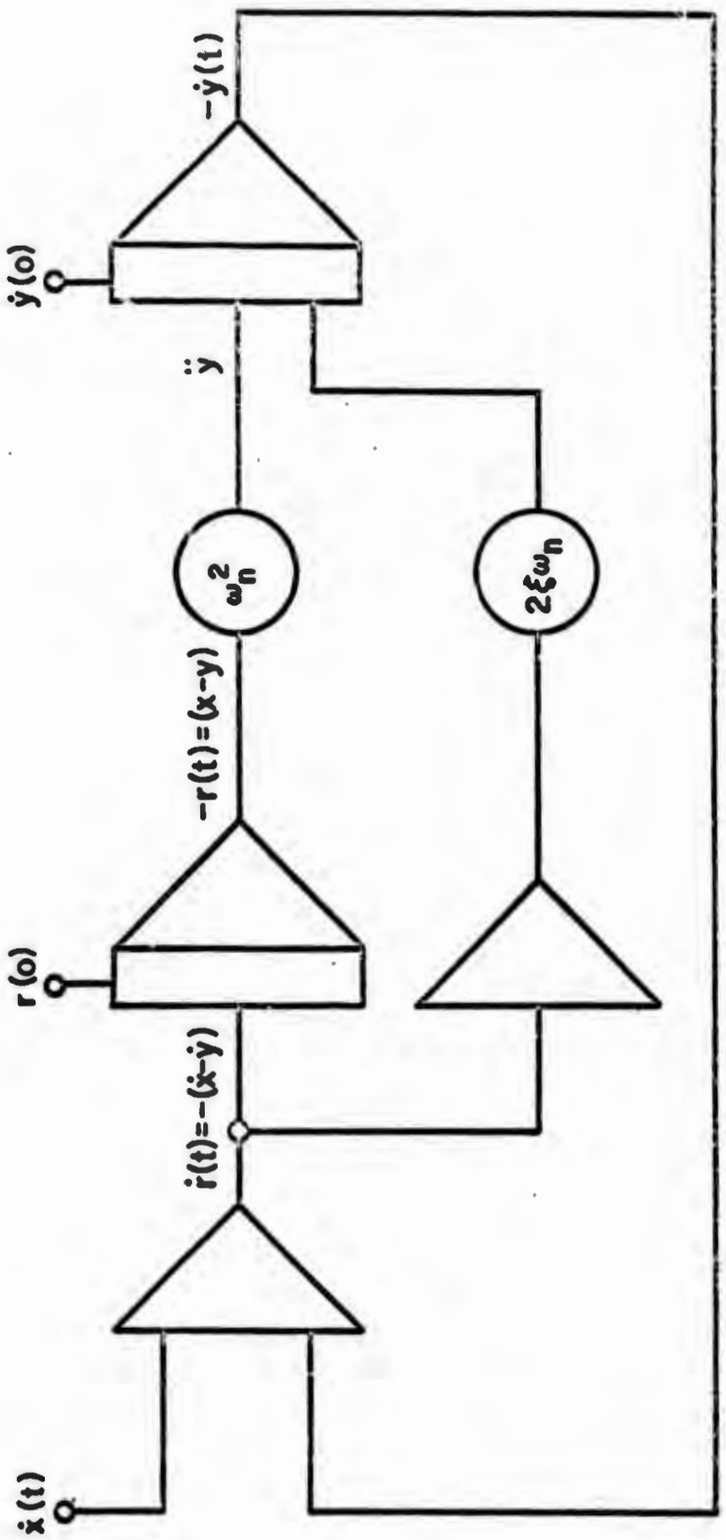

FIGURE 3.

ANALOG COMPUTER BLOCK DIAGRAM FOR COMPUTATION OF SHOCK AND FOURIER SPECTRA FROM VELOCITY INPUTS

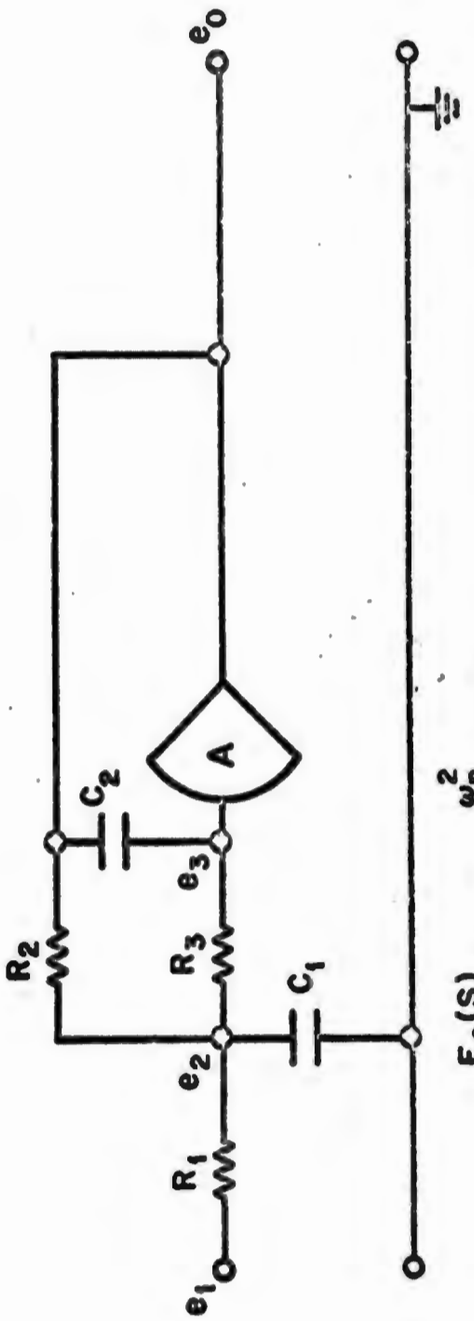

$$\frac{E_0(S)}{E_1(S)} = \frac{\omega_n^2}{S^2+2\xi\omega_n S+\omega_n^2}$$

$$R_1 = R_2 = \xi/\beta \quad R_3 = \xi/2\beta \quad C_1 = \frac{2\beta}{\xi^2\omega_n} \quad C_2 = \frac{\beta}{\omega_n}$$

FIGURE 4.

ACTIVE RC NETWORK FOR COMPUTATION OF SHOCK AND FOURIER SPECTRA FROM ACCELERATION INPUTS

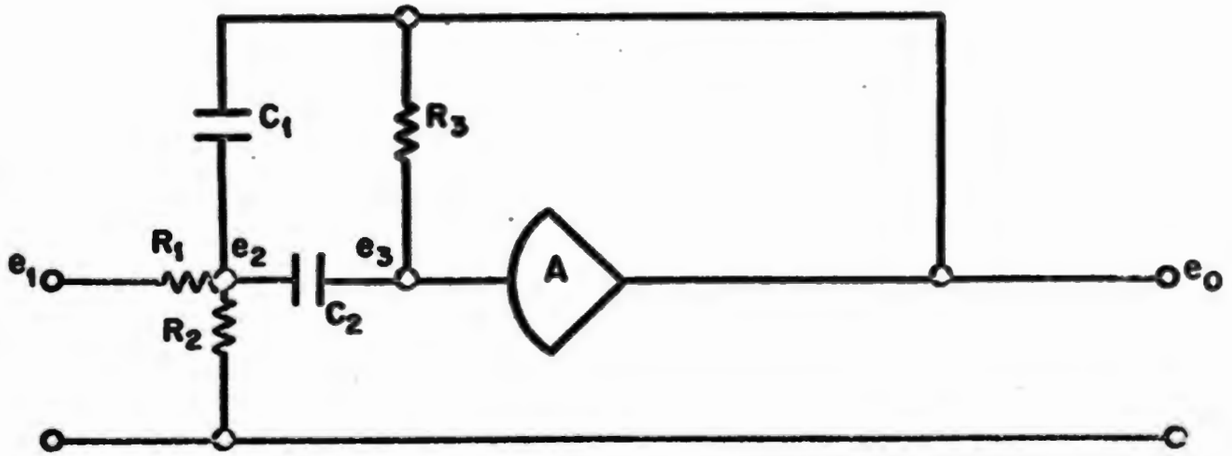

FOR A>>1

$$\frac{E_o}{E_i} = \frac{-\omega_o S}{S^2 + 2\xi\omega_n S + \omega_n^2}$$

$$C_2 = C_1 = C = \frac{\beta}{\omega_n} \qquad R_1 = \frac{1}{\beta} \qquad R_2 = \frac{\xi}{(1-\xi)\beta} \qquad R_3 = \frac{1}{\xi\beta}$$

FIGURE 5

ACTIVE RC NETWORK FOR COMPUTATION OF SHOCK AND FOURIER SPECTRA FROM VELOCITY INPUTS

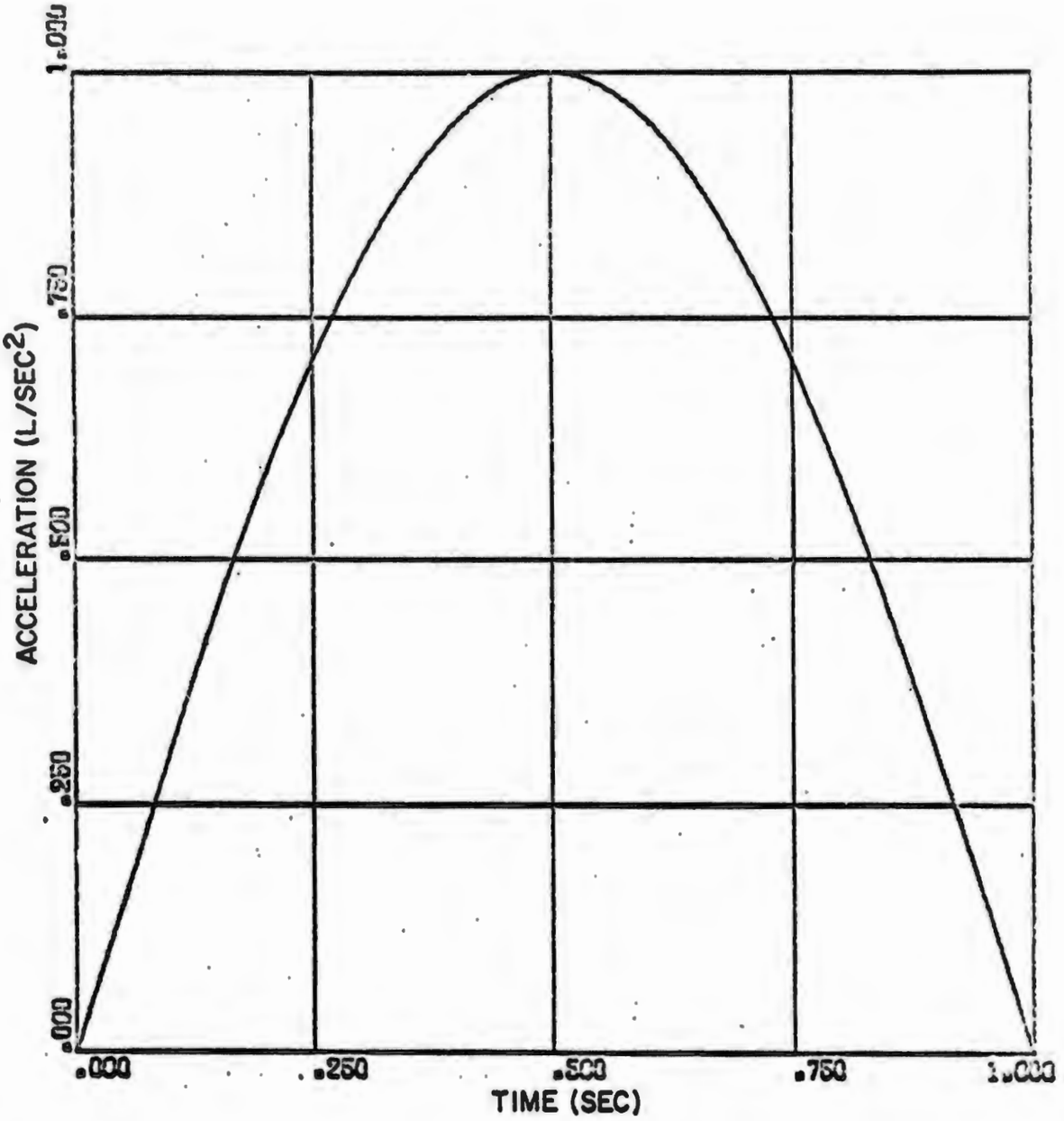

FIGURE 6.

HALF-SINE ACCELERATION INPUT FUNCTION

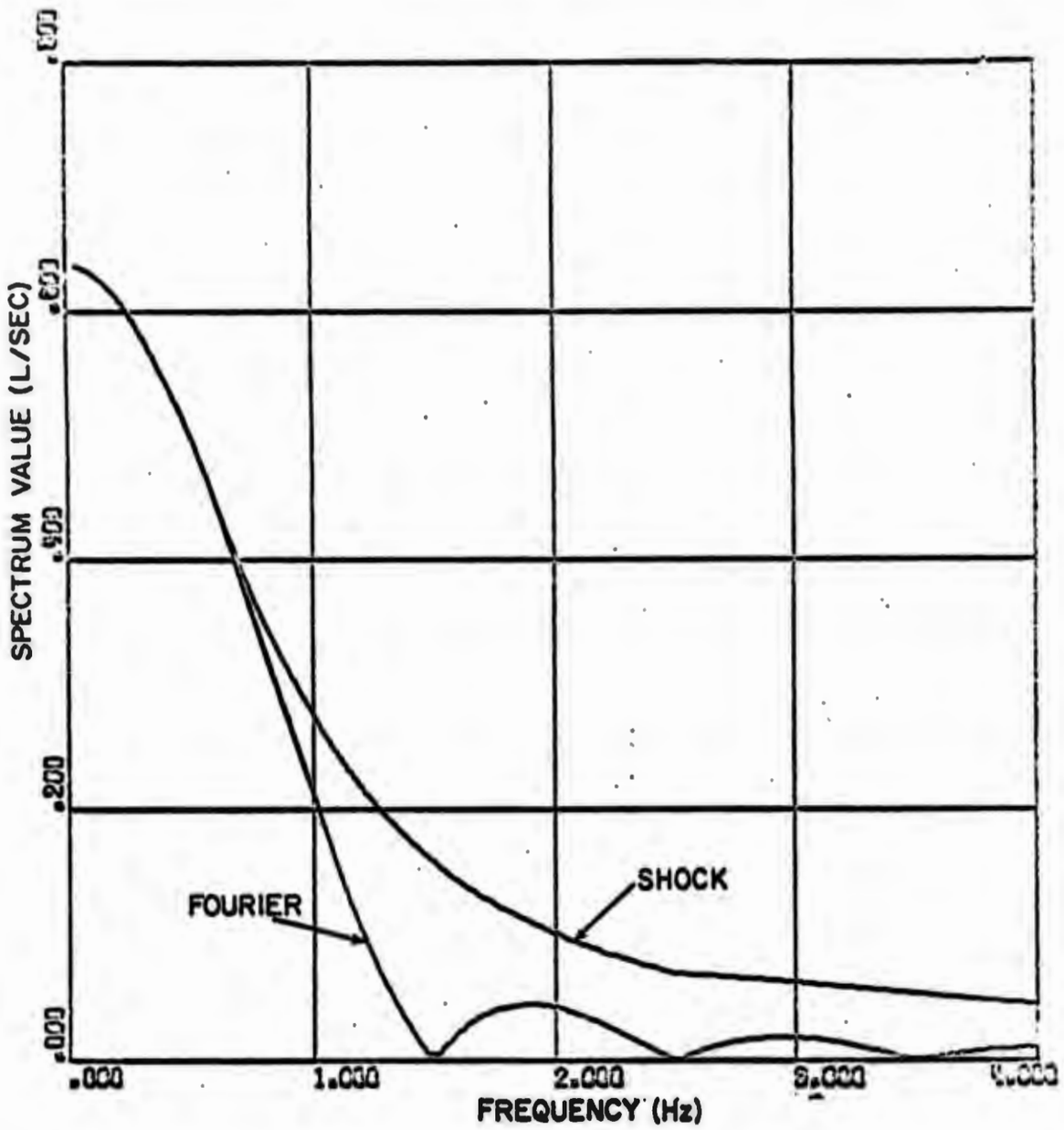

FIGURE 7.

FOURIER SPECTRUM AND UNDAMPED VELOCITY SHOCK SPECTRUM FOR HALF-SINE ACCELERATION INPUT COMPUTED USING A NYQUIST RATE OF 500 HZ AND THE O'HARA TECHNIQUE

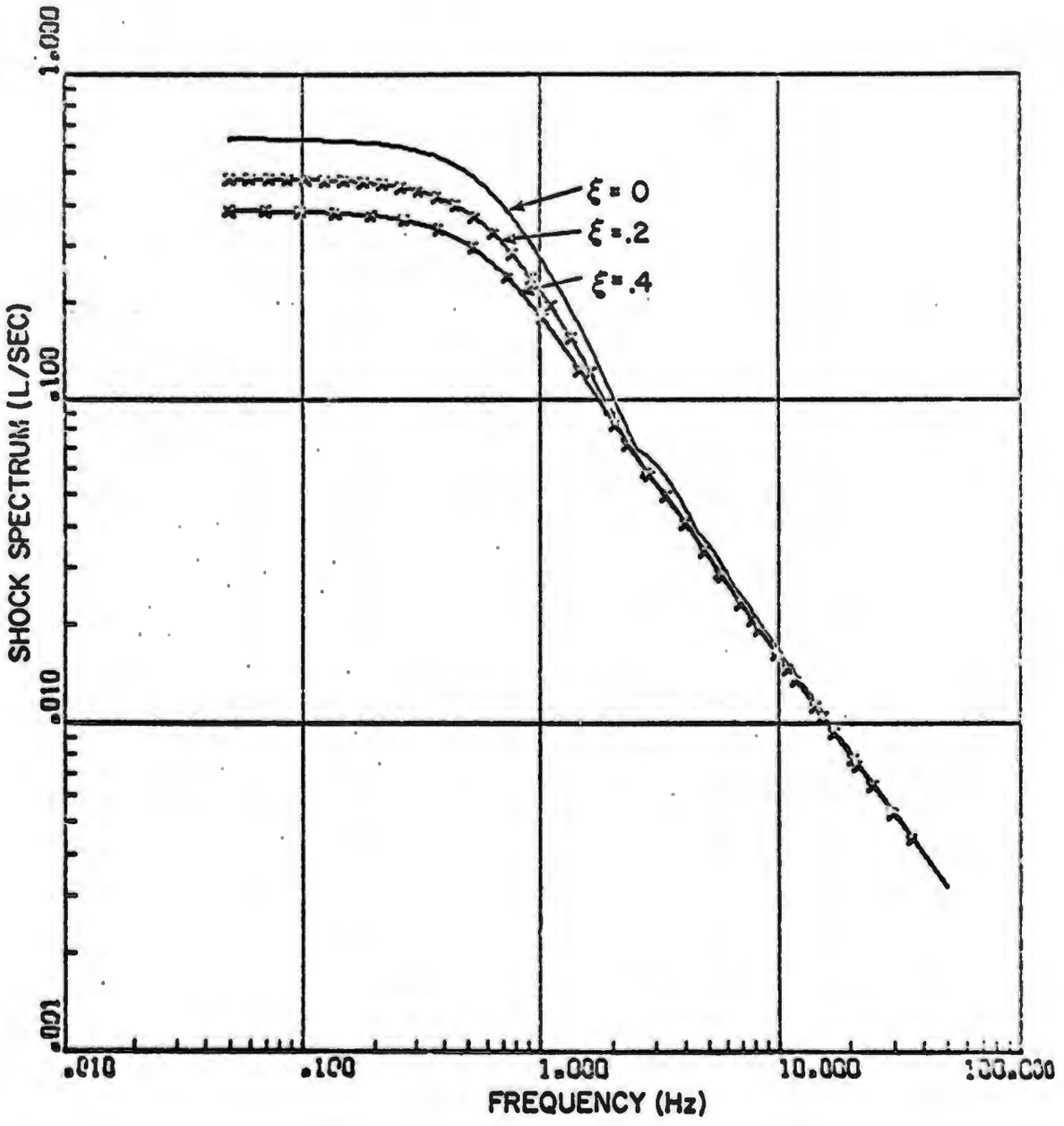

FIGURE 8.

UNDAMPED CONSTANT FREQUENCY INCREMENT VELOCITY SHOCK SPECTRUM AND DAMPED CONSTANT PERCENTAGE VELOCITY SHOCK SPECTRUM FOR HALF-SINE INPUT COMPUTED USING A NYQUIST RATE OF 500 HZ AND THE O'HARA TECHNIQUE

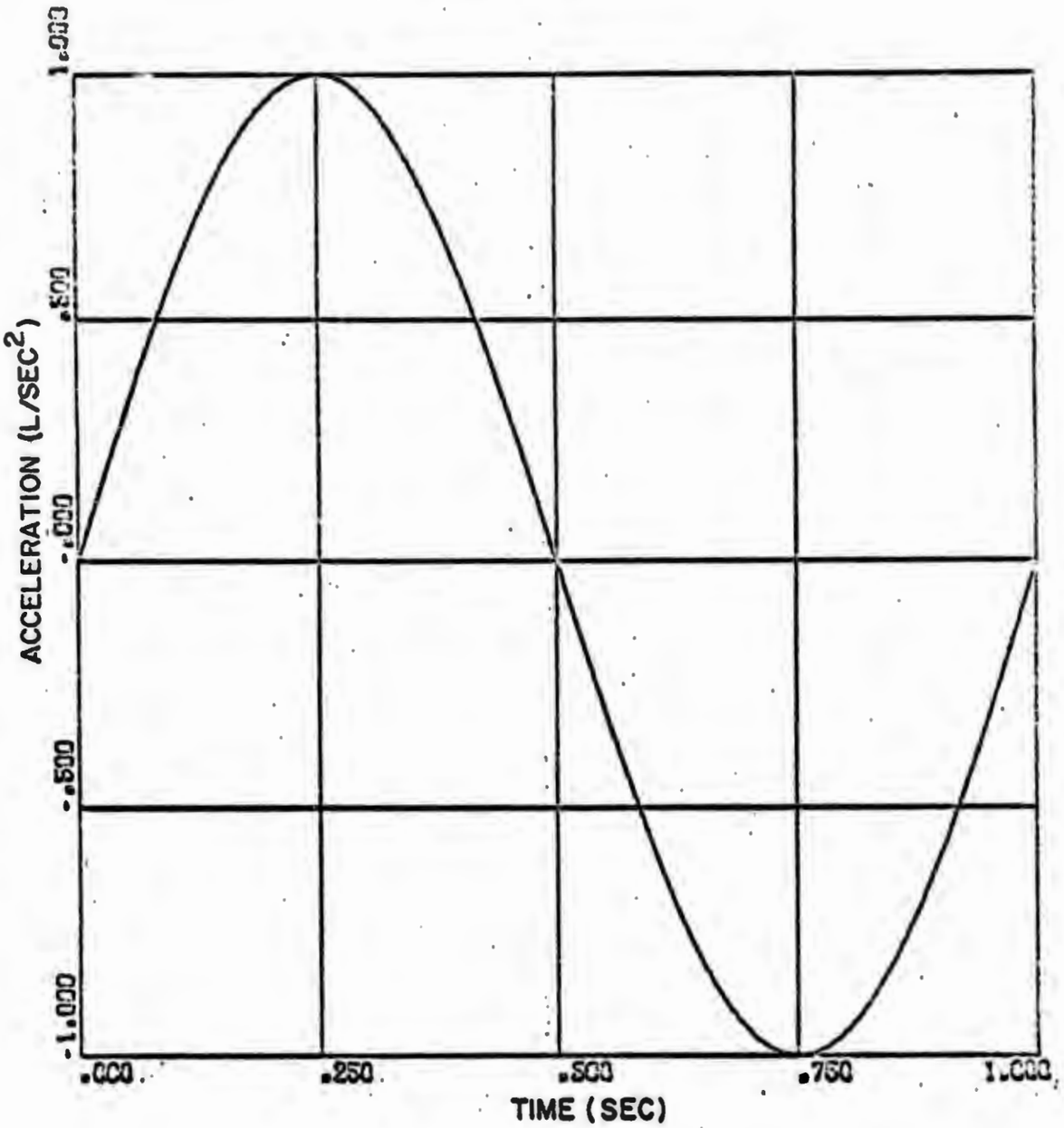

FIGURE 9.

FULL-SINE ACCELERATION INPUT FUNCTION

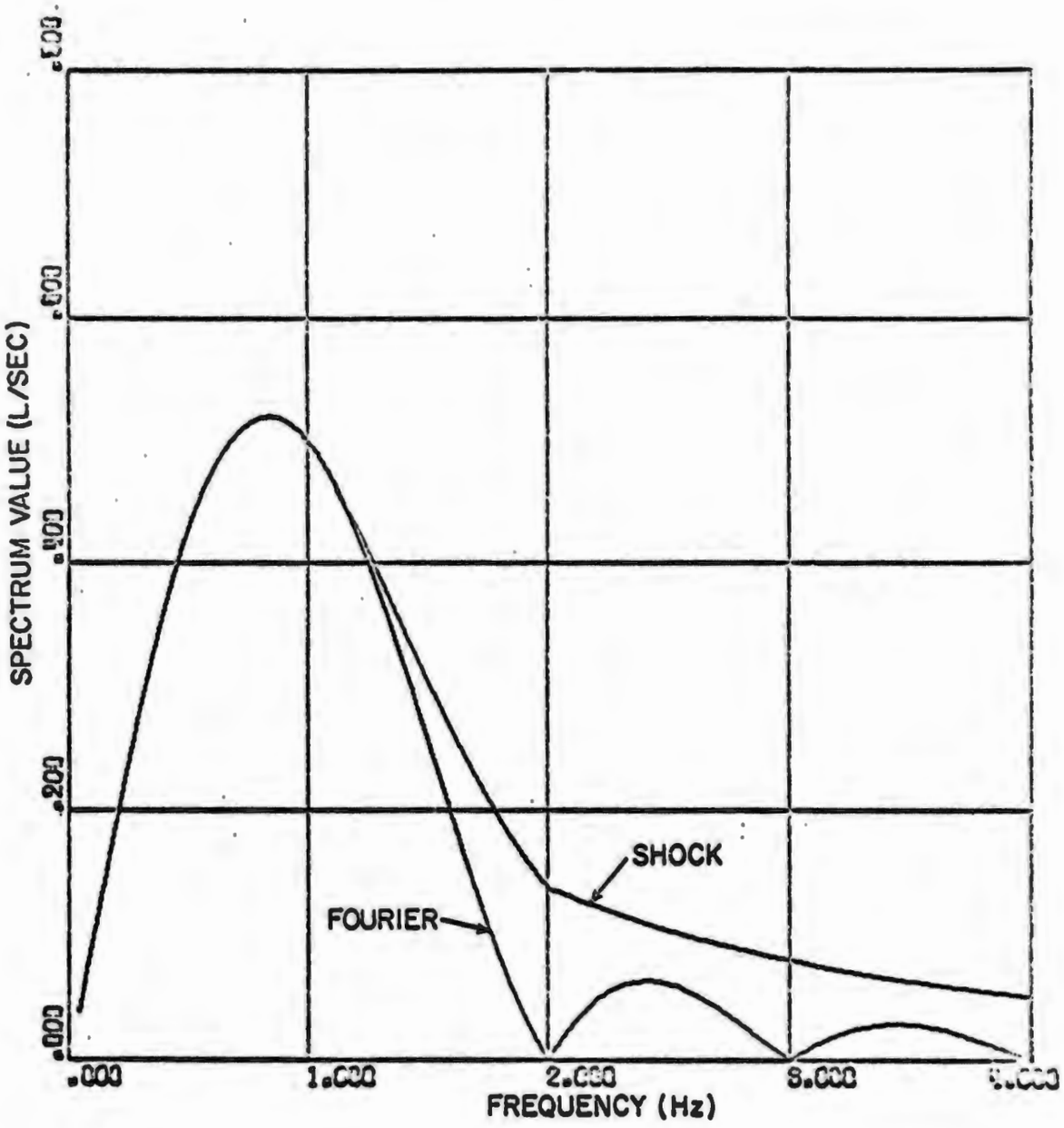

FIGURE 10.

FOURIER SPECTRUM AND UNDAMPED VELOCITY SHOCK SPECTRUM FOR FULL-SINE ACCELERATION INPUT COMPUTED USING A NYQUIST RATE OF 500 HZ AND THE O'HARA TECHNIQUE

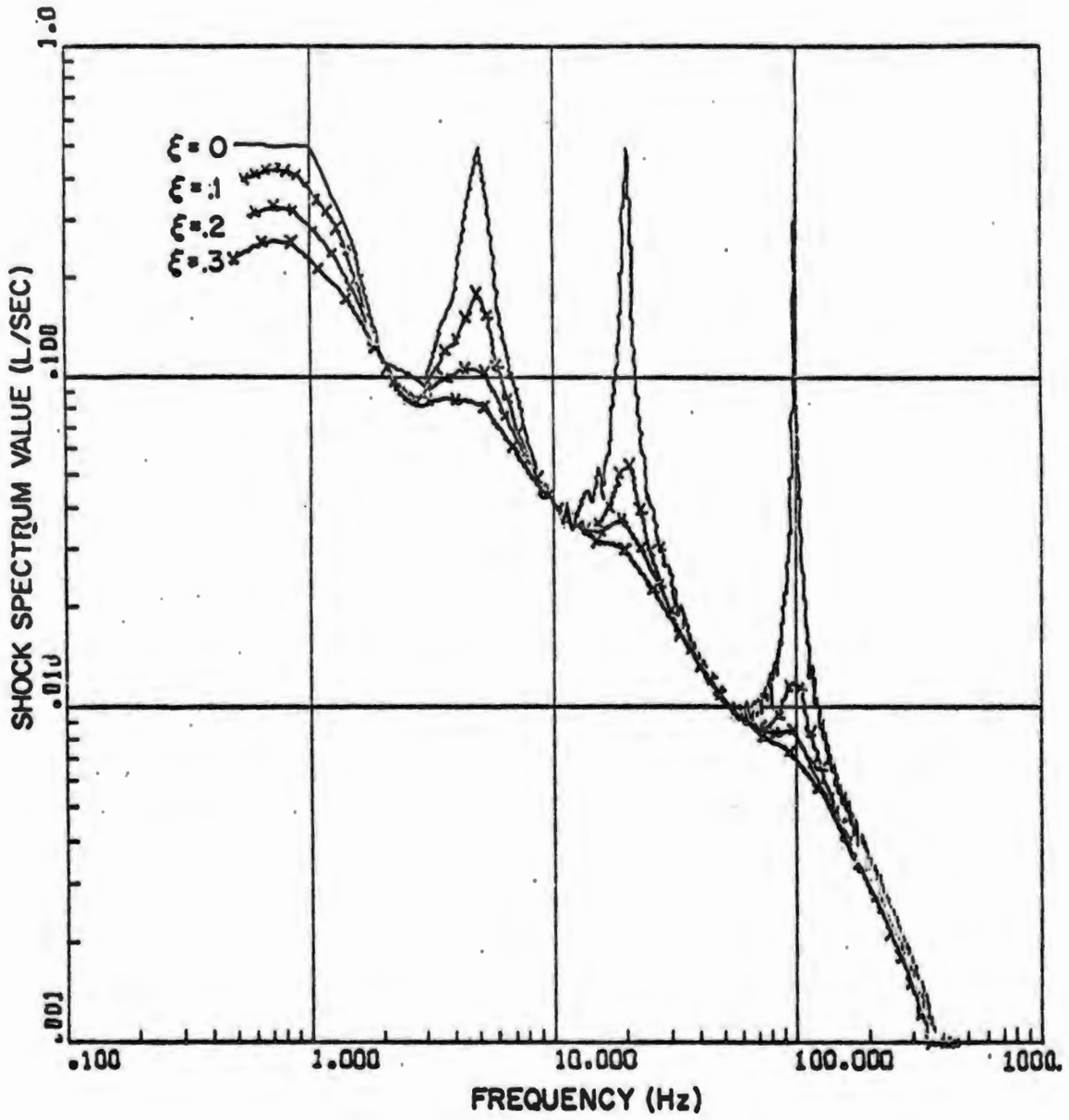

FIGURE 11.

UNDAMPED CONSTANT FREQUENCY INCREMENT VELOCITY SHOCK SPECTRUM AND DAMPED CONSTANT PERCENTAGE VELOCITY SHOCK SPECTRUM FOR COMBINED SINUSOID INPUT COMPUTED USING A NYQUIST RATE OF 500 HZ AND THE O'HARA TECHNIQUE

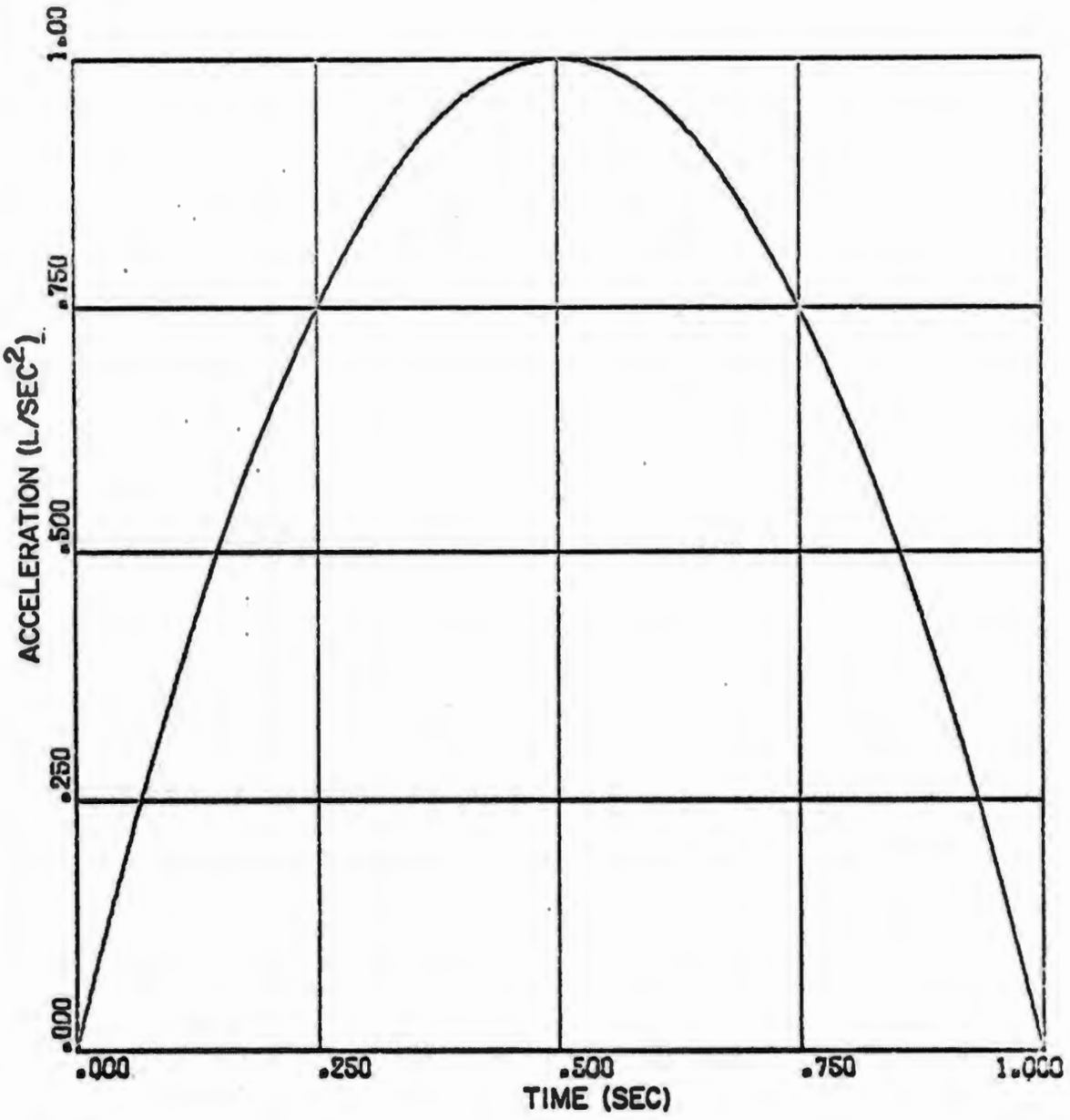

FIGURE 12.

INVERTED PARABOLA INPUT FUNCTION

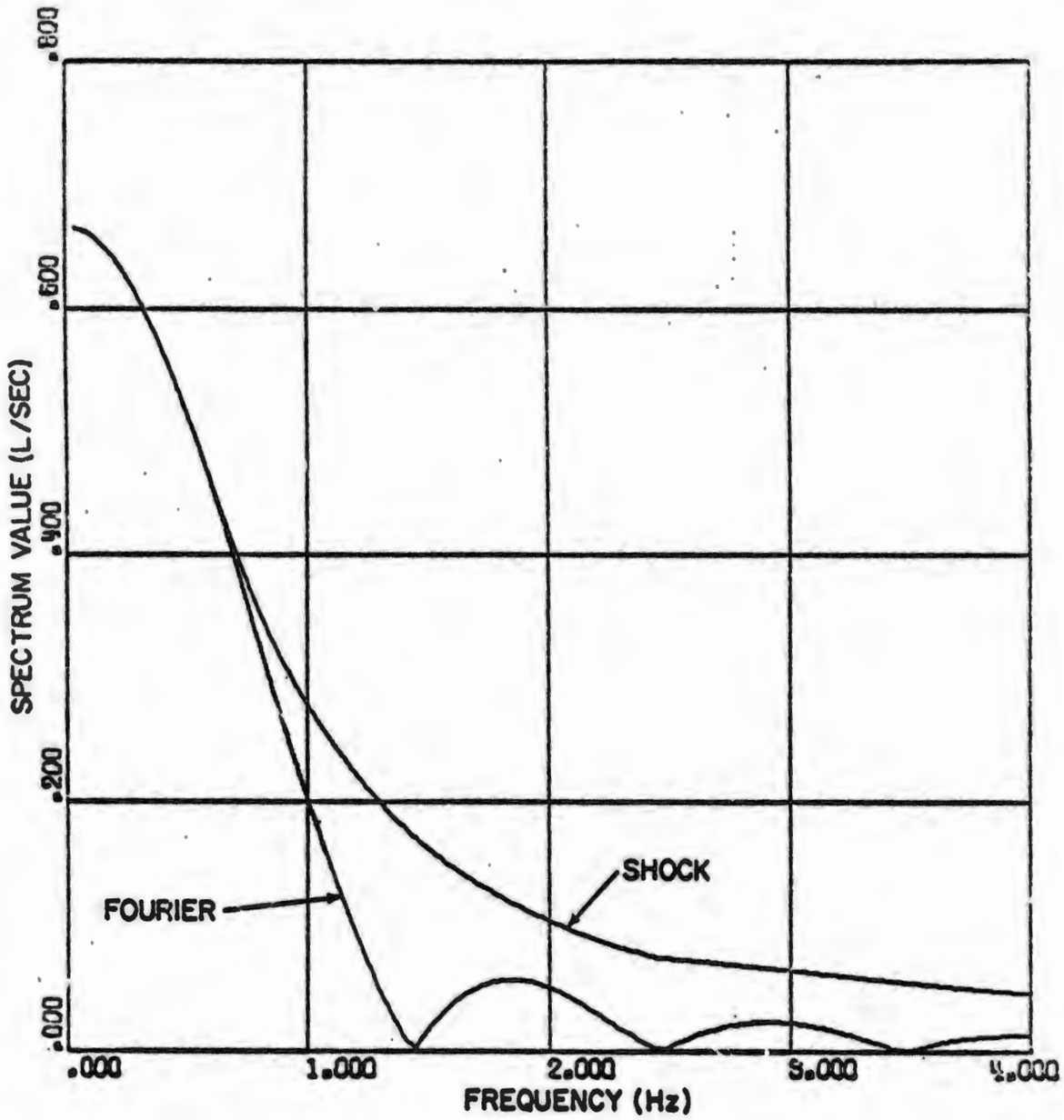

FIGURE 13.

FOURIER SPECTRUM AND UNDAMPED VELOCITY SHOCK SPECTRUM FOR INVERTED PARABOLA INPUT COMPUTED USING A NYQUIST RATE OF 500 HZ AND THE O'HARA TECHNIQUE

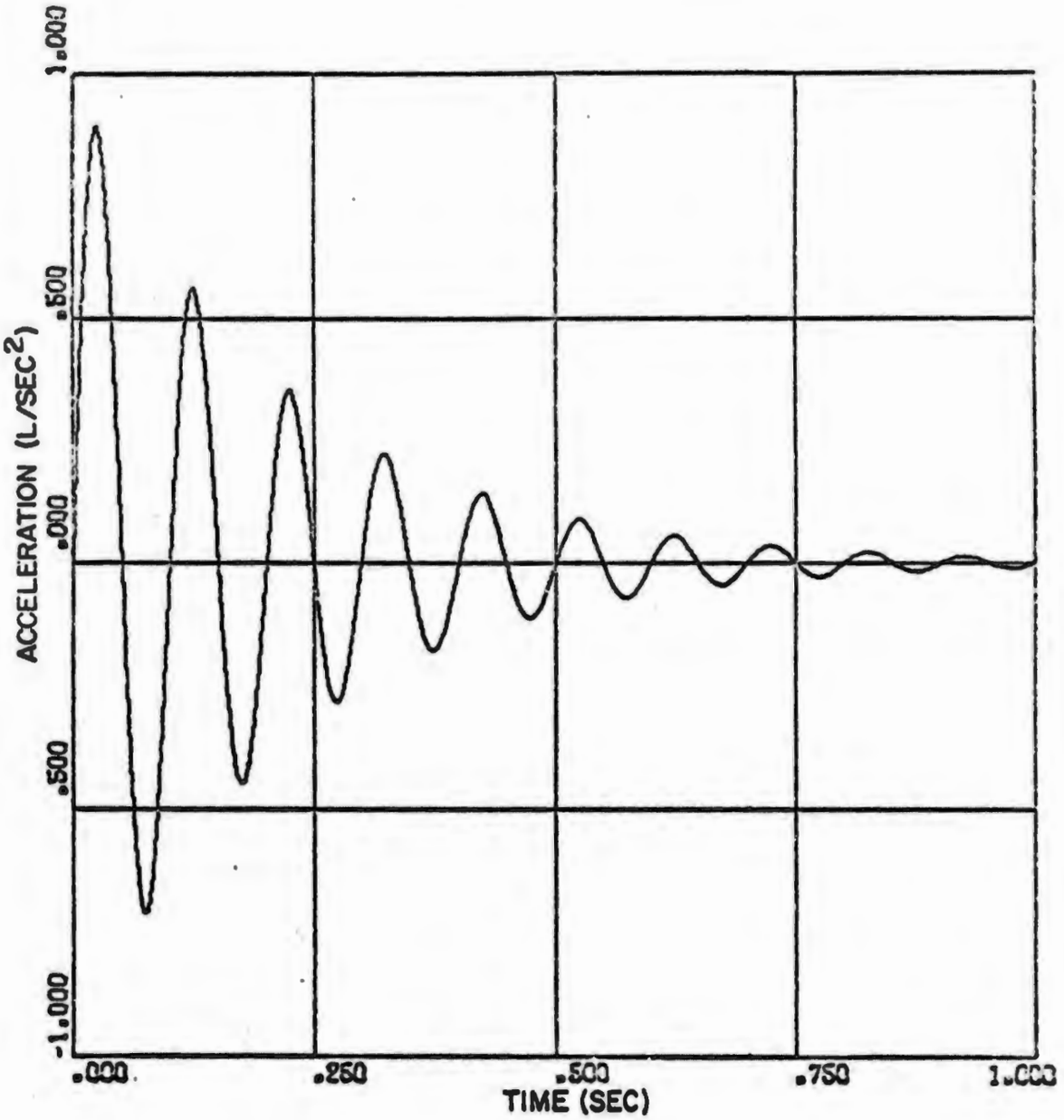

FIGURE 14.

DECAYING SINUSOID INPUT FUNCTION

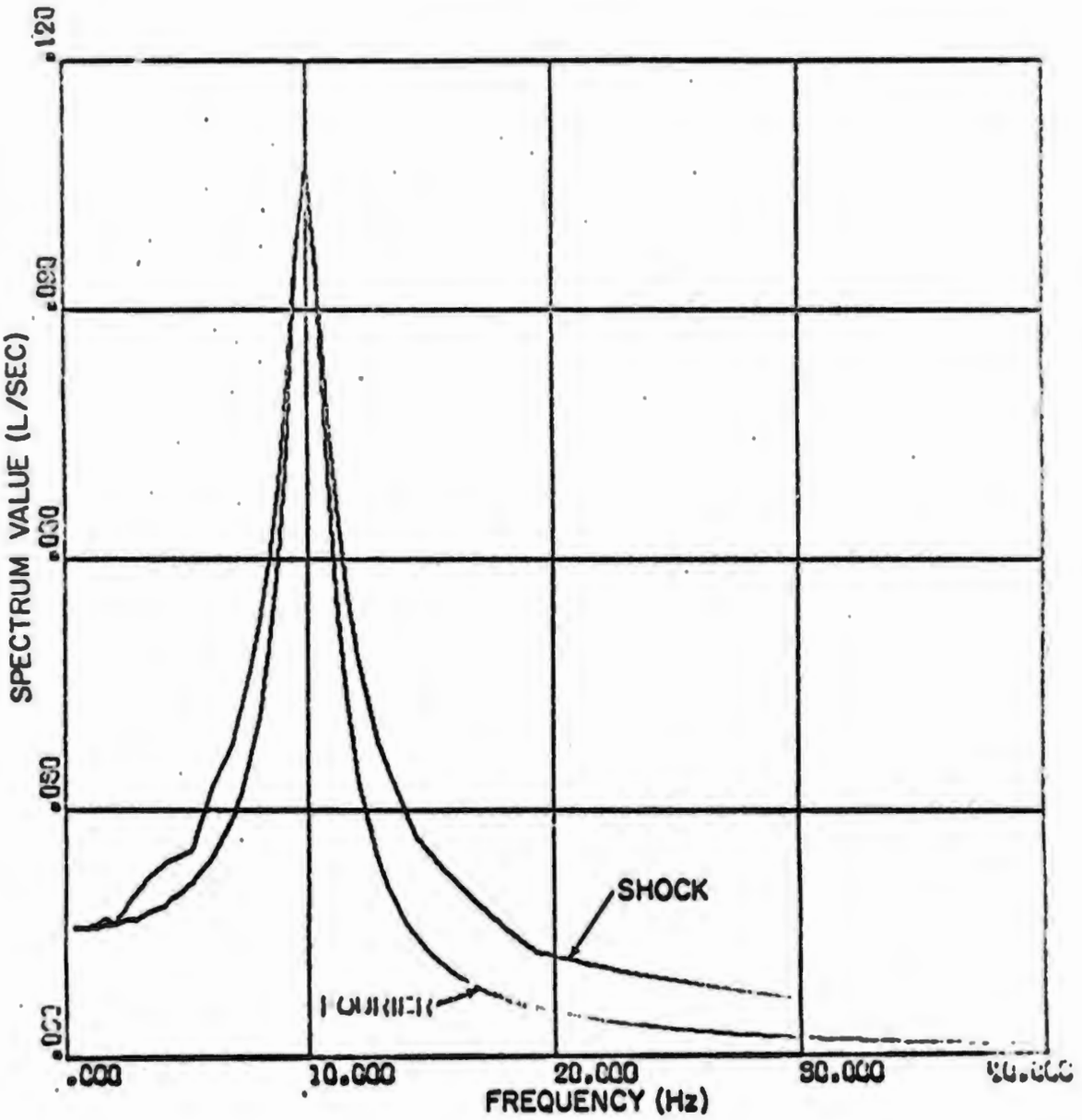

FIGURE 15.

FOURIER SPECTRUM AND UNDAMPED VELOCITY SHOCK SPECTRUM FOR DECAYING SINUSOID ACCELERATION INPUT COMPUTED USING A NYQUIST RATE OF 500 HZ AND THE O'HARA TECHNIQUE

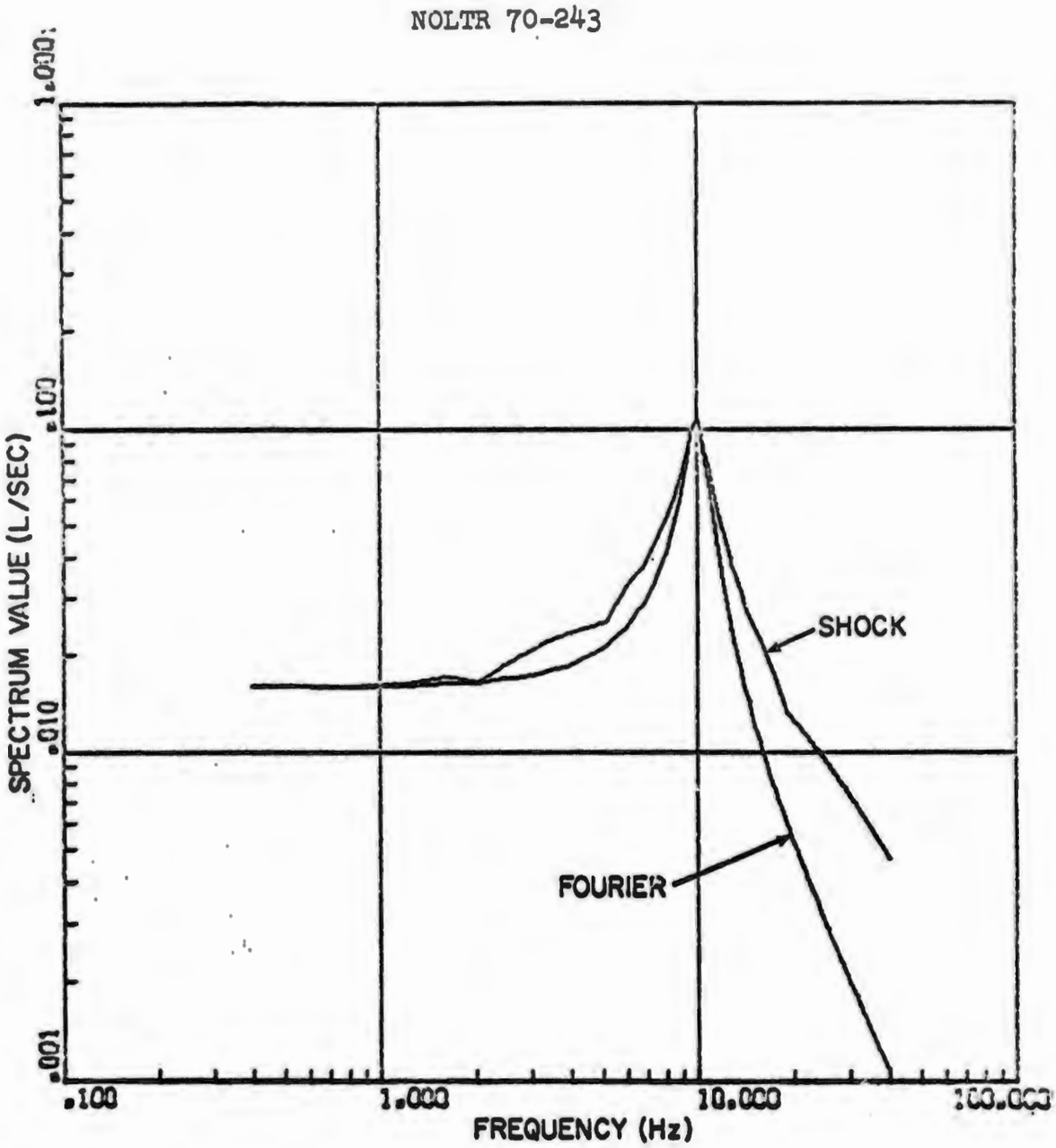

FIGURE 16.

LOG-LOG DISPLAY OF FOURIER AND UNDAMPED VELOCITY SHOCK SPECTRUM FOR DECAYING SINUSOID ACCELERATION INPUT COMPUTED USING A NYQUIST RATE OF 500 HZ AND THE O'HARA TECHNIQUE

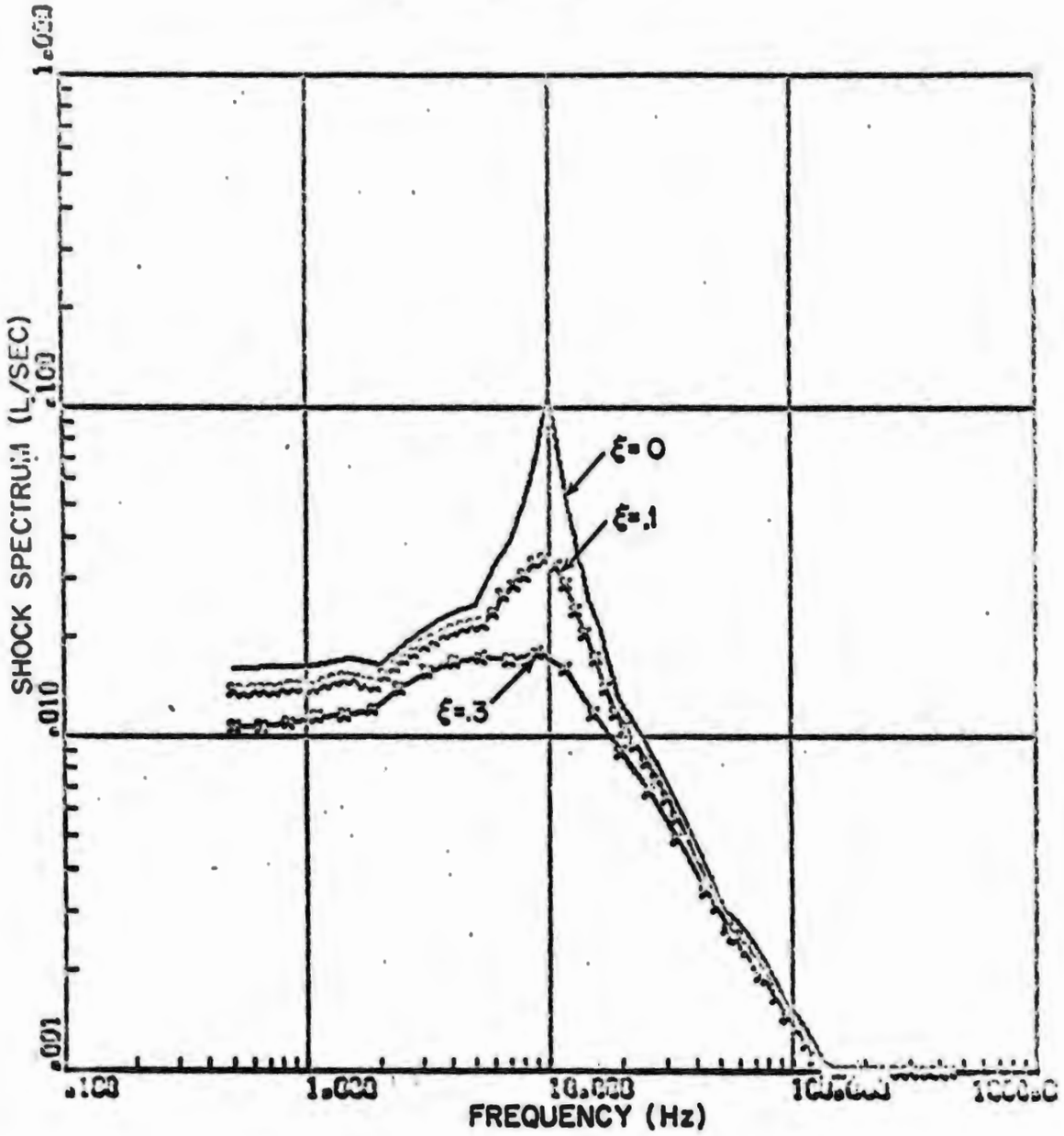

FIGURE 17.

UNDAMPED CONSTANT FREQUENCY INCREMENT VELOCITY SHOCK SPECTRUM AND DAMPED CONSTANT PERCENTAGE VELOCITY SHOCK SPECTRUM FOR DECAYING SINUSOID INPUT ACCELERATION COMPUTED USING A NYQUIST RATE OF 500 HZ AND THE O'HARA TECHNIQUE

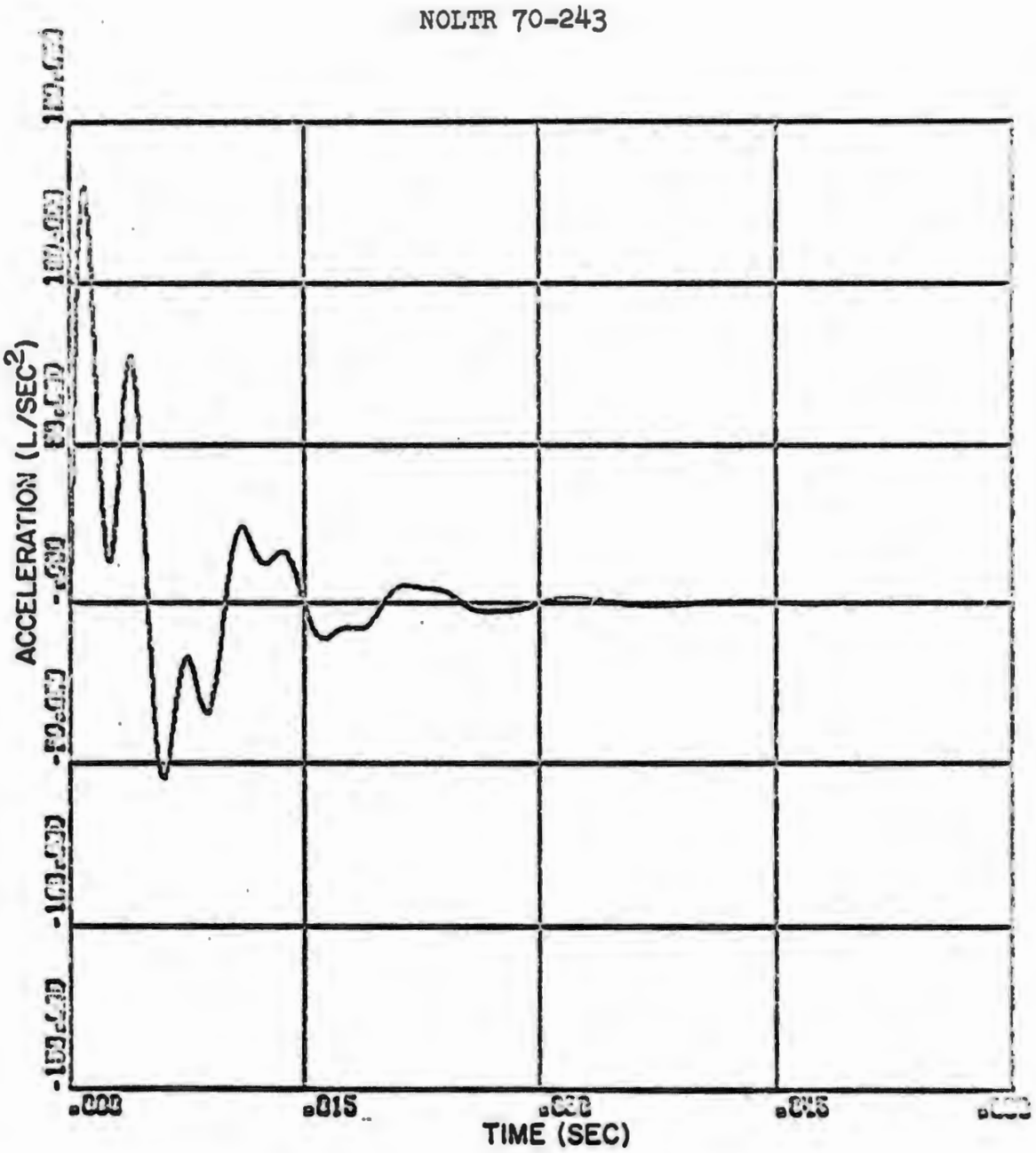

FIGURE 18.

COMBINED DECAYING SINUSOIDS ACCELERATION INPUT

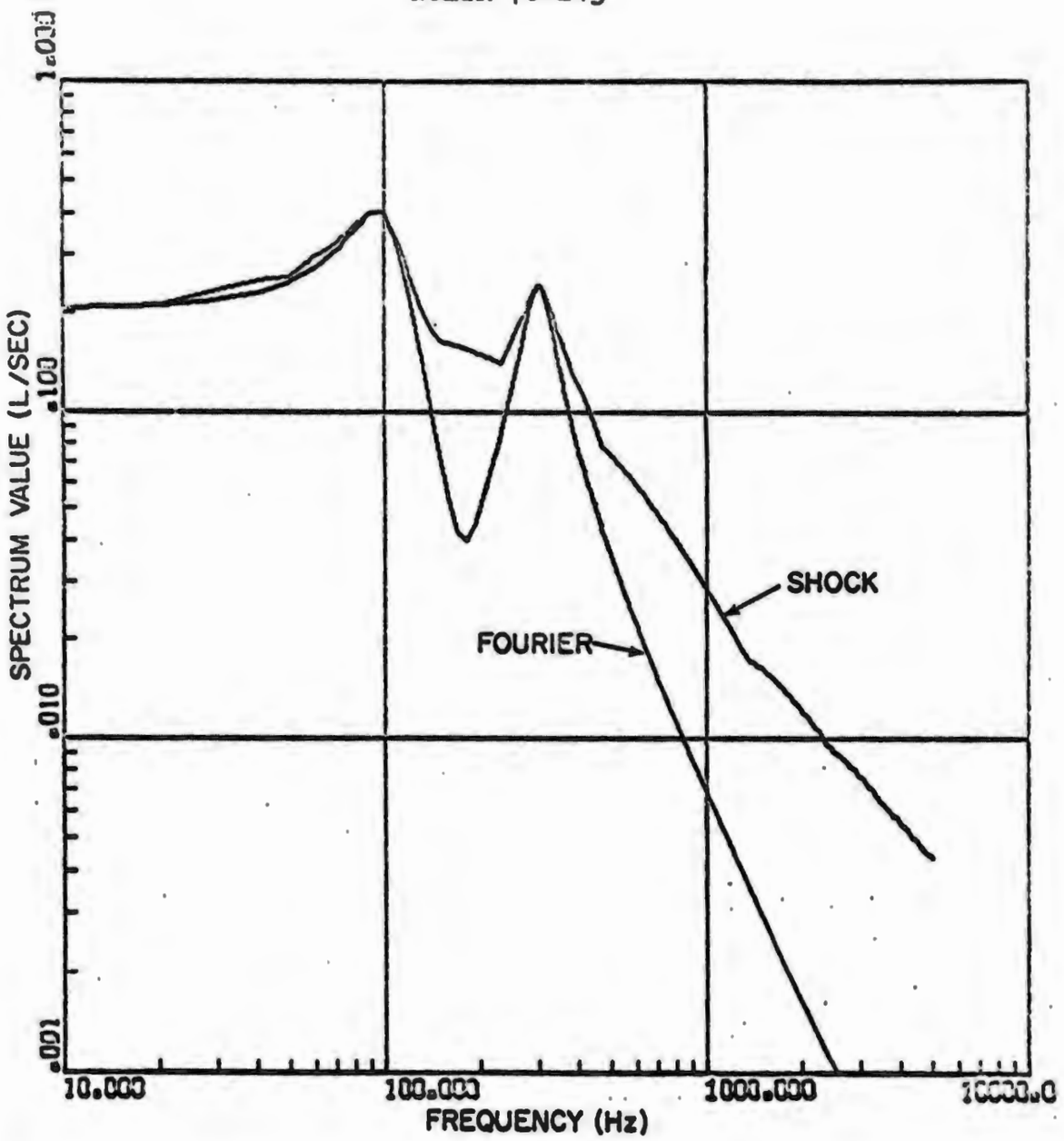

FIGURE 19.

LOG-LOG DISPLAY OF FOURIER SPECTRUM AND UNDAMPED VELOCITY SHOCK SPECTRUM FOR COMBINED DECAYING SINUSOIDS COMPUTED USING A NYQUIST RATE OF 5000 HZ AND THE O'HARA TECHNIQUE

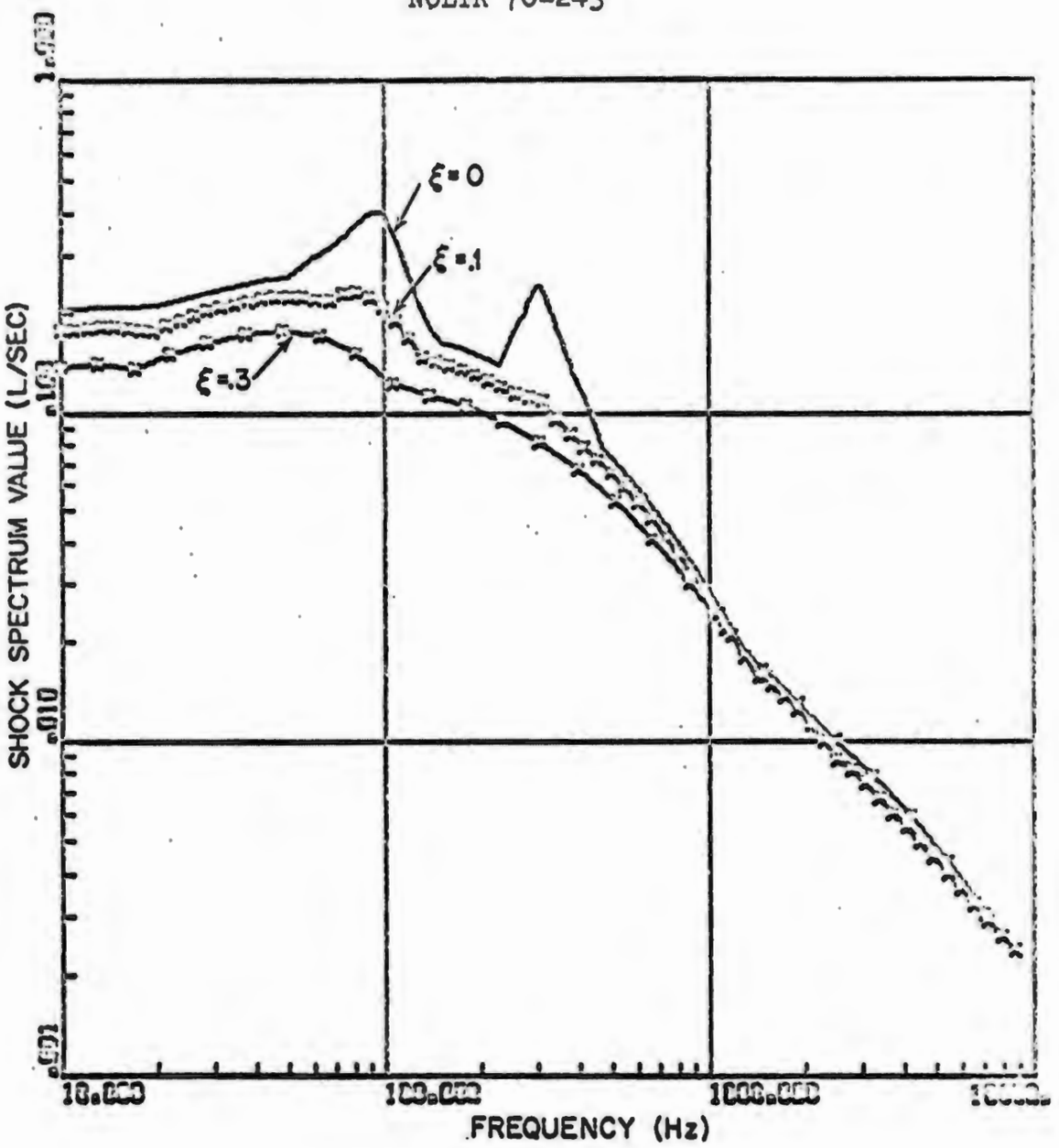

FIGURE 20.

UNDAMPED CONSTANT FREQUENCY INCREMENT VELOCITY SHOCK SPECTRUM AND DAMPED CONSTANT PERCENTAGE VELOCITY SHOCK SPECTRUM FOR COMBINED DECAYING SINUSOIDS COMPUTED USING A NYQUIST RATE OF 8333.3 HZ AND THE O'HARA TECHNIQUE

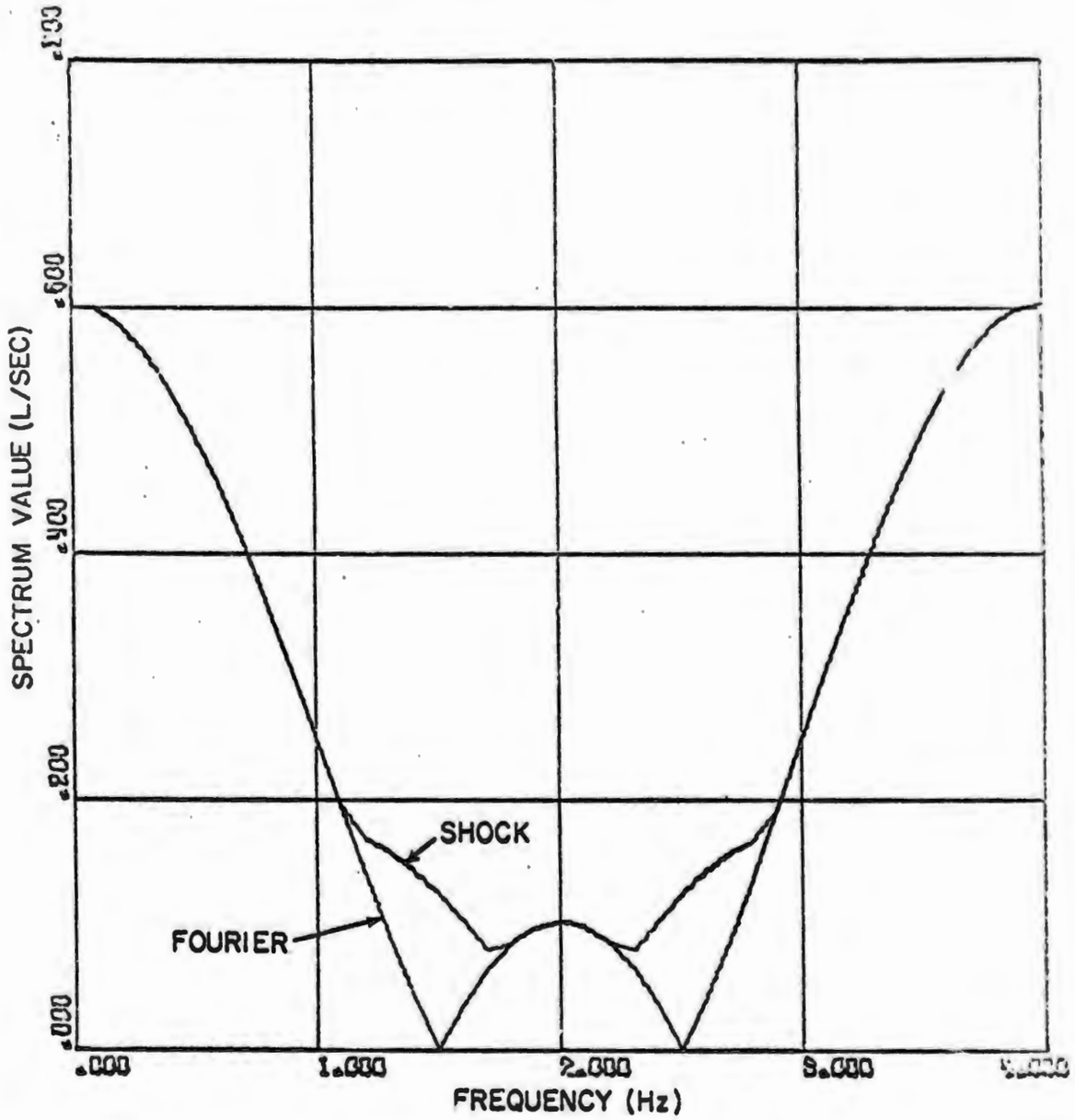

FIGURE 21.

FOURIER SPECTRUM AND UNDAMPED VELOCITY SHOCK SPECTRUM FOR HALF-SINE ACCELERATION INPUT COMPUTED USING A NYQUIST RATE OF 2 HZ

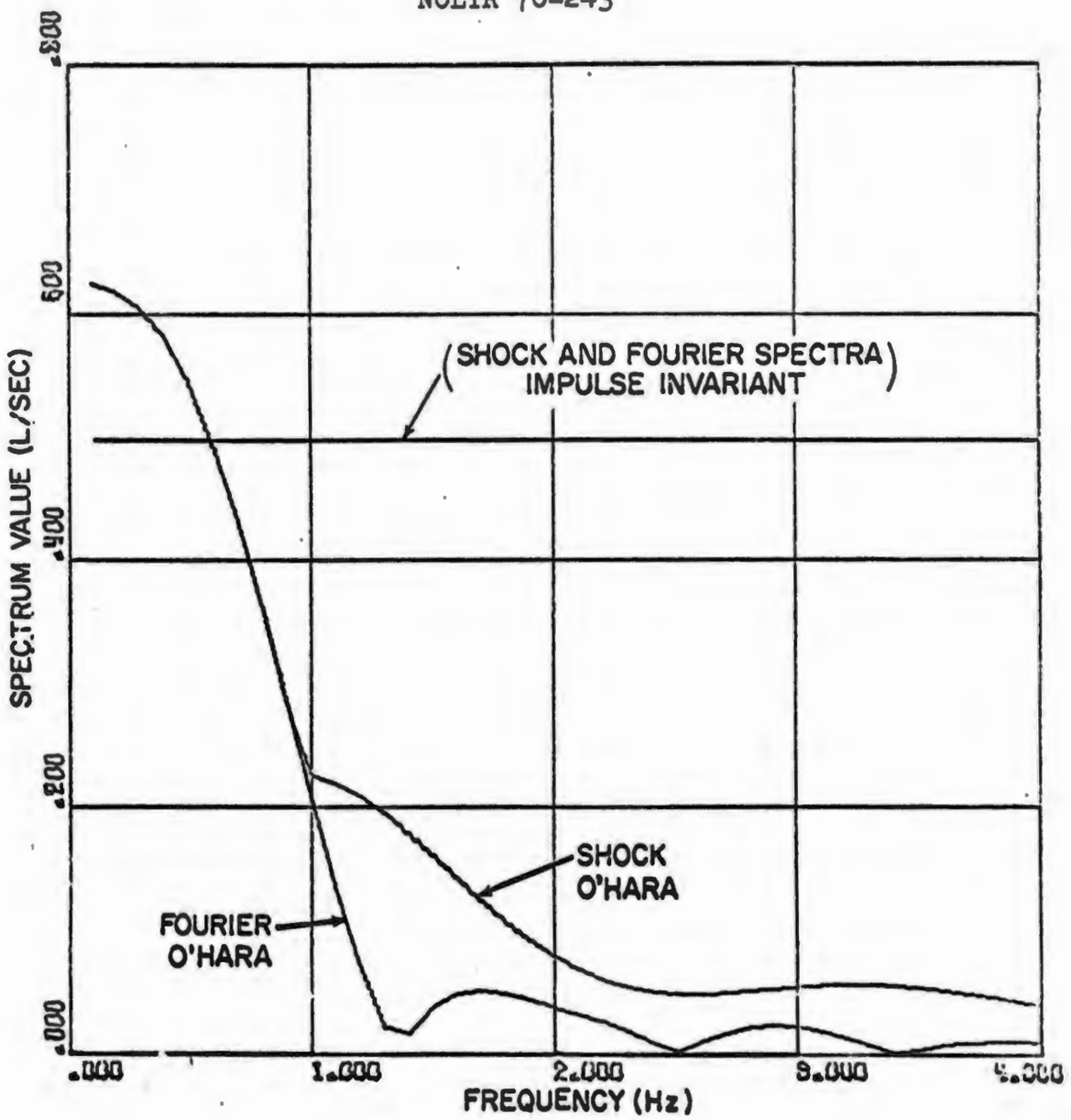

FIGURE 22.

FOURIER SPECTRUM AND UNDAMPED VELOCITY SHOCK SPECTRUM FOR THE HALF-SINE ACCELERATION INPUT COMPUTED WITH TWO SAMPLES OR A NYQUIST RATE OF 1 HZ, AND BOTH THE O'HARA AND IMPULSE INVARIANT TECHNIQUES

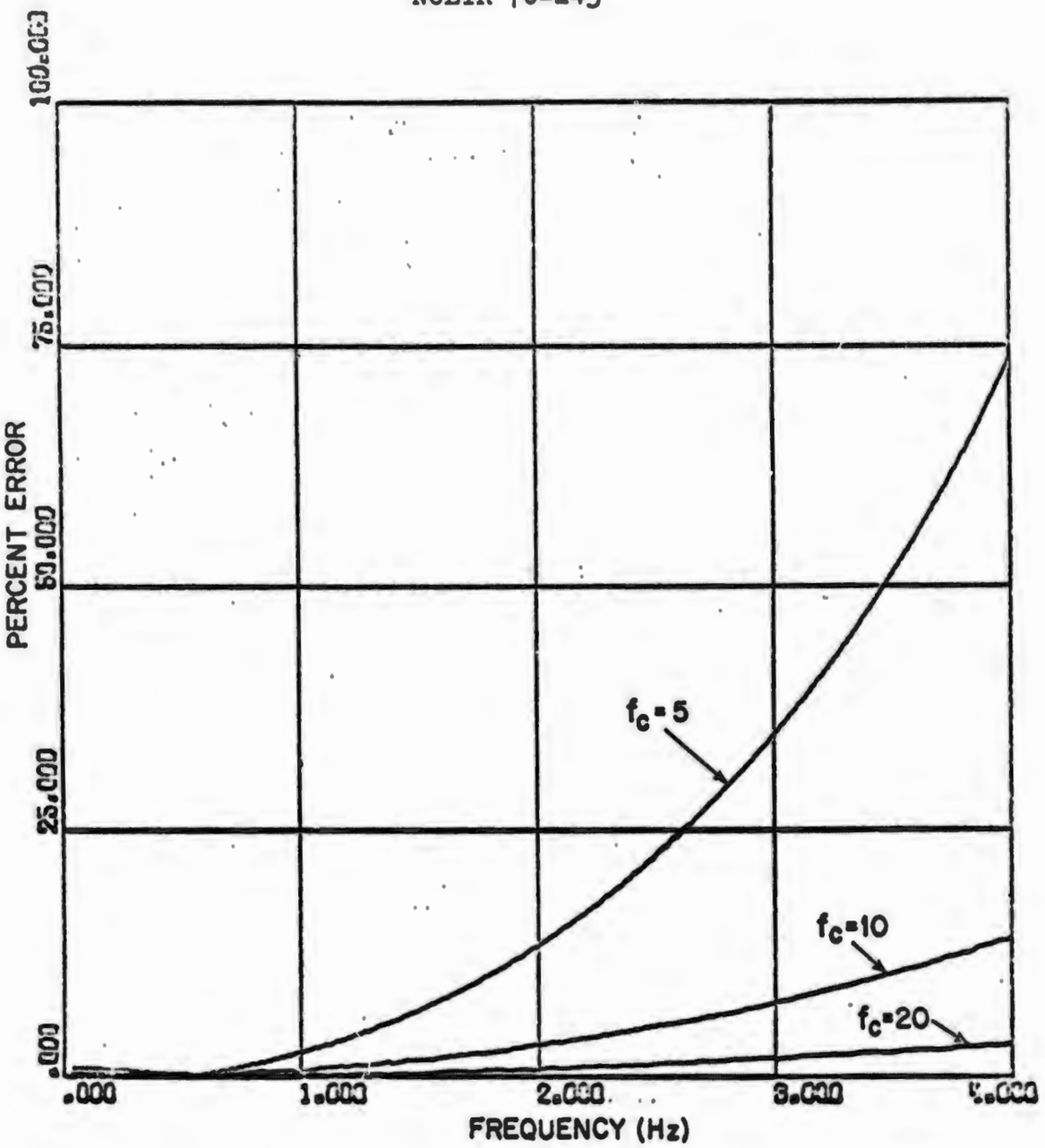

FIGURE 23.

FOURIER SPECTRUM ERROR VERSUS FREQUENCY FOR THE HALF-SINE ACCELERATION INPUT USING AN IMPULSE INVARIANT TECHNIQUE AND DIFFERENT NYQUIST RATES

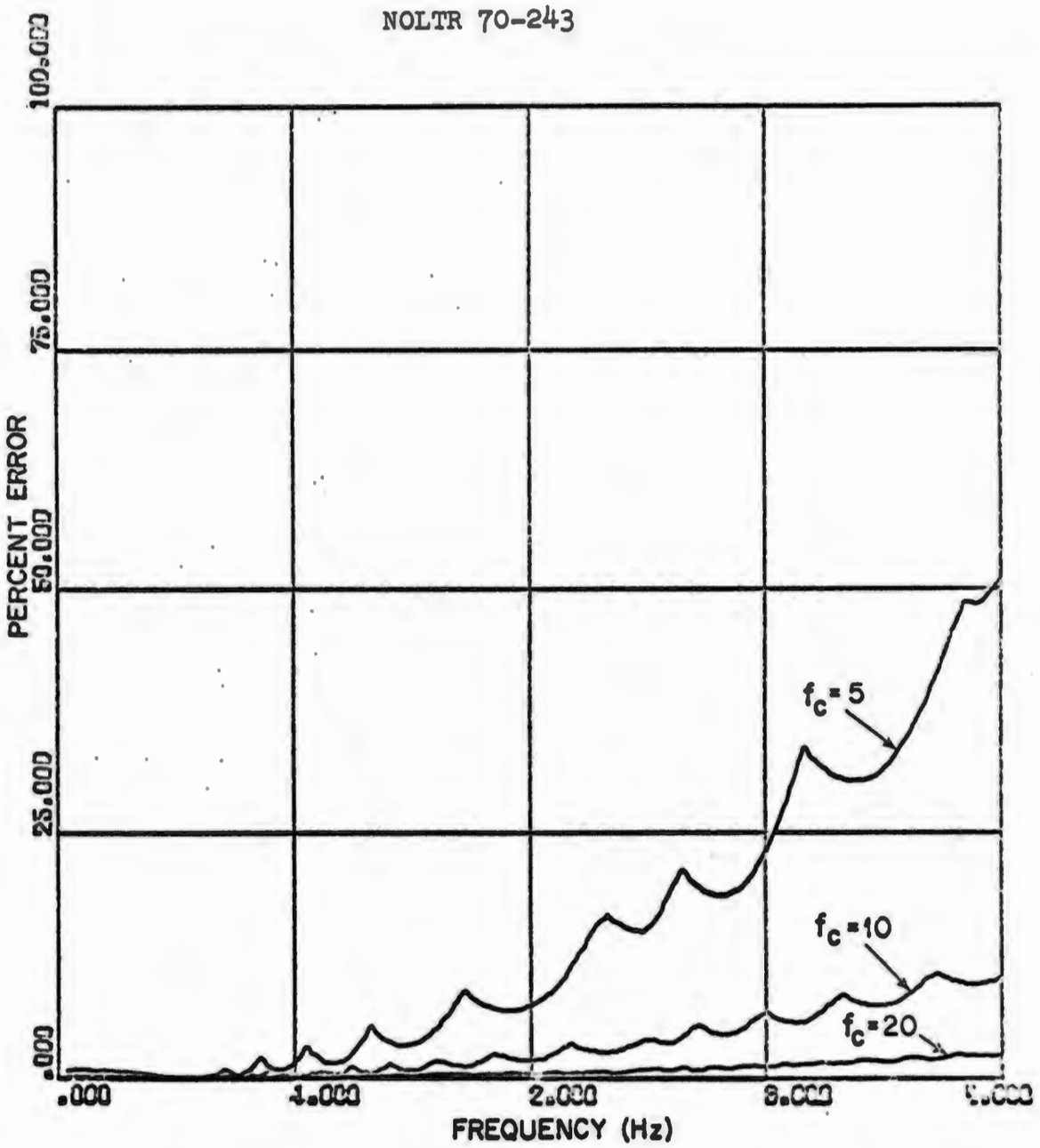

FIGURE 24.

VELOCITY SHOCK SPECTRUM ERROR VERSUS FREQUENCY FOR THE HALF-SINE ACCELERATION INPUT USING AN IMPULSE INVARIANT TECHNIQUE AND DIFFERENT NYQUIST RATES

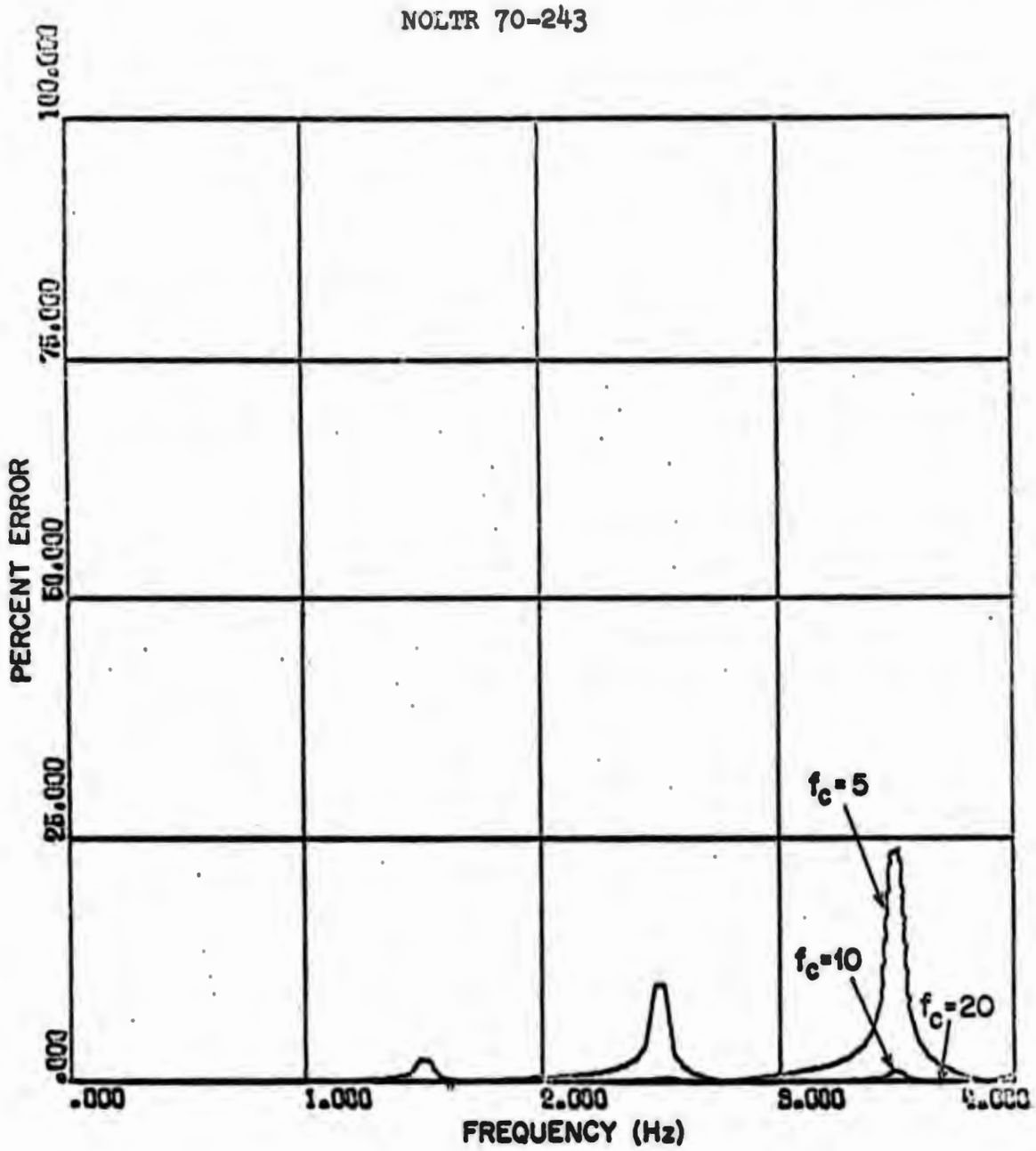

FIGURE 25.

FOURIER SPECTRUM ERROR VERSUS FREQUENCY FOR THE HALF-SINE ACCELERATION INPUT USING THE O'HARA TECHNIQUE AND DIFFERENT NYQUIST RATES

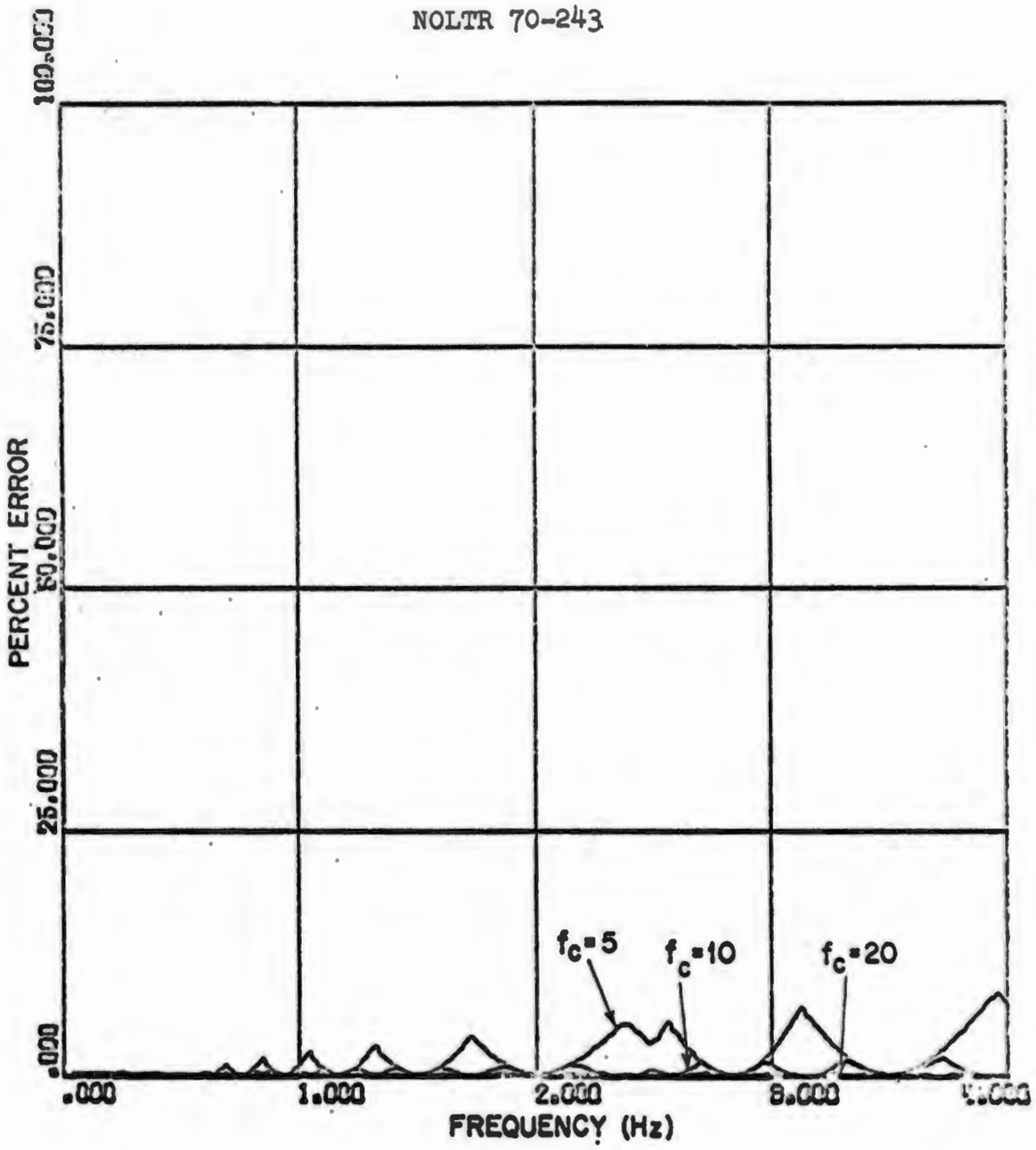

FIGURE 26.

VELOCITY SHOCK SPECTRUM ERROR VERSUS FREQUENCY FOR THE HALF-SINE ACCELERATION INPUT USING THE O'HARA TECHNIQUE AND DIFFERENT NYQUIST RATES

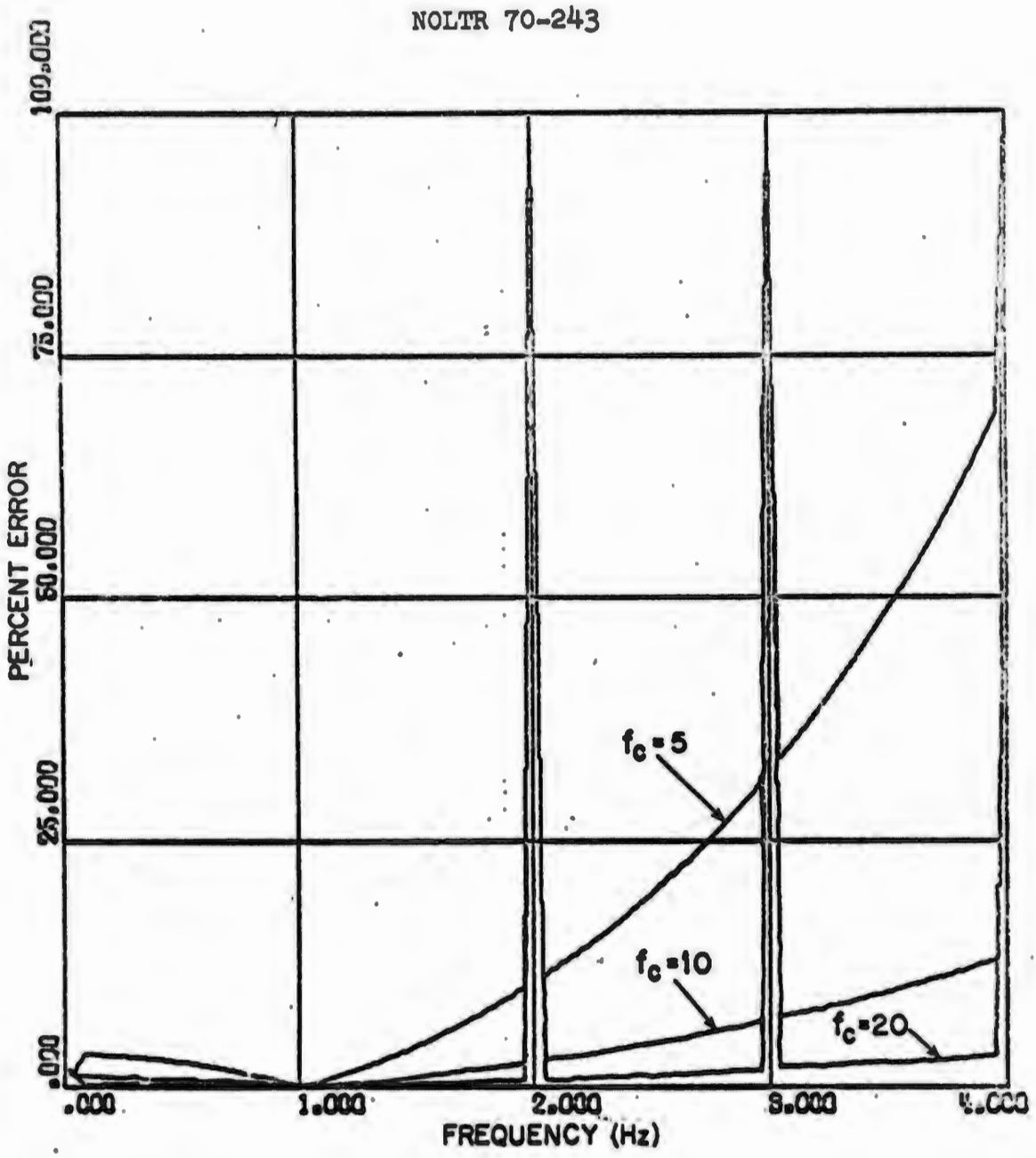

FIGURE 27.

FOURIER SPECTRUM ERROR VERSUS FREQUENCY FOR THE FULL-SINE ACCELERATION INPUT USING AN IMPULSE INVARIANT TECHNIQUE AND DIFFERENT NYQUIST RATES

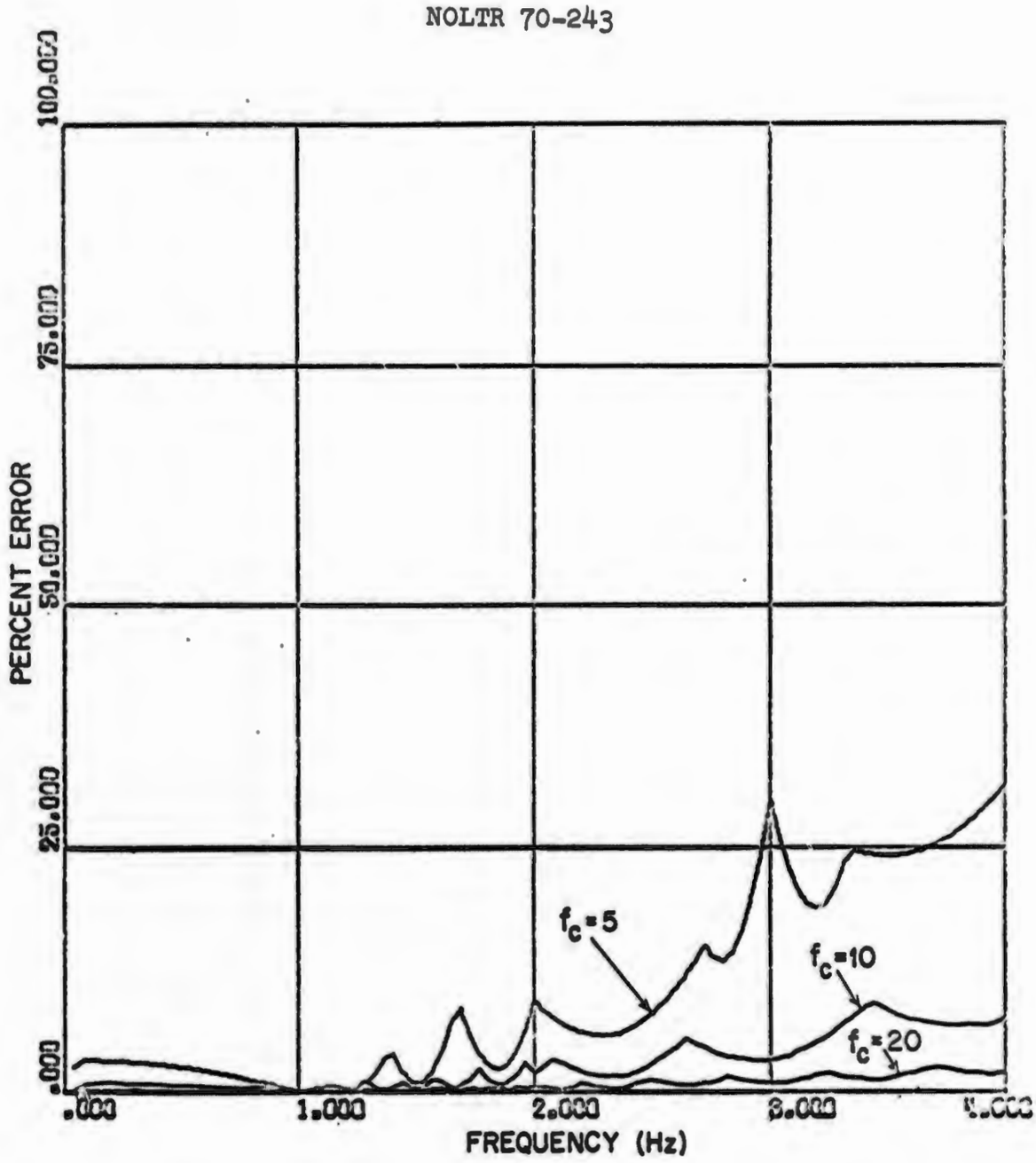

FIGURE 28.

VELOCITY SHOCK SPECTRUM ERROR VERSUS FREQUENCY FOR THE FULL-SINE ACCELERATION INPUT USING AN IMPULSE INVARIANT TECHNIQUE AND DIFFERENT NYQUIST RATES

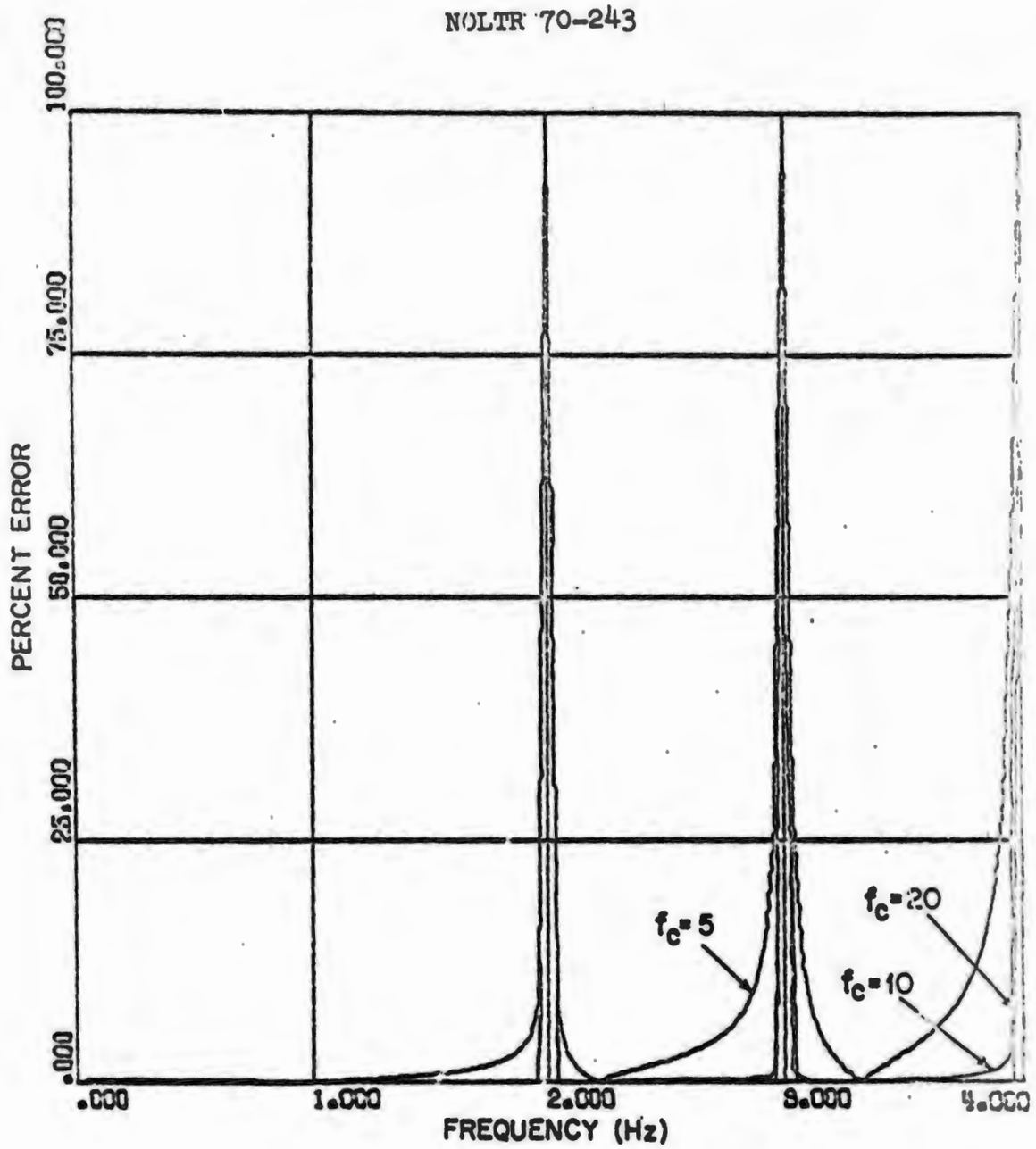

FIGURE 29.

FOURIER SPECTRUM ERROR VERSUS FREQUENCY FOR THE FULL-SINE ACCELERATION INPUT USING THE O'HARA TECHNIQUE AND DIFFERENT NYQUIST RATES

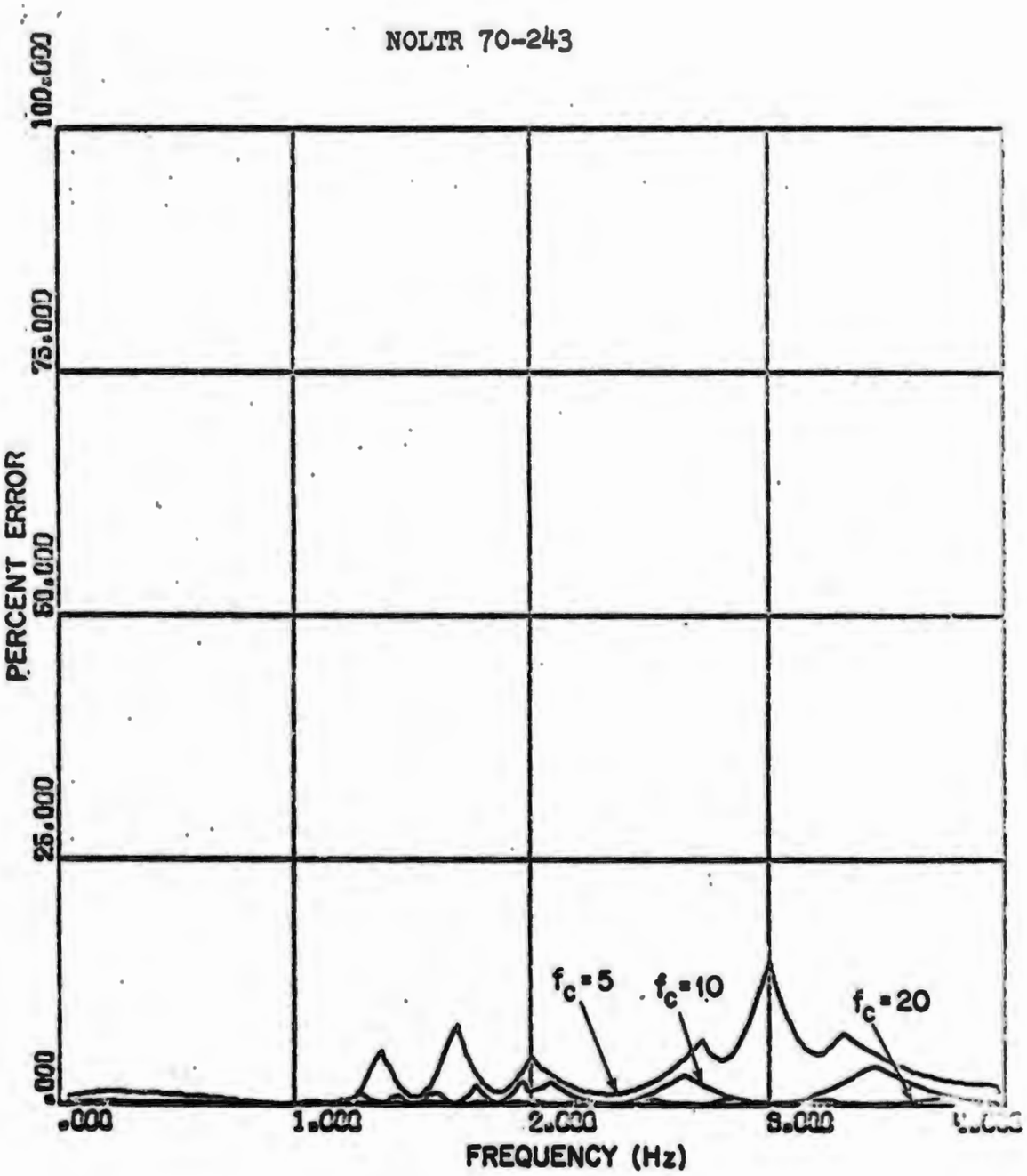

FIGURE 30.

VELOCITY SHOCK SPECTRUM ERROR VERSUS FREQUENCY FOR THE FULL-SINE ACCELERATION INPUT USING THE O'HARA TECHNIQUE AND DIFFERENT NYQUIST RATES

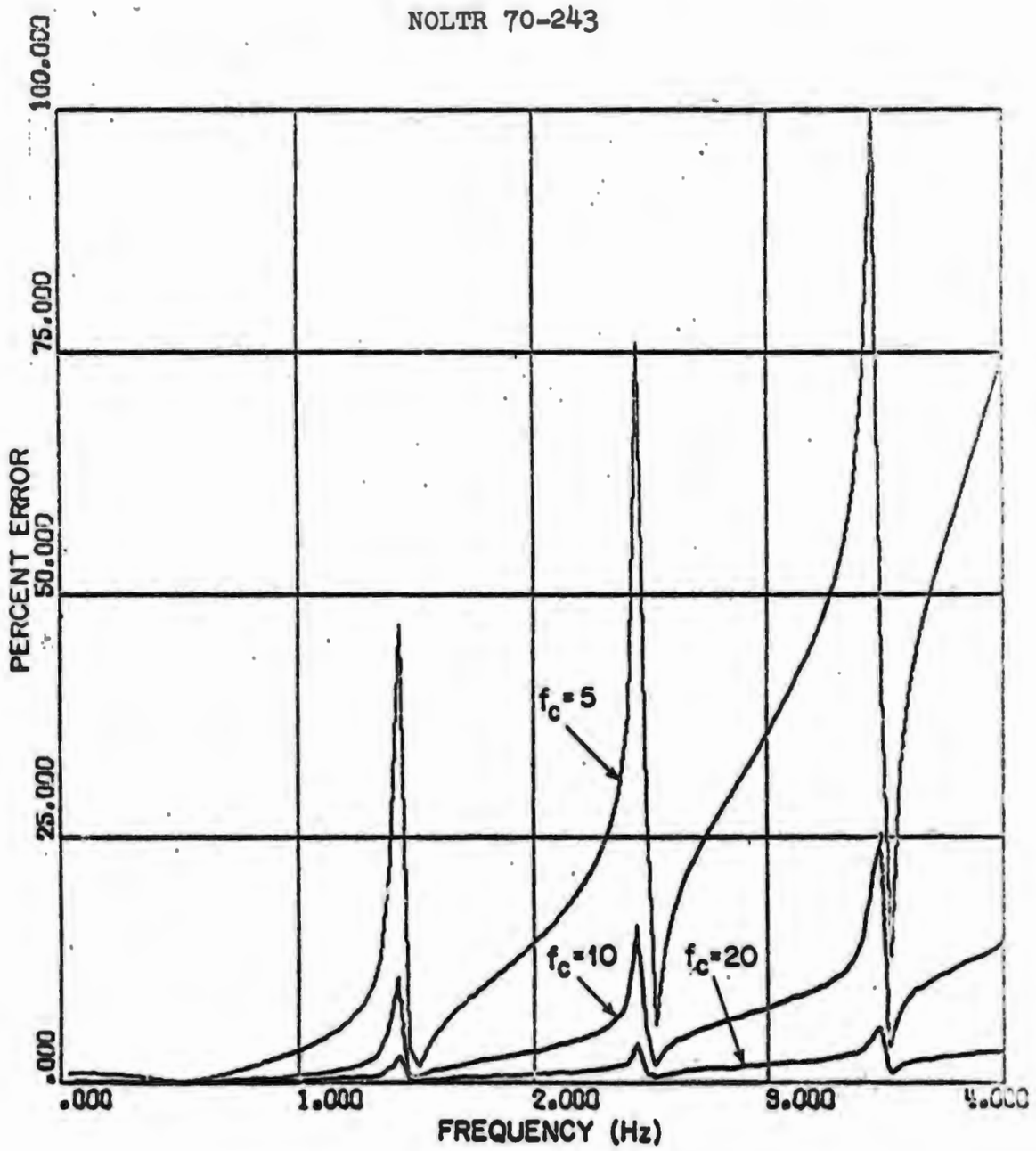

FIGURE 31.

FOURIER SPECTRUM ERROR VERSUS FREQUENCY FOR THE INVERTED PARABOLA ACCELERATION INPUT USING AN IMPULSE INVARIANT TECHNIQUE AND DIFFERENT NYQUIST RATES

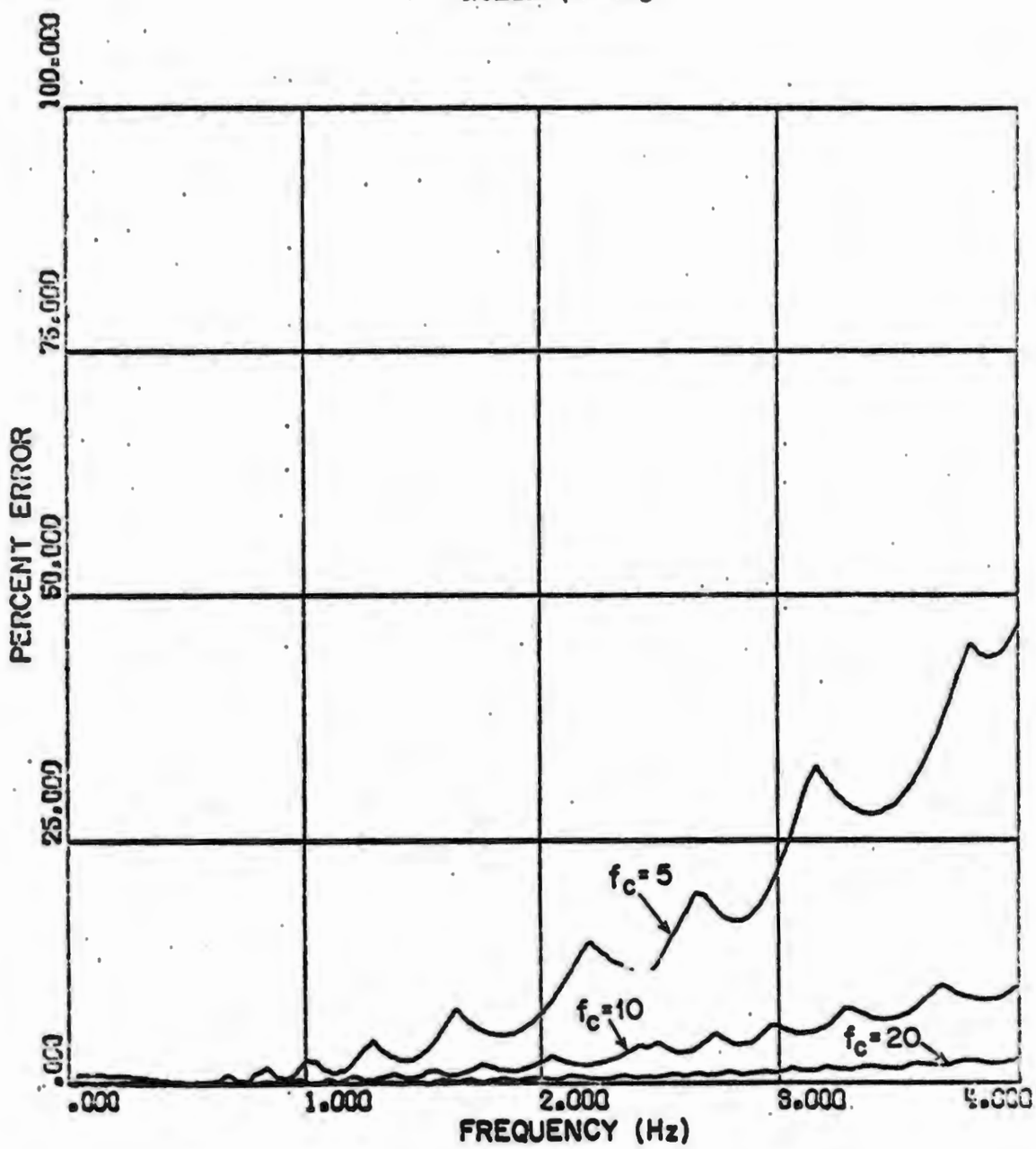

FIGURE 32.

VELOCITY SHOCK SPECTRUM ERROR VERSUS FREQUENCY FOR THE INVERTED PARABOLA ACCELERATION INPUT USING AN IMPULSE INVARIANT TECHNIQUE AND DIFFERENT NYQUIST RATES

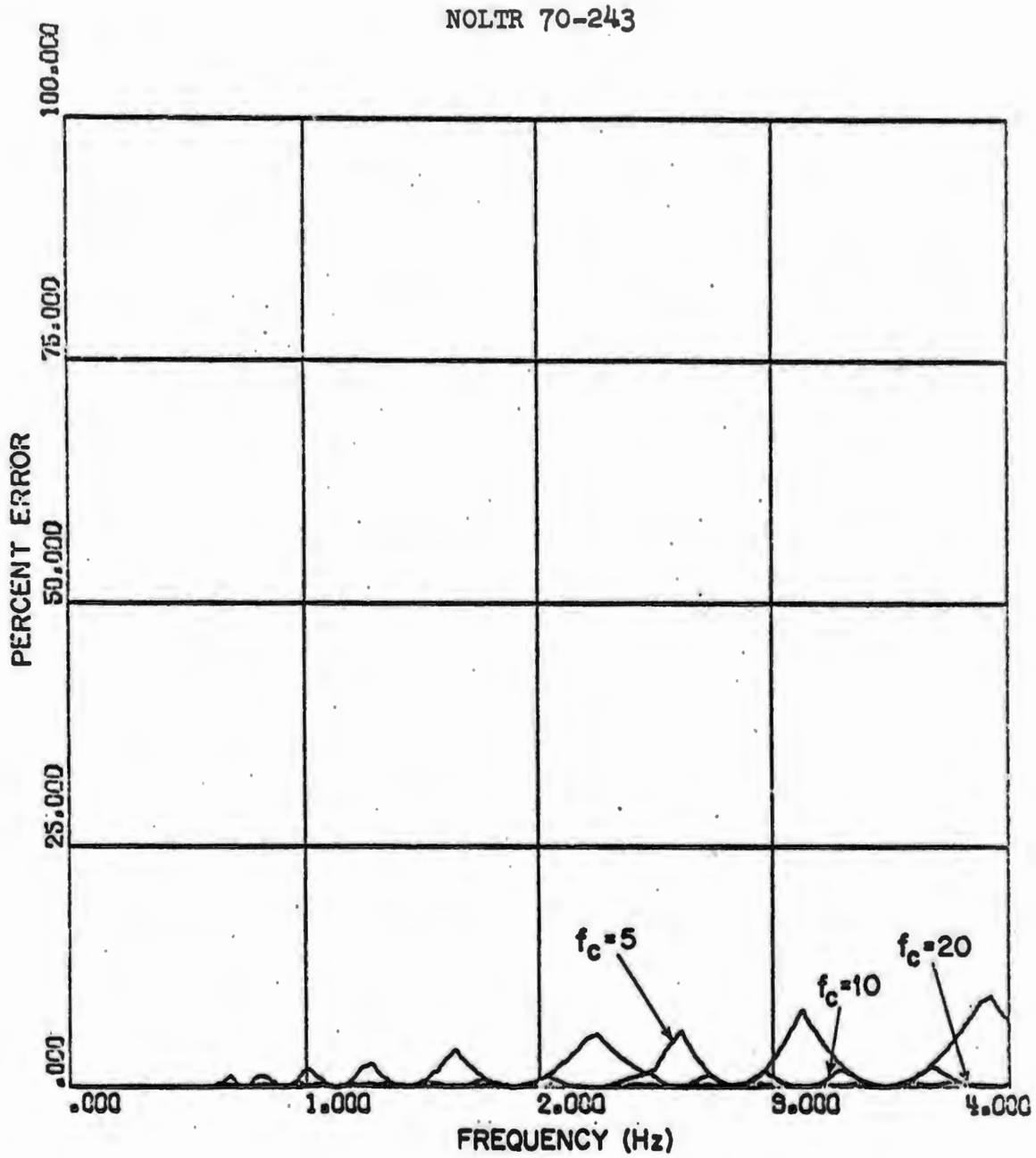

FIGURE 33.

VELOCITY SHOCK SPECTRUM ERROR VERSUS FREQUENCY FOR THE INVERTED PARABOLA ACCELERATION INPUT USING THE O'HARA TECHNIQUE AND DIFFERENT NYQUIST RATES

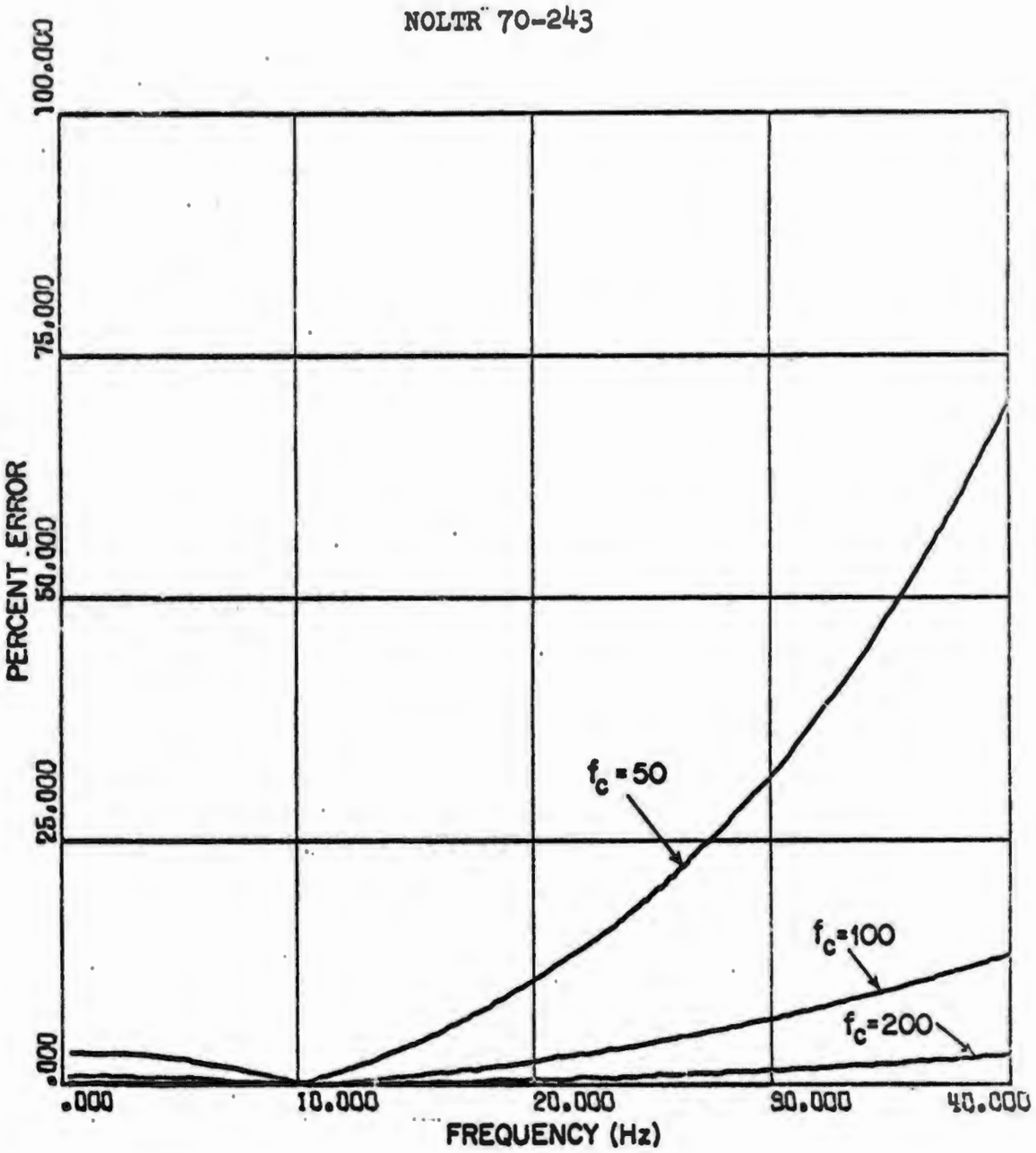

FIGURE 34.

FOURIER SPECTRUM ERROR VERSUS FREQUENCY FOR THE DECAYING SINUSOID ACCELERATION INPUT USING AN IMPULSE INVARIANT TECHNIQUE AND DIFFERENT NYQUIST RATES

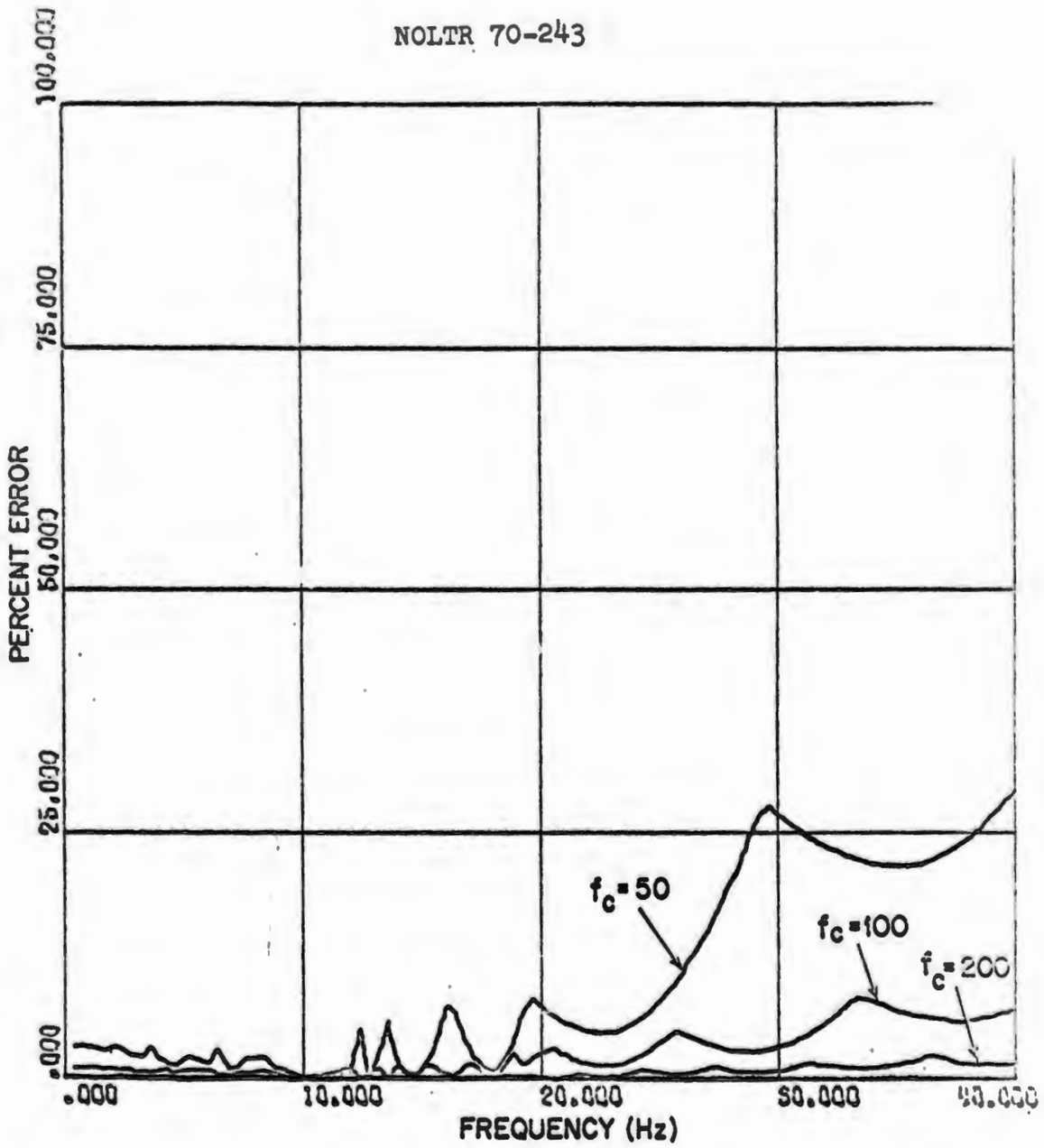

FIGURE 35.

VELOCITY SHOCK SPECTRUM ERROR VERSUS FREQUENCY FOR THE DECAYING SINUSOID ACCELERATION INPUT USING AN IMPULSE INVARIANT TECHNIQUE AND DIFFERENT NYQUIST RATES

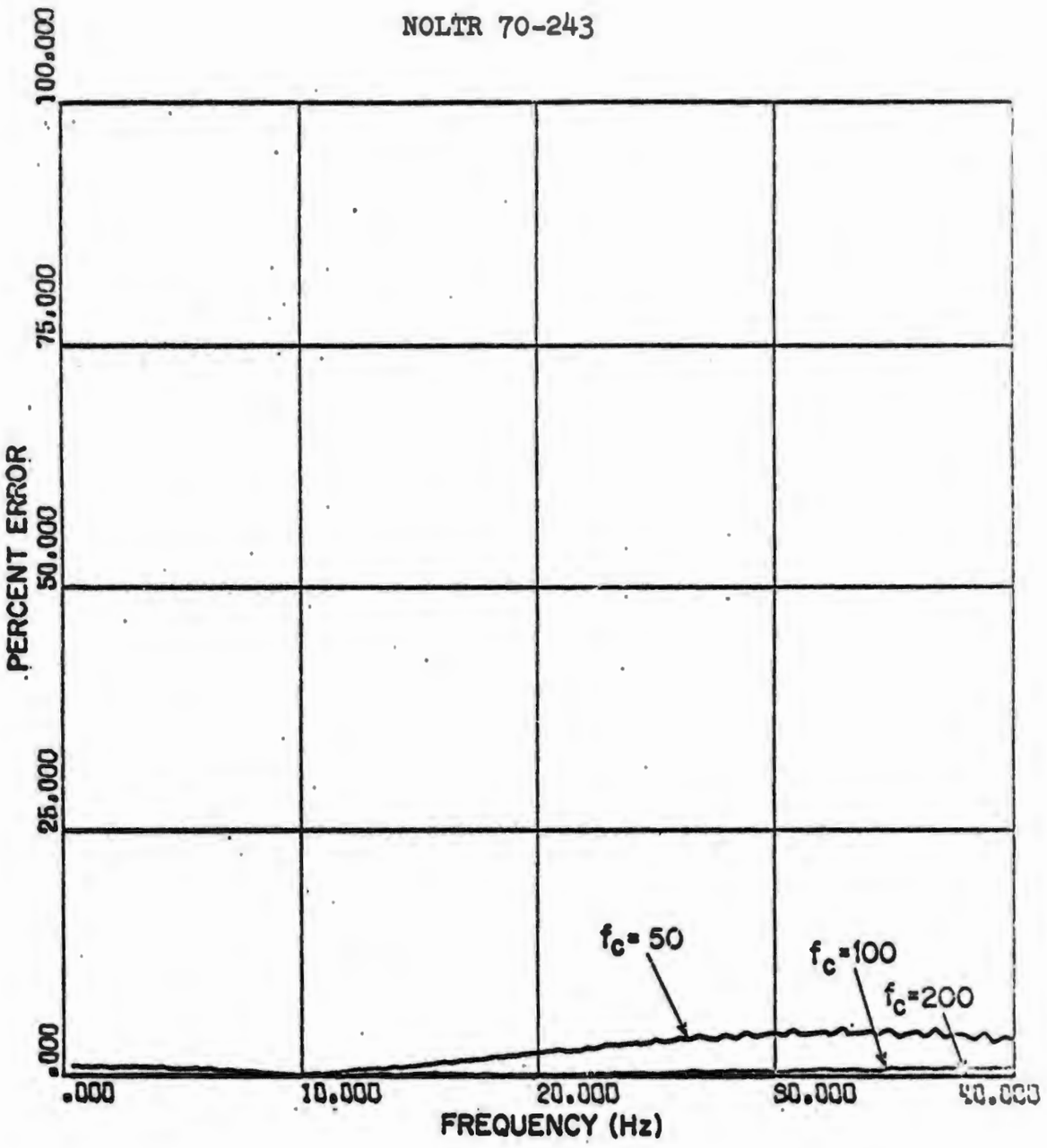

FIGURE 36.

FOURIER SPECTRUM ERROR VERSUS FREQUENCY FOR THE DECAYING SINUSOID ACCELERATION INPUT USING THE O'HARA TECHNIQUE AND DIFFERENT NYQUIST RATES

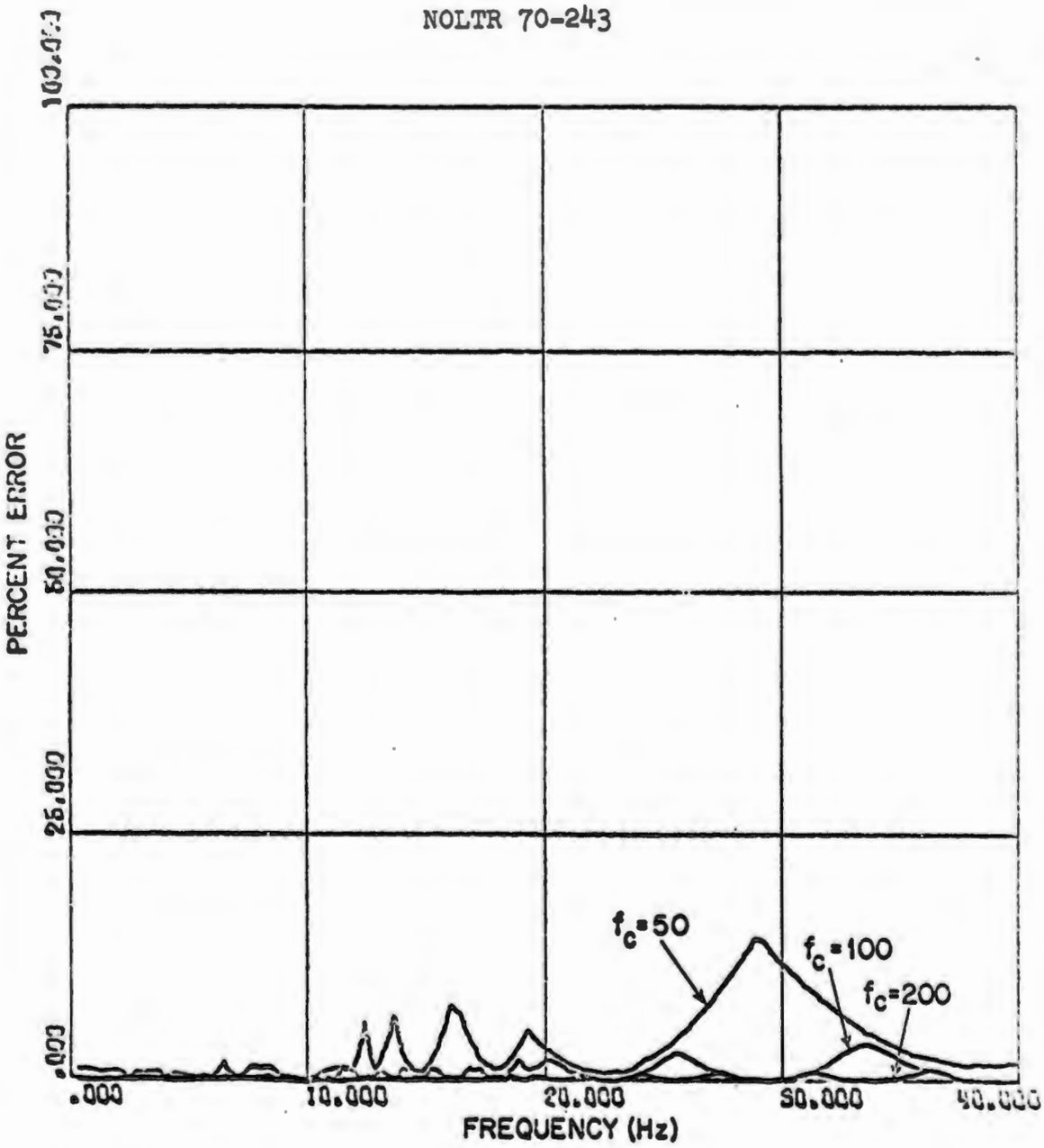

FIGURE 37.

VELOCITY SHOCK SPECTRUM ERROR VERSUS FREQUENCY FOR THE DECAYING SINUSOID ACCELERATION INPUT USING THE O'HARA TECHNIQUE AND DIFFERENT NYQUIST RATES

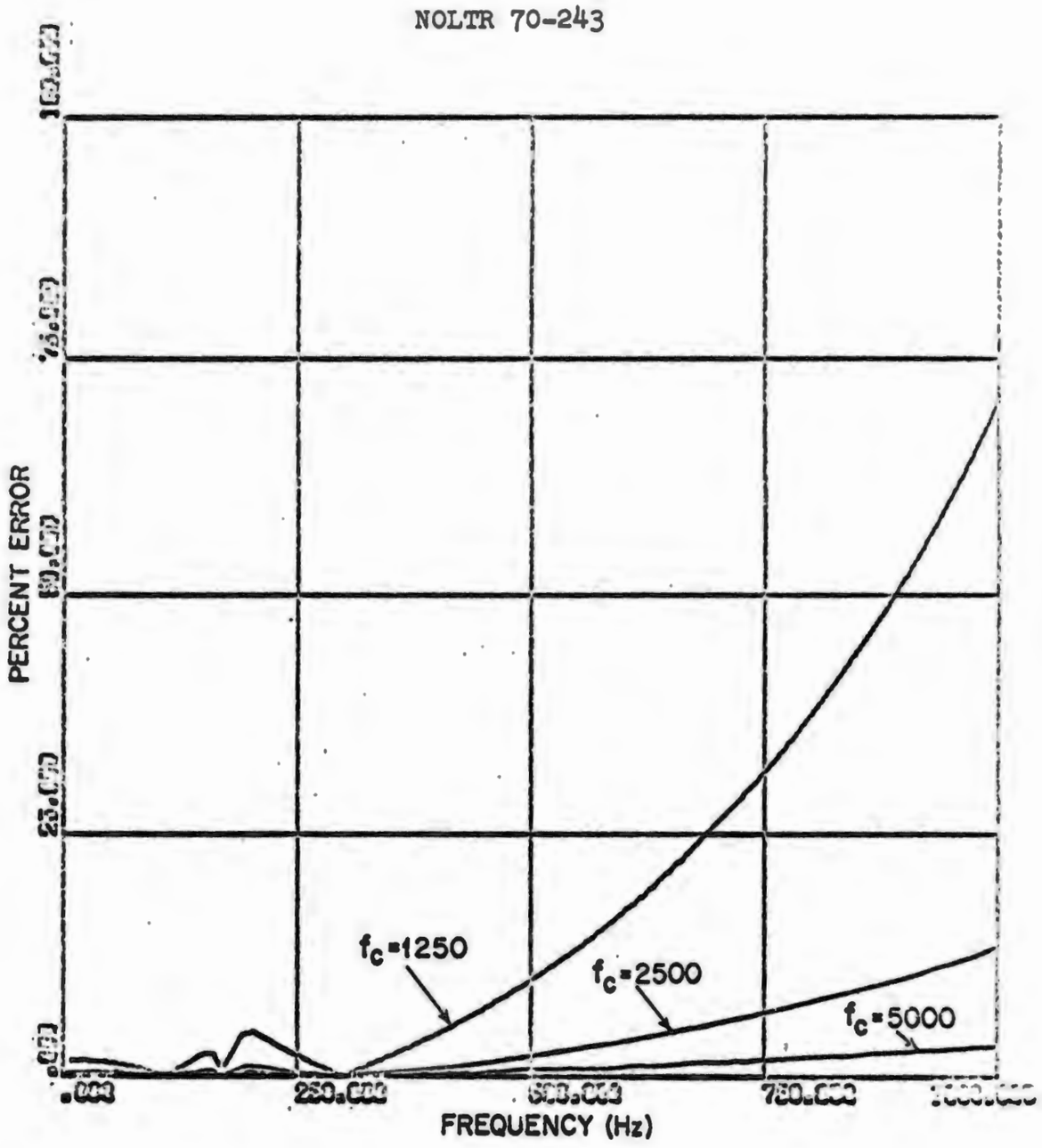

FIGURE 38.

FOURIER SPECTRUM ERROR VERSUS FREQUENCY FOR THE COMBINED DECAYING SINUSOIDS ACCELERATION INPUT USING AN IMPULSE INVARIANT TECHNIQUE AND DIFFERENT NYQUIST RATES

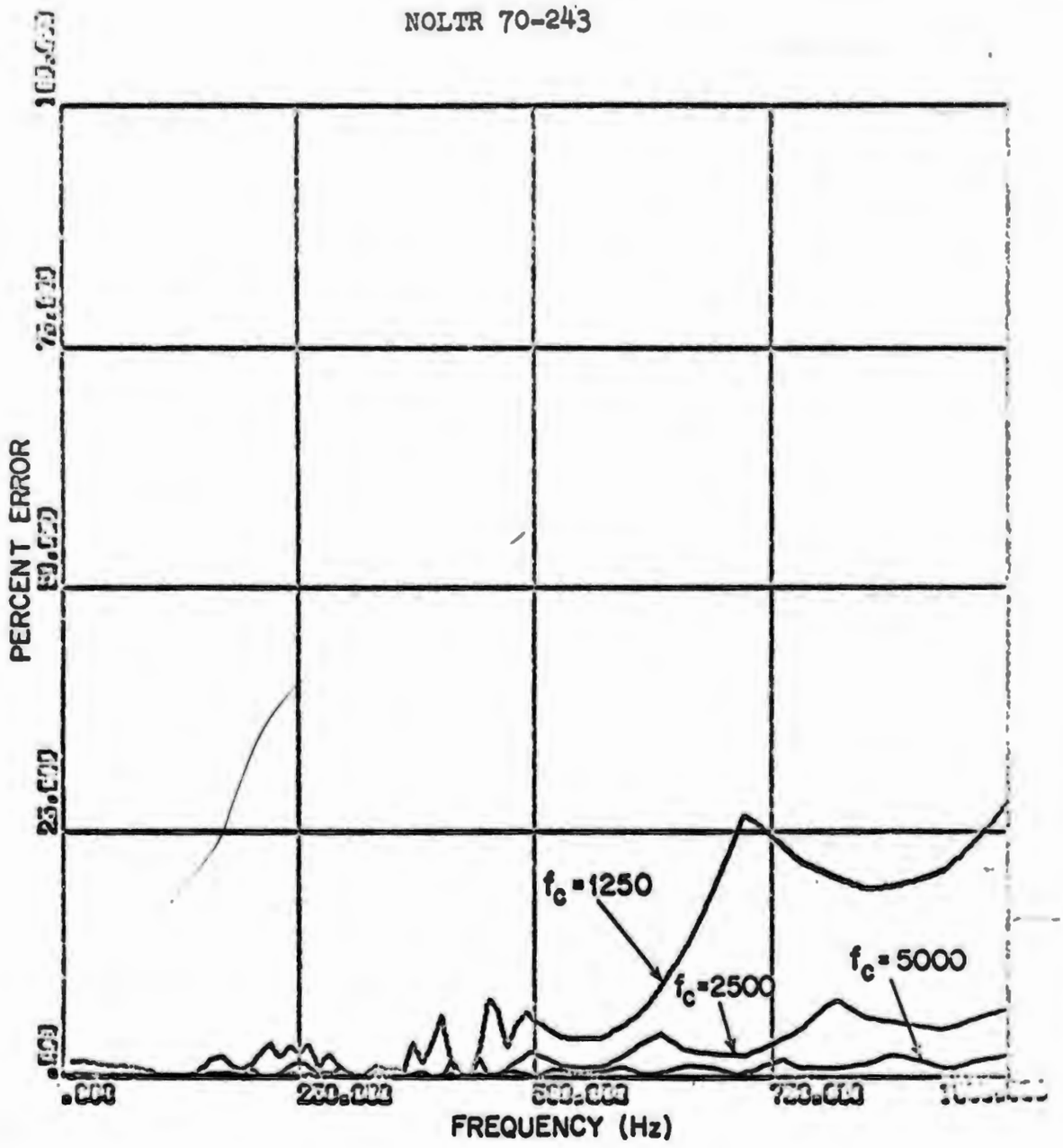

FIGURE 39.

VELOCITY SHOCK SPECTRUM ERROR VERSUS FREQUENCY FOR THE COMBINED DECAYING SINUSOIDS ACCELERATION INPUT USING AN IMPULSE INVARIANT TECHNIQUE AND DIFFERENT NYQUIST RATES

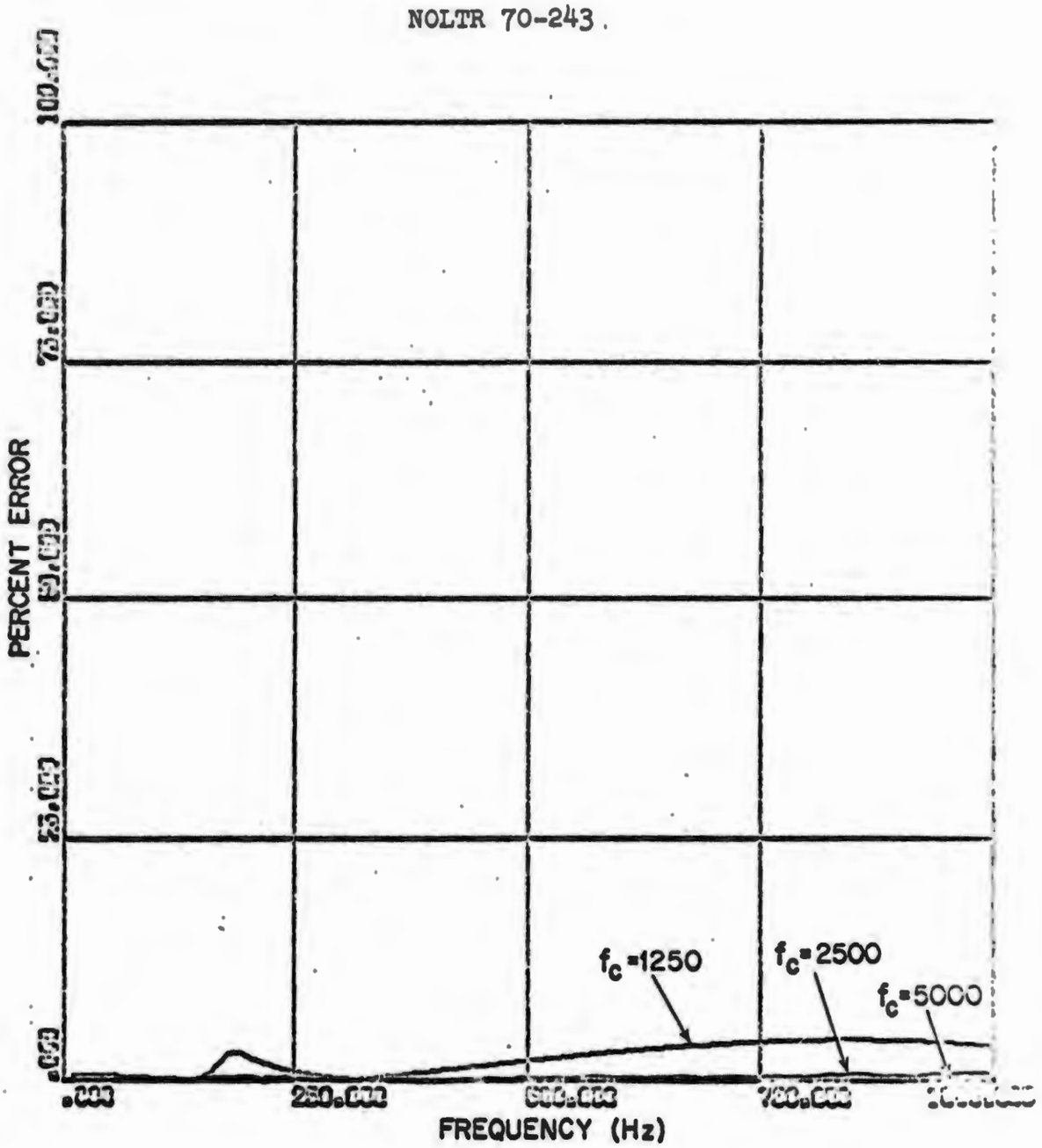

FIGURE 40.

FOURIER SPECTRUM ERROR VERSUS FREQUENCY FOR THE COMBINED DECAYING SINUSOID ACCELERATION INPUT USING THE O'HARA TECHNIQUE AND DIFFERENT NYQUIST RATES

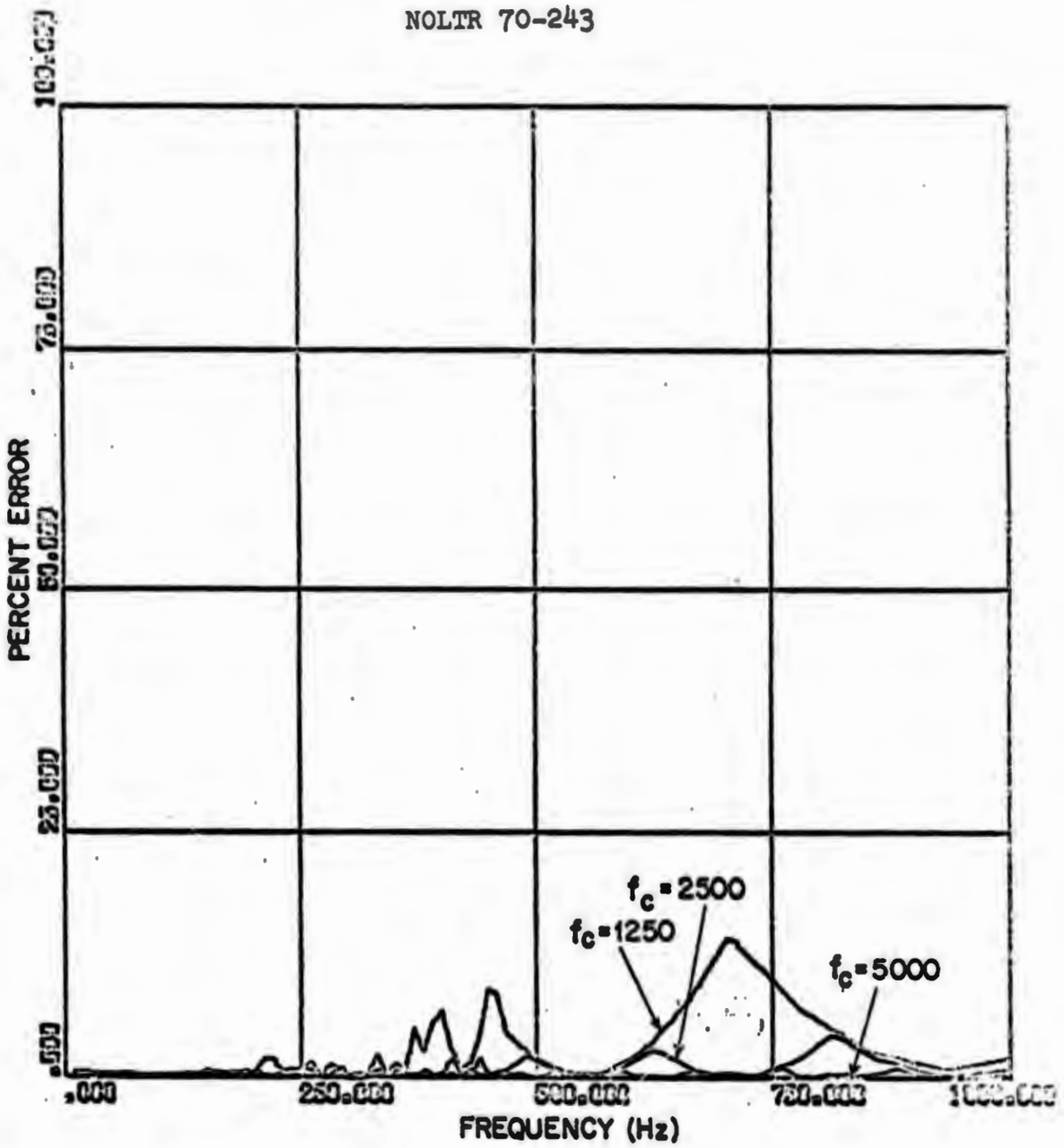

FIGURE 41.

VELOCITY SHOCK SPECTRUM ERROR VERSUS FREQUENCY FOR THE COMBINED DECAYING SINUSOIDS ACCELERATION INPUT USING THE O'HARA TECHNIQUE AND DIFFERENT NYQUIST RATES

TABLE 1

TIMING TABLE FOR FOURIER AND UNDAMPED SHOCK SPECTRA, $T = M (T_{oh} + NT_i)$

	Method	Iteration Time (ms/data)	Overhead Time (ms)	Example 1 N = 1024 M = 512 (sec)	Example 2 N = 4096 M = 2048 (min)	Example 3 N = 8192 M = 4096 (min)
Acceleration Input	O'Hara	.57	2.3	300	79	318
	Direct Method	.22	1.6	116	31	125
	Z-Transform	.12	2.3	64	17	67
Velocity Input	O'Hara	.46	2.1	243	65	259
	Direct Method	.23	1.6	123	33	130
	Z-Transform	.15	2.2	80	21	84
Fast Fourier $T = K(N \log_2 N)$ $K = .234$ ms/data				2.4 sec	11.5 sec	25.0 sec

TABLE 2

NUMBER OF SPECTRUM SAMPLES REQUIRED USING THE DAMPED SAMPLING FORMULA FOR VARIOUS FREQUENCY RANGES AND DAMPING RATIOS

	Damping Ratio ζ					
Range $\frac{f_{max}}{\Delta f}$	.01	.02	.05	.1	.2	.5
100	462	232	94	48	25	11
500	624	313	127	65	34	15
1000	694	348	141	72	37	17
5000	855	430	174	89	46	21
10000	925	465	188	96	50	22

SELECTED BIBLIOGRAPHY

1. O'Hara, G. J., and Petak, L. P., "The Effect of a Second Mode and Nearby Structures on Shock Design Values." NRL Report 6676, April 1968

2. Papoulis, A., The Fourier Integral and Its Applications, McGraw-Hill Book Company, Inc., New York, 1962

3. Frankland, J. M., "Effects of Impact on Simple Elastic Structures," DTMB Report 481, April 1942

4. Mindlin, Raymond D., "Dynamics of Package Cushioning," Bell System Technical Journal, Vol. 24, 1945

5. Biot, M. A., "Analytical and Experimental Methods in Engineering Seismology," Trans, ASCE 108:365, 1943

6. Garner, Murray F., and Barnes, John L., Transients in Linear Systems, John Wiley & Sons, Inc., New York, 1942

7. Gertel, M., and Holland, R., "Definition of Shock Design and Test Criteria Using Shock and Fourier Spectra of Transient Environments," The Shock and Vibration Bulletin 35, Part 6, Washington, D.C., 1966

8. Ostergren, S. M., "Shock Testing to Shock Spectra Specifications," The Shock and Vibration Bulletin 35, Part 6, Washington, D.C., 1966

9. O'Hara, G. J., and Cunniff, P. F., "Elements of Normal Mode Theory," NRL Report 6002, November 1963

10. Hurty, Walter C., and Rubinstein, Moshe F., Dynamics of Structures, Prentice-Hall, Inc., Englewood Cliffs, N. J., May 1965

11. Weber, Ernst, Linear Transient Analysis, John Wiley & Sons, Inc., New York, 1954

12. Collins, R. P., "A Computer Simulation Study of the Effects of Equipment Loading on Foundation Shock Spectra," Master of Science Thesis, University of Maryland, June 1966

13. Harris, Cyril M., and Crede, Charles E., (ed), Shock and Vibration Handbook, Vol. 2, McGraw-Hill Book Co., Inc., 1961

14. O'Hara, G. J., "A Numerical Procedure for Shock and Fourier Analysis," NRL Report 5772, June 1962

15. Kuo, Benjamin C., Analysis and Synthesis of Sampled-Data Control Systems, Prentice-Hall, Inc., 1963

16. Hamming, Richard W., Numerical Methods for Scientists and Engineers, McGraw-Hill Book Company, Inc., 1962

17. Kaufman, Myron N., "Real-Time Spectrum Analysis in Vibration and Shock Testing," Test Engineering & Management, Oakhurst, N. J., June 1969

18. "Real Time Spectrum Analysis," Signal Analysis Industries Corp., New York

19. Mebane, William W., "Analog Shock-Spectrum Analyzer," NOLTR 67-97, Naval Ordnance Laboratory, White Oak, Maryland, June 1967

20. Barnes, Ward P., "A Spectral Analyzer for Shock Environment," Shock, Vibration and Associated Environments Part IV, Bulletin 29, June 1961

21. Jackson, Albert S., Analog Computation, McGraw-Hill Book Co., Inc., New York 1960

22. Reed, R. S., "A Digital Computer Program for the Analysis of Wave-Form Data (Multi-Record Wave Investigator for Sine and Random Date - MR WISARD), NOLTR 69-28, Naval Ordnance Laboratory, White Oak, Maryland, January 1969

23. Michellich, M. O., "Dynamic Data Analysis System," The Shock and Vibration Bulletin 40, Part 7, Washington, D.C., 1969

24. Jury, Eliahu I., Sampled-Data Control Systems, John Wiley & Sons, Inc., New York, 1958

25. Cooley, J. S., and Tukey, J. W., "An Algorithm for the Machine Calculation of Complex Fourier Series," Math Computation, Vol. 19, No. 90, pp. 297-301, 1965

26. Gentleman, W. M., and Sande, G., "Fast Fourier Transforms - For Fun and Profit," Proceeding of the Fall Computer Conference, 1966

27. Enochson, Loren D., and Otnes, Robert K., "Programming and Analysis for Digital Time Series Data," The Shock and Vibration Information Center, SVM-3, 1968

28. Langdon, Bruce, "Fast Finite Discrete Fourier Transform," SHARE Program Library, SDA 3483, January 1967

29. Lane, D. W., "Digital Shock Spectrum Analysis by Recursive Filtering," Shock, Vibration and Associated Environments Part II, Bulletin No. 33, February 1964

30. Jones, G. K., and On, F. J., "Prediction of Interface Random and Transient Environments Through the Use of Mechanical Impedance Concepts," The Shock and Vibration Bulletin 40, Part 3, Washington, D. C., 1969

31. Favour, J. D., LeBrun, J. M., and Young, J. P., "Transient Waveform Control of Electromagnetic Vibration Test Equipment," The Shock and Vibration Bulletin 40, Part 5, Washington, D. C., 1969

32. Stockham, Thomas G., Jr., "High-Speed Convolution and Correlation," Proceedings - Spring Joint Computer Conference, 1966

33. Melodia, Anthony C., "Mathematical Model and Computer Program for Transient Shock Analysis," Report 2263, DTMB, February 1967

34. Pipes, Louis A., Matrix Methods for Engineering, Prentice-Hall, Inc., Englewood Cliffs, N. J., 1963

BLANK PAGE

APPENDIX A

EXAMPLE OF APPLICATION OF SHOCK AND FOURIER SPECTRA TO COMPLEX SYSTEMS

In order to demonstrate the application of the shock and Fourier spectra to complex systems, two systems, one mechanical and one electrical, were chosen. The two lumped parameter systems are shown in Figure A-1. The problem is to derive an estimate of the peak displacement and voltage values which occur in the two systems given the shock and Fourier spectra of the input base motion and the input voltage respectively.

The equations of motion for the mechanical system are derived using D'Alembert's principle as follows. The summation of forces on mass 1 is given by

$$F_1 = m_1\ddot{x}_1 = -k_1(x_1-x_0) - k_2(x_1-x_2) - c_1(\dot{x}_1-\dot{x}_0) - c_2(\dot{x}_1-\dot{x}_2) \tag{145}$$

The summation of forces on mass 2 is given by

$$F_2 = m_2\ddot{x}_2 = -k_2(x_2-x_1) - c_2(\dot{x}_2-\dot{x}_1) \tag{146}$$

Substitution of the values shown yields

$$(\ddot{x}_1+.02\dot{x}_1+.2x_1) - (.01x_2+.1x_2) = (.01\dot{x}_0+.1x_0) \tag{147}$$

$$- (.01\dot{x}_1+.1x_1) + (\ddot{x}_2+.01\dot{x}_2+.1x_2) = 0$$

The Laplace transform of this equation with no initial conditions is given in matrix notation by

$$\begin{vmatrix} (s^2+.02s+.02) - (.01s+.1) \\ -(.01s+.1) \quad (s^2+.01s+.1) \end{vmatrix} \begin{Bmatrix} \bar{x}_1(s) \\ \bar{x}_2(s) \end{Bmatrix} = \begin{Bmatrix} (.01s+.1) \\ 0 \end{Bmatrix} x_0(s) \tag{148}$$

The equations can be written in terms of the relative displacement $r_1 = x_1 - x_0$, and $r_2 = x_2 - x_0$ which yields in matrix form.

$$\begin{vmatrix} (s^2+.02s+.2) - (.01s+.1) \\ -(.01s+.1) \quad (s^2+.01s+.1) \end{vmatrix} \begin{Bmatrix} r_1(s) \\ r_2(s) \end{Bmatrix} = \begin{Bmatrix} -\ddot{x}_0(s) \\ -\ddot{x}_0(s) \end{Bmatrix} \tag{149}$$

The solution by multiplication by the inverse of the square matrix [34] is given by

$$\begin{Bmatrix} r_1(s) \\ r_2(s) \end{Bmatrix} = \frac{1}{D} \begin{vmatrix} (s^2+.01s+.1) \quad (.01s+.1) \\ (.01s+.1) \quad (s^2+.02s+.2) \end{vmatrix} \begin{Bmatrix} -\ddot{x}_0(s) \\ -\ddot{x}_0(s) \end{Bmatrix} \tag{150}$$

$$D = s^4+.03s^3+.3001s^2+.002s+.01$$

$$= (s+.002-j.195)\ (s+.002+j.195)\ (s+.013-j.511)\ (s+.013+j.511)$$

Therefore the transfer characteristics of the base and the relative motion of the masses is given by

$$\frac{r_1(s)}{\ddot{x}_0(s)} = \frac{-(s^2+.02s+.2)}{(s^4+.03s^3+.3001s^2+.002s+.01)} \tag{151}$$

$$\frac{r_2(s)}{\ddot{x}_0(s)} = \frac{-(s^2+.03s+.3)}{(s^4+.03s^3+.3001s^2+.002s+.01)} \tag{152}$$

These are equations of the form shown in equation 31. The impulse response can be simply derived by evaluation of the residues at each of the four roots of the denominator. Only the magnitude of the residues will be determined. The responses of the two masses relative to the base for an impulsive base acceleration are given by

$$r_1(t) = 3.70 \exp(-.002t) \sin(.195t) \tag{153}$$

$$+.54 \exp(-.013t) \sin(.511t)$$

$$r_2(t) = 6.02 \exp(-.002t) \sin(.195t)$$

$$- .342 \exp(-.013t) \sin(.511t)$$

The response of mass 1 relative to mass 2 with this input is given by

$$r_1(t) - r_2(t) = -2.32 \exp(-.002t) \sin(.195t) + .882 \exp(-.013t) \sin(.511t) \quad (154)$$

The phase angle was computed for several of the residue pairs and proved to be very small. These equations and the shock and Fourier spectra values can be used to establist a bound on the response of the masses to a complex input. The critical frequencies are $\omega_1 = .195$ and $\omega_2 = .511$ which are $f_1 = .031$ Hz and $f_2 = .081$ Hz. The undamped velocity shock and Fourier spectra values for the half-sine input are shown in Figure 7 and have the value .63 at .031 Hz and .62 at .081 Hz. The undamped shock spectrum value will be used for convenience. The relative responses of the masses can therefore be bounded as follows

$$r_1(t) \leq (3.70)(.63) + (.54)(.62) = 2.66L$$

$$r_2(t) \leq (6.02)(.63) + (.342)(.62) = 4.00L$$

$$r_1(t)-r_2(t) \leq (2.32)(.63) + (.882)(.62) = 1.00L \quad (155)$$

Where L is the unit of length associated with the acceleration input. The same technique can now be applied to the electrical network of Figure A-1B. The required equations can be written using Laplace transforms with no initial conditions and the summation of nodal currents as

$$\sum i_2 = \frac{E_1(s)-E_2(s)}{R_1+L_1 s} + \frac{E_3(s)-E_2(s)}{R_2+L_2 s} - E_2(s)C_1 s = 0 \qquad (156)$$

$$\sum i_3 = \frac{E_2(s)-E_3(s)}{R_2+L_2 s} - E_3(s)C_2 s = 0 \qquad (157)$$

This can be written in matrix notation with substitution of the values shown in Figure A-1.

$$\begin{vmatrix} (s^2+10s+2\times10^4) & (-10^4) \\ (-10^4) & (s^2+10s+10^4) \end{vmatrix} \begin{Bmatrix} E_2(s) \\ E_3(s) \end{Bmatrix} = \begin{Bmatrix} 10^4 E_1(s) \\ 0 \end{Bmatrix} \qquad (158)$$

The solution is again accomplished by multiplication by the inverse of the square matrix which yields

$$\begin{Bmatrix} E_2(s) \\ E_3(s) \end{Bmatrix} = \frac{1}{D} \begin{vmatrix} (s^2+10s+10^4) & (10^4) \\ (10^4) & (s^2+10s+2\times10^4) \end{vmatrix} \begin{Bmatrix} 10^4 E_1(s) \\ 0 \end{Bmatrix} \qquad (159)$$

$$D = s^4+20s^3+3.01\times10^4 s^2+3\times10^5+10^8$$

$$= (s+5.02-j61.73)\,(s+5.02+j61.73)\,(s+4.98-j161.36)\,(s+4.98+j161.36)$$

The Laplace transforms of the impulse response is therefore

$$\frac{E_2(s)}{E_1(s)} = \frac{10^4\,(s^2+10s+10^4)}{s^4+20s^3+3.01\times10^4 s^2+3\times10^5 s+10^8} \qquad (160)$$

$$\frac{E_3(s)}{E_1(s)} = \frac{10^8}{s^4+20s^3+3.01x10^4s^2+3x10^5s+10^8} \qquad (161)$$

The two voltage responses to an impulse, $e_1(t) = \delta(0)$, are found using residues as before yielding

$$e_2(t) = +45.1 \exp(-5.02t) \sin(61.73t) + 45.0 \exp(-4.98t) \sin(161.36t)$$

$$e_3(t) = +72.8 \exp(-5.02t) \sin(61.73t) - 27.8 \exp(-4.98t) \sin(161.36t) \qquad (162)$$

The damping ratio for the two frequencies is .08 and .03 for the first and second modes respectively. The approximate bounds for the responses of the network to the decaying sinusoid input (Figure 14) can be obtained using the shock spectrum value for the .1 and 0 damping values from Figure 17. For the angular frequency 61.73 rad/sec or 9.82 Hz and $\zeta = .1$, the value is approximately .032; for the angular frequency of 161.36 rad/sec or 25.68 Hz and $\zeta = 0$ the value is approximately .008. Therefore the bounds on the two responses is approximated by

$$e_2(t) \leq 45.1\ (.032) + 45.0\ (.008) = 1.803 \text{ volts}$$

$$e_3(t) \leq 72.8\ (.032) + 27.8\ (.008) = 2.55 \text{ volts} \qquad (163)$$

The residual response can be bounded using the Fourier spectrum values with the assumption of no damping at these same frequencies from Figure 15; the values of the Fourier

integral for the first and second natural frequencies are .105 and .005 respectively.

$$e(t) \leq 45.1\ (.105) + 45.0\ (.005) = 4.95 \text{ volts}$$

$$e(t) \leq 73.8\ (.105) + 27.8\ (.005) = 7.89 \text{ volts} \qquad (164)$$

Without damping, the bound is much greater as seen in equations (163) and (164).

A major problem associated with the shock spectrum technique results from the effects of loading. In both of the above examples it was assumed that the presence of the structure or network had no effect on the base or voltage source. The problem can be demonstrated by returning to the matrix equation (148). The solution for $X_1(s)$ and $X_2(s)$ can be accomplished by multiplication by the inverse of the square matrix as before which yields

$$\begin{Bmatrix} X_1(s) \\ X_2(s) \end{Bmatrix} = \frac{1}{D} \begin{vmatrix} (s^2+.01+.1) & (.01s+.1) \\ (.01s+.1) & (s^2+.02s+.2) \end{vmatrix} \begin{Bmatrix} (.01s+.1) \\ 0 \end{Bmatrix} X_0(s) \qquad (165)$$

Where D is the determinant of the square matrix and is given again by

$$D = s^4+.03s^3+.3001s^2+.002s+.01$$

$$= (s+.002-j.195)\ (s+.002+j.195)\ (s+.013-j.511)\ (s+.013+j.511)$$

The transmissibility for the two masses is given in terms of Laplace transforms as

$$\frac{X_1(s)}{X_0(s)} = \frac{(s^2+.01s+.1)\ (.01s+.1)}{(s^4+.03s^3+.3001s^2+.002s+.01)} \tag{166}$$

$$\frac{X_2(s)}{X_0(s)} = \frac{.0001(s^2+20s+100)}{(s^4+.03s^3+.3001s^2+.002s+.01)} \tag{167}$$

Both transmissibilities have the same four complex poles which represent the fixed base natural frequencies of the total system. The transmissibility $\frac{X_1(s)}{X_0(s)}$ has three zeros, one occurring at s = -10 and the other occurring as the complex conjugate pair s = -.005±j.316. These zeros are identical to the fixed-base natural frequencies of the mass two. If the response of mass one was measured without mass two, and the shock and Fourier spectrum of this response were used to predict the response of mass two when placed on mass one, the computation would be in error because the simple, no longer massless oscillator has restricted the motion of the base at exactly the frequency of importance. This problem has been called Fourier and shock spectrum dip and is well discussed in references [1] and [2].

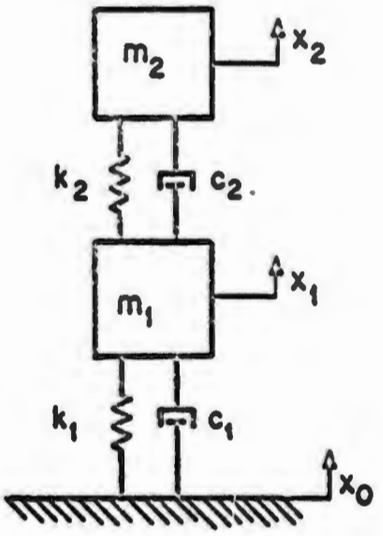

$$m_1 = m_2 = 10 \frac{\text{lb sec}^2}{\text{in}}$$

$$c_1 = c_2 = 0.1 \frac{\text{lb sec}}{\text{in}}$$

$$k_1 = k_2 = 1 \frac{\text{lb}}{\text{in}}$$

FIGURE A-1A

TWO-DEGREE-OF-FREEDOM SPRING MASS SYSTEM

$R_1 = R_2 = 1$ OHM

$L_1 = L_2 = .1$ HENRY

$c_1 = c_2 = .001$ FARAD

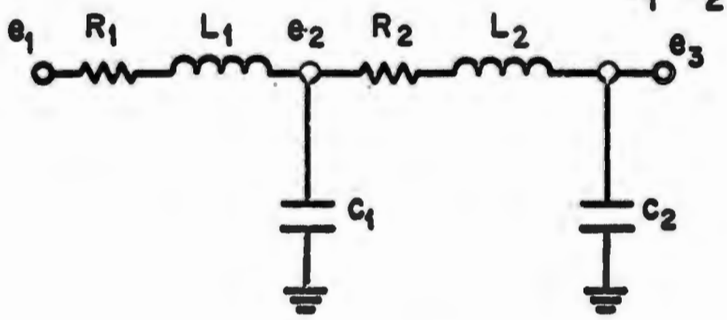

FIGURE A-1B

TWO-DEGREE-OF-FREEDOM PASSIVE RLC NETWORK

BLANK PAGE

APPENDIX B

PREDICTION OF ALIASING ERRORS

The aliasing errors discussed in Chapter IV are predictable for transients which have a known Fourier transform. In order to demonstrate the significance of the aliasing errors, the error will be estimated for two transients which have Fourier integrals which are easily expressed in closed form. The two transients are

a. The square pulse

$$f(t) = 1, \; -T/2 \leq t \leq T/2$$

$$f(t) = 0, \; t < -T/2, \; t > T/2 \qquad (168)$$

b. The displaced half-sine pulse

$$f(t) = \cos(\pi t), \; -T/2 \leq t \leq T/2$$

$$f(t) = 0, \; t < T/2, \; t > T/2 \qquad (169)$$

The two functions have been shifted back $T/2$ seconds to eliminate the phase angle from the derivation. The Fourier integral of the functions are

a. $$F(\omega) = \frac{T \sin\left(\frac{\omega T}{2}\right)}{\left(\frac{\omega T}{2}\right)}$$

$$\text{b.}\quad F(\omega) = \frac{2T}{\pi}\,\frac{\cos\left(\frac{\omega T}{2}\right)}{\left(1 - \left(\frac{\omega T}{\pi}\right)^2\right)} \tag{170}$$

The derivation will be normalized by setting T = 1 and using $f = \frac{\omega}{2\pi}$. The envelopes of the two functions are given by

$$\text{a.}\quad \left|F(f)\right| \leq \frac{1}{\pi f}$$

$$\text{b.}\quad \left|F(f)\right| \leq \frac{2}{\pi(1 - 4f^2)} \tag{171}$$

The expression for the half-sine envelope can be considerably simplified if $4f^2 \gg 1$. Assuming this to be the case, the simplified expression is as follows:

$$\text{b.}\quad \left|F(f)\right| \leq \frac{2}{4\pi f^2} \tag{172}$$

In order to estimate the significance of the aliasing errors, the error caused by the aliasing will be compared to the true spectrum value. The aliased frequencies are given by [16] $f_a = 2nf_c \pm f$, $n = 1,2,3,\ldots$ Therefore the first two frequencies which are folded into f where $0 \leq f \leq f_c$ are given by $2f_c - f$ and $2f_c + f$. The error caused by the first two folded frequencies can be estimated by the ratio of the sum of the aliased envelope values and the correct value as

$$\text{a.}\quad \frac{\left|F(2f_c-f)\right| + \left|F(2f_c+f)\right|}{\left|F(f)\right|} = \frac{\frac{f}{f_c}}{1 - \frac{f^2}{4f_c^2}} \qquad (173)$$

$$\text{b.}\quad \frac{\left|F(2f_c-f)\right| + \left|F(2f_c+f)\right|}{\left|F(f)\right|} = \frac{8\frac{f^2}{f_c^2} + 2\frac{f^4}{f_c^4}}{\left(4 - \frac{f^2}{f_c^2}\right)^2} \qquad (174)$$

Therefore if the two functions are sampled well above the fundamental frequency, 1/T, the aliasing error is a function of the roll-off rate and is approximated by the equations above. Consider sampling the two functions with a Nyquist rate of 10 which corresponds to a sampling rate of 20 samples per second for the one second transient. The approximate errors in the Fourier spectra at 4 Hz are given as

$$\text{a.}\quad \frac{.4}{1 - \frac{1}{4}(.4)^2} = .417 = 41.7\%$$

$$\text{b.}\quad \frac{8(.4)^2 + 2(.4)^4}{(4 - (.4)^2)^2} = .090 = 9.0\% \qquad (175)$$

The value for the half-sine is less than the value from Figure 23, but it seems to be a fair approximation.

APPENDIX C

ACTIVE RC-NETWORK ANALYSIS

In order to demonstrate that the active RC-networks of Figures 4 and 5 have transfer functions which are analogous to the required single degree-of-freedom oscillator, the circuits will be analyzed here. The circuits can be analyzed by summing the currents into nodes e_2 and e_3, and noting that the current into the operational amplifier is virtually zero and the gain is extremely high.

The nodal equations for the circuit shown in Figure 4, using Laplace transforms and no initial conditions, are

$$\sum I_2(s) = \frac{E_1(s)-E_2(s)}{R_1} + \frac{E_0(s)-E_2(s)}{R_2} + \frac{E_3(s)-E_2(s)}{R_3} - C_1 s E_2(s) = 0 \quad (176)$$

$$\sum I_3(s) = \frac{E_2(s)-E_3(s)}{R_3} + C_2 s(E_0(s)-E_3(s)) = 0$$

and

$$E_0(s) = -AE_3(s)$$

The solution of these equations with the gain A approaching infinity is given by

$$\frac{E_0(s)}{E_1(s)} = \frac{-\frac{1}{R_1 R_3 C_2 C_1}}{s^2 + \frac{1}{C_1}\left(\frac{1}{R_1} + \frac{1}{R_2} + \frac{1}{R_3}\right)s + \frac{1}{R_2 R_3 C_2 C_1}} \quad (177)$$

Substitution of the oscillator parameters from Figure 4 yields

$$\frac{E_0(s)}{E_1(s)} = \frac{-\omega_n^2}{s^2+2\zeta\omega_n s+\omega_n^2} \tag{178}$$

The equivalent solution for the active RC-network of Figure 5 is as follows. The summation of nodal currents is.

$$\sum I_2(s) = \frac{E_1(s)-E_2(s)}{R_1} + \frac{E_0(s)-E_2(s)}{\frac{1}{C_1 s}} + \frac{E_3(s)-E_2(s)}{\frac{1}{C_2 s}} - \frac{E_2(s)}{R_2} = 0 \tag{179}$$

$$\sum I_3(s) = \frac{E_2(s)-E_3(s)}{\frac{1}{C_2 s}} + \frac{E_0(s)-E_3(s)}{R_3}$$

and

$$E_0(s) = -AE_3(s)$$

The solution again as the gain approaches infinity is given by

$$\frac{E_0(s)}{E_1(s)} = \frac{-\frac{1}{R_1 C_1} s}{s^2 + \frac{(C_1+C_2)}{R_3 C_1 C_2} s + \frac{(R_1+R_2)}{R_1 R_2 R_3 C_1 C_2}} \tag{180}$$

Substitution of the oscillator parameters for Figure 5 yields

$$\frac{E_0(s)}{E_1(s)} = \frac{-\omega_n s}{s^2+2\zeta\omega_n s+\omega_n^2} \qquad (181)$$

Neglecting initial conditions, this transfer function is equivalent to that required in equation (17).

APPENDIX D

FOURIER AND SHOCK SPECTRA FORTRAN IV SUBROUTINES

```
      SUBROUTINE DMA002(A,N,H,W,SS,FS,RDO)                          DMA0  20
C THIS ROUTINE COMPUTES THE SHOCK AND FOURIER SPECTRUM VALUES        DMA0  30
C BY DIRECT SOLUTION OF THE DIFFERENTIAL EQUATION FOR THE            DMA0  40
C SAMPLED ACCELERATION INPUT.                                        DMA0  50
      DIMENSION A(1)                                                 DMA0  60
      WH=W*H                                                         DMA0  70
      CS=COS(WH)                                                     DMA0  80
      SN=SIN(WH)                                                     DMA0  90
      SS=0                                                           DMA0 100
      SNW=SN*W                                                       DMA0 110
      SWN=SN/W                                                       DMA0 120
      R=0.                                                           DMA0 130
      RD=RDO/H-A(1)                                                  DMA0 140
      DO 2 I=2,N                                                     DMA0 150
      AR=ABS(R)                                                      DMA0 160
      IF(AR.GT.SS)SS=AR                                              DMA0 170
      RS=R                                                           DMA0 180
      R=RD*SWN+R*CS                                                  DMA0 190
    2 RD=RD*CS-RS*SNW-A(I)                                           DMA0 200
      FS=SQRT(R*R+(RD/W)**2)*WH                                      DMA0 210
      SS=WH*SS                                                       DMA0 220
      IF(FS.GT.SS)SS=FS                                              DMA0 230
      RETURN                                                         DMA0 240
      END                                                            DMA0 250
```

```
      SUBROUTINE DMV002(V,N,H,W,SS,FS,RDO)                              DMV0  20
C THIS ROUTINE COMPUTES THE VELOCITY SHOCK SPECTRUM AND                  DMV0  30
C FOURIER SPECTRUM OF THE SAMPLED VELOCITY FUNCTION ( V )               DMV0  40
C BY DIRECT EVALUATION OF THE DIFFERENTIAL EQUATION WITH                 DMV0  50
C THE ASSUMPTION THAT THE ACCELERATION IS IMPULSIVE.                     DMV0  60
      DIMENSION V(1)                                                     DMV0  70
      WH=W*H                                                             DMV0  80
      CS=COS(WH)                                                         DMV0  90
      SN=SIN(WH)                                                         DMV0 100
      SS=0                                                               DMV0 110
      SNW=SN*W                                                           DMV0 120
      SWN=SN/W                                                           DMV0 130
      R=0.                                                               DMV0 140
      RD=RDO                                                             DMV0 150
      DO 2 I=2,N                                                         DMV0 160
      RS=R                                                               DMV0 170
      R=RD*SWN+R*CS                                                      DMV0 180
      AR=ABS(R)                                                          DMV0 190
      IF(AR.GT.SS)SS=AR                                                  DMV0 200
    2 RD=RD*CS-RS*SNW-V(I)+V(I-1)                                        DMV0 210
      FS=SQRT(R*R+(RD/W)**2)*W                                           DMV0 220
      SS=W*SS                                                            DMV0 230
      IF(FS.GT.SS)SS=FS                                                  DMV0 240
      RETURN                                                             DMV0 250
      END                                                                DMV0 260
```

```
      SUBROUTINE ZTA002(A,N,H,W,SS,FS,RDO)                              ZTA0  20
C THIS ROUTINE COMPUTES THE VELOCITY SHOCK SPECTRUM AND FOURIER          ZTA0  30
C INTEGRAL VALUE FROM THE SAMPLED ACCELERATION USING THE                 ZTA0  40
C Z-TRANSFORM TECHNIQUE.                                                 ZTA0  50
      DIMENSION A(1)                                                     ZTA0  60
      R=0.                                                               ZTA0  70
      R1=0.                                                              ZTA0  80
      R2=0.                                                              ZTA0  90
      SS=0.                                                              ZTA0 100
      RDH=RDO/H                                                          ZTA0 110
      A(1)=A(1)+RDH                                                      ZTA0 120
      WH=W*H                                                             ZTA0 130
      CS=COS(WH)                                                         ZTA0 140
      SN=SIN(WH)                                                         ZTA0 150
      SNW=SN*W                                                           ZTA0 160
      SWN=SN/W                                                           ZTA0 170
      D1=2.*CS                                                           ZTA0 180
      NN=N+1                                                             ZTA0 190
      DO 2 I=2,NN                                                        ZTA0 200
      R=A(I-1)+D1*R1-R2                                                  ZTA0 210
      AR=ABS(R)                                                          ZTA0 220
      IF(AR.GT.SS)SS=AR                                                  ZTA0 230
      R2=R1                                                              ZTA0 240
    2 R1=R                                                               ZTA0 250
      A(1)=A(1)-RDH                                                      ZTA0 260
      R=D1*R1-R2                                                         ZTA0 270
      RD=(R-R1*CS)*W/SN                                                  ZTA0 280
      HSN=H*SN                                                           ZTA0 290
      FS=SQRT(R1*R1+(RD/W)**2)*HSN                                       ZTA0 300
      SS=SS*HSN                                                          ZTA0 310
      IF(FS.GT.SS)SS=FS                                                  ZTA0 320
      RETURN                                                             ZTA0 330
      END                                                                ZTA0 340
```

```
      SUBROUTINE ZTV002(V,N,H,W,SS,FS,RDO)                              ZTV0  20
C THIS ROUTINE COMPUTES THE SHOCK AND FOURIER SPECTRUM VALUES            ZTV0  30
C FROM THE SAMPLED VELOCITY ( V ) USING THE Z-TRANSFORM TECH-            ZTV0  40
C NIQUE                                                                  ZTV0  50
      DIMENSION V(1)                                                     ZTV0  60
      WH=W*H                                                             ZTV0  70
      CS=COS(WH)                                                         ZTV0  80
      SN=SIN(WH)                                                         ZTV0  90
      SS=0                                                               ZTV0 100
      SNW=SN*W                                                           ZTV0 110
      SWN=SN/W                                                           ZTV0 120
      B0=-H                                                              ZTV0 130
      B1=H*CS                                                            ZTV0 140
      D1=-2.*CS                                                          ZTV0 150
      D2=1.                                                              ZTV0 160
      R=0.                                                               ZTV0 170
      R1=0.                                                              ZTV0 180
      R2=0.                                                              ZTV0 190
      RD=RDO                                                             ZTV0 200
      DO 2 I=2,N                                                         ZTV0 210
      R=CS*(V(I-1)+R1+R1)-R2-V(I)                                        ZTV0 220
      AR=ABS(R)                                                          ZTV0 230
      IF(AR.GT.SS)SS=AR                                                  ZTV0 240
      R2=R1                                                              ZTV0 250
    2 R1=R                                                               ZTV0 260
      R=CS*(R1+R1+V(N))-R2-V(N)                                          ZTV0 270
      RD=(R-R1*CS)*W/SN                                                  ZTV0 280
      FS=SQRT(R1*R1+(RD/W)**2)*WH                                        ZTV0 290
      SS=SS*WH                                                           ZTV0 300
      IF(FS.GT.SS)SS=FS                                                  ZTV0 310
      RETURN                                                             ZTV0 320
      END                                                                ZTV0 330
```

```
      SUBROUTINE OHA002(A,N,H,W,SS,FS,RD0)                              OHA0  20
C THIS ROUTINE COMPUTES THE VELOCITY SHOCK SPECTRUM AND                  OHA0  30
C FOURIER INTEGRAL VALUE AT FREQUENCY W OF THE SAMPLED ACCELER-          OHA0  40
C ATION USING O'HARA'S TECHNIQUE                                         OHA0  50
      DIMENSION A(21)                                                    OHA0  60
      WH=W*H                                                             OHA0  70
      CS=COS(WH)                                                         OHA0  80
      SN=SIN(WH)                                                         OHA0  90
      SS=0                                                               OHA0 100
      SNW=SN*W                                                           OHA0 110
      SWN=SN/W                                                           OHA0 120
      H2=H*H                                                             OHA0 130
      W2=W*W                                                             OHA0 140
      C1=-(1.-CS)/W2                                                     OHA0 150
      C2=-(1.-SWN/H)/W2                                                  OHA0 160
      C3=-(SN/WH/2.-(1.-CS)/W2/H2)/W2                                    OHA0 170
      D1=-SN/W                                                           OHA0 180
      D2=-(1.-CS)/W2/H                                                   OHA0 190
      D3=-((1.+CS)/H/W/2.-SN/W2/H2)/W                                    OHA0 200
      R=0                                                                OHA0 210
      A0=A(1)                                                            OHA0 220
      A1=A(2)-A(1)                                                       OHA0 230
      A2=A(3)-A(2)-A1                                                    OHA0 240
      RD=RD0                                                             OHA0 250
      R=R*CS+RD*SWN+A0*C1+A1*C2+A2*C3                                    OHA0 260
      RS=0.                                                              OHA0 270
      RD=RD*CS-RS*SNW+A0*D1+A1*D2+A2*D3                                  OHA0 280
      SS=ABS(R)                                                          OHA0 290
      DO 2 I=3,N                                                         OHA0 300
      A0=A(I-1)                                                          OHA0 310
      A1=A(I)-A(I-1)                                                     OHA0 320
      A2=A1-A(I-1)+A(I-2)                                                OHA0 330
      RS=R                                                               OHA0 340
      R=R*CS+RD*SWN+A0*C1+A1*C2+A2*C3                                    OHA0 350
      AR=ABS(R)                                                          OHA0 360
      IF(AR.GT.SS)SS=AR                                                  OHA0 370
      RD=RD*CS-RS*SNW+A0*D1+A1*D2+A2*D3                                  OHA0 380
    2 CONTINUE                                                           OHA0 390
      FS=SQRT(R*R+(RD/W)**2)*W                                           OHA0 400
      SS=W*SS                                                            OHA0 410
      IF(FS.GT.SS)SS=FS                                                  OHA0 420
      RETURN                                                             OHA0 430
      END                                                                OHA0 440
```

```
      SUBROUTINE OHV002(V,N,H,W,SS,FS,RDO)                              OHV0  20
C THIS ROUTINE COMPUTES THE FOURIER AND SHOCK SPECTRUM VALUE             OHV0  30
C FROM THE SAMPLED VELOCITY FUNCTION ( V ) AT A FREQUENCY                OHV0  40
C OF ( W ) RADIANS PER SECOND. THE OUTPUT IS IN THE FORM OF              OHV0  50
C THE VELOCITY. THE METHOD EMPLOYED IS THAT USED BY O'HARA.              OHV0  60
      DIMENSION V(21)                                                   OHV0  70
      WH=W*H                                                            OHV0  80
      CS=COS(WH)                                                        OHV0  90
      SN=SIN(WH)                                                        OHV0 100
      SNW=SN*W                                                          OHV0 110
      SWN=SN/W                                                          OHV0 120
      H2=H*H                                                            OHV0 130
      W2=W*W                                                            OHV0 140
      C1=-(1.-CS)/W2/H                                                  OHV0 150
      C2=-((1.+CS)/H/2.-SN/W/H2)/W2                                     OHV0 160
      D1=-SN/W/H                                                        OHV0 170
      D2=-((1.-CS)/WH-SN/2.)/W/H                                        OHV0 180
      R=0                                                               OHV0 190
      RD=RDO                                                            OHV0 200
      V1=V(2)-V(1)                                                      OHV0 210
      V2=V(3)-V(2)-V1                                                   OHV0 220
      R=R*CS+RD*SWN+V1*C1+V2*C2                                         OHV0 230
      SS=ABS(R)                                                         OHV0 240
      RD=RD*CS-RS*SNW+V1*D1+V2*D2                                       OHV0 250
      DO 2 I=3,N                                                        OHV0 260
      RS=R                                                              OHV0 270
      V1=V(I)-V(I-1)                                                    OHV0 280
      V2=V1-V(I-1)+V(I-2)                                               OHV0 290
      R=R*CS+RD*SWN+V1*C1+V2*C2                                         OHV0 300
      AR=ABS(R)                                                         OHV0 310
      IF(AR.GT.SS)SS=AR                                                 OHV0 320
      RD=RD*CS-RS*SNW+V1*D1+V2*D2                                       OHV0 330
    2 CONTINUE                                                          OHV0 340
      FS=SQRT(R*R+(RD/W)**2)*W                                          OHV0 350
      SS=W*SS                                                           OHV0 360
      IF(FS.GT.SS)SS=FS                                                 OHV0 370
      RETURN                                                            OHV0 380
      END                                                               OHV0 390
```

```
      SUBROUTINE DVSSDM(A,N,H,W,SS,Z,RD0)                                DADT  20
C     THIS ROUTINE COMPUTES THE DAMPED VELOCITY SHOCK SPECTRUM FROM THE  DADT  30
C     SAMPLED ACCELERATION USING THE DIRECT METHOD.                      DADT  40
      DIMENSION A(1)                                                     DADT  50
      SS=0                                                               DADT  60
      WH=W*H                                                             DADT  70
      RZ=SQRT(1.-Z*Z)                                                    DADT  80
      PH=RZ*WH                                                           DADT  90
      CS=COS(PH)                                                         DADT 100
      SN=SIN(PH)                                                         DADT 110
      WHZ=-Z*WH                                                          DADT 120
      E=EXP(WHZ)                                                         DADT 130
      P=W*RZ                                                             DADT 140
      SRZ=SN/RZ                                                          DADT 150
      C1=E*(CS+Z*SRZ)                                                    DADT 160
      C2=E*SRZ/W                                                         DADT 170
      D1=-E*SRZ*W                                                        DADT 180
      D2=E*(CS-Z*SRZ)                                                    DADT 190
      R=0                                                                DADT 200
      RD=RD0                                                             DADT 210
      DO 2 I=1,N                                                         DADT 220
      RS=R                                                               DADT 230
      R=R*C1+RD*C2                                                       DADT 240
      AR=ABS(R)                                                          DADT 250
      IF(AR.GT.SS)SS=AR                                                  DADT 260
      RD=RS*D1+RD*D2-A(I)                                                DADT 270
    2 CONTINUE                                                           DADT 280
      PHM=RD*RZ/(R*W+RD*Z)                                               DADT 290
      PHP=ATAN(PHM)                                                      DADT 300
      EPP=-Z*PHP/RZ                                                      DADT 310
      RMAX=EXP(EPP)*(R*COS(PHP)+(W*Z*R+RD)*SIN(PHP)/P)                   DADT 320
      RMAX=ABS(RMAX)                                                     DADT 330
      IF(RMAX.GT.SS)SS=RMAX                                              DADT 340
      SS=WH*SS                                                           DADT 350
      RETURN                                                             DADT 360
      END                                                                DADT 370
```

```
      SUBROUTINE DVSSDM(V,N,H,W,SS,Z,RDO)                                DMVV  20
C     THIS ROUTINE COMPUTES THE DAMPED VELOCITY SHOCK SPECTRUM FROM THE  DMVV  30
C     SAMPLED VELOCITY BY THE DIRECT METHOD.                             DMVV  40
      DIMENSION V(1)                                                     DMVV  50
      SS=0                                                               DMVV  60
      WH=W*H                                                             DMVV  70
      RZ=SQRT(1.-Z*Z)                                                    DMVV  80
      PH=RZ*WH                                                           DMVV  90
      CS=COS(PH)                                                         DMVV 100
      SN=SIN(PH)                                                         DMVV 110
      WHZ=-Z*WH                                                          DMVV 120
      E=EXP(WHZ)                                                         DMVV 130
      P=W*RZ                                                             DMVV 140
      SRZ=SN/RZ                                                          DMVV 150
      C1=E*(CS+Z*SRZ)                                                    DMVV 160
      C2=E*SRZ/W                                                         DMVV 170
      D1=-E*SRZ*W                                                        DMVV 180
      D2=E*(CS-Z*SRZ)                                                    DMVV 190
      R=0                                                                DMVV 200
      RD=RDO-V(1)                                                        DMVV 210
      DO 2 I=2,N                                                         DMVV 220
      RS=R                                                               DMVV 230
      R=R*C1+RD*C2                                                       DMVV 240
      AR=ABS(R)                                                          DMVV 250
      IF(AR.GT.SS)SS=AR                                                  DMVV 260
      RD=RS*D1+RD*D2+V(I-1)-V(I)                                         DMVV 270
    2 CONTINUE                                                           DMVV 280
      PHM=RD*RZ/(R*W+RD*Z)                                               DMVV 290
      PHP=ATAN(PHM)                                                      DMVV 300
      EPP=-Z*PHP/RZ                                                      DMVV 310
      RMAX=EXP(EPP)*(R*COS(PHP)+(W*Z*R+RD)*SIN(PHP)/P)                   DMVV 320
      RMAX=ABS(RMAX)                                                     DMVV 330
      IF(RMAX.GT.SS)SS=RMAX                                              DMVV 340
      SS=WH*SS                                                           DMVV 350
      RETURN                                                             DMVV 360
      END                                                                DMVV 370
```

```
      SUBROUTINE DVSSZT(A,N,H,W,SS,Z,RDO)                                DVSZ  20
C     THIS ROUTINE COMPUTES THE DAMPED VELOCITY SHOCK SPECTRUM FROM THE  DVSZ  30
C     SAMPLED ACCELERATION USING THE Z-TRANFORM TECHNIGUE.               DVSZ  40
      DIMENSION A(1)                                                     DVSZ  50
      WH=W*H                                                             DVSZ  60
      RZ=SQRT(1.-Z*Z)                                                    DVSZ  70
      P=W*RZ                                                             DVSZ  80
      PH=P*H                                                             DVSZ  90
      CS=COS(PH)                                                         DVSZ 100
      SN=SIN(PH)                                                         DVSZ 110
      E=EXP(-Z*WH)                                                       DVSZ 120
      SS=0                                                               DVSZ 130
      B1=-H*E*SN/P                                                       DVSZ 140
      D1=-2.*E*CS                                                        DVSZ 150
      D2=E*E                                                             DVSZ 160
      RD=0.                                                              DVSZ 170
      R=0.                                                               DVSZ 180
      R1=0.                                                              DVSZ 190
      R2=0.                                                              DVSZ 200
      NN=N+1                                                             DVSZ 210
      DO 2 I=2,NN                                                        DVSZ 220
      R=A(I-1)-D1*R1-D2*R2                                               DVSZ 230
      AR=ABS(R)                                                          DVSZ 240
      IF(AR.GT.SS)SS=AR                                                  DVSZ 250
      R2=R1                                                              DVSZ 260
    2 R1=R                                                               DVSZ 270
      R=-D1*R1-D2*R2                                                     DVSZ 280
      RD=(R-R1*CS)*W/SN                                                  DVSZ 290
      PHM=RD*RZ/(R*W+RD*Z)                                               DVSZ 300
      PHP=ATAN(PHM)                                                      DVSZ 310
      EPP=-Z*PHP/RZ                                                      DVSZ 320
      RMAX=EXP(EPP)*(R*COS(PHP)+(W*Z*R+RD)*SIN(PHP)/P)                   DVSZ 330
      RMAX=ABS(RMAX)                                                     DVSZ 340
      IF(RMAX.GT.SS)SS=RMAX                                              DVSZ 350
      SS=W*SS*B1                                                         DVSZ 360
      RETURN                                                             DVSZ 370
      END                                                                DVSZ 380
```

```
      SUBROUTINE DVVSZT(V,N,H,W,SS,Z,RD0)                                DVVZ  20
C     THIS ROUTINE COMPUTES THE DAMPED VELOCITY SHOCK SPECTRUM FROM THE  DVVZ  30
C     SAMPLED VELOCITY USING THE Z-TRANSFORM TECHNIQUE.                  DVVZ  40
      DIMENSION V(1)                                                     DVVZ  50
      WH=W*H                                                             DVVZ  60
      RZ=SQRT(1.-Z*Z)                                                    DVVZ  70
      P=W*RZ                                                             DVVZ  80
      PH=P*H                                                             DVVZ  90
      CS=COS(PH)                                                         DVVZ 100
      SN=SIN(PH)                                                         DVVZ 110
      E=EXP(-Z*WH)                                                       DVVZ 120
      B0=-H                                                              DVVZ 130
      B1=-H*(Z/RZ*SN-CS)*E                                               DVVZ 140
      D1=-2.*E*CS                                                        DVVZ 150
      D2=E*E                                                             DVVZ 160
      RD=0.                                                              DVVZ 170
      R=0.                                                               DVVZ 180
      R1=0.                                                              DVVZ 190
      R2=0.                                                              DVVZ 200
      R=(V(1)-RD0)*B0                                                    DVVZ 210
      SS=ABS(R)                                                          DVVZ 220
      NN=N+1                                                             DVVZ 230
      DO 2 I=2,NN                                                        DVVZ 240
      R=V(I)*B0+V(I-1)*B1-D1*R1-D2*R2                                    DVVZ 250
      AR=ABS(R)                                                          DVVZ 260
      IF(AR.GT.SS)SS=AR                                                  DVVZ 270
      R2=R1                                                              DVVZ 280
    2 R1=R                                                               DVVZ 290
      R=-D1*R1-D2*R2                                                     DVVZ 300
      RD=(R-R1*CS)*W/SN                                                  DVVZ 310
      PHM=RD*RZ/(R*W+RD*Z)                                               DVVZ 320
      PHP=ATAN(PHM)                                                      DVVZ 330
      EPP=-Z*PHP/RZ                                                      DVVZ 340
      RMAX=EXP(EPP)*(R*COS(PHP)+(W* *R+RD)*SIN(PHP)/P)                   DVVZ 350
      RMAX=ABS(RMAX)                                                     DVVZ 360
      IF(RMAX.GT.SS)SS=RMAX                                              DVVZ 370
      SS=W*SS                                                            DVVZ 380
      RETURN                                                             DVVZ 390
      END                                                                DVVZ 400
```

```
      SUBROUTINE DVSSOH(A,N,H,W,SS,Z,RDO)                                DASO  20
C     THIS ROUTINE COMPUTES THE DAMPED VELOCITY SHOCK SPECTRUM FROM THE  DASO  30
C     SAMPLED ACCELERATION USING THE METHOD OF O'HARA.                   DASO  40
      DIMENSION A(1)                                                     DASO  50
      SS=0                                                               DASO  60
      W2=W*W                                                             DASO  70
      WH=W*H                                                             DASO  80
      Z2=Z*Z                                                             DASO  90
      RZ=SQRT(1.-Z2)                                                     DASO 100
      WH2=WH*WH                                                          DASO 110
      PH=RZ*WH                                                           DASO 120
      H2=H*H                                                             DASO 130
      CS=COS(PH)                                                         DASO 140
      SN=SIN(PH)                                                         DASO 150
      WHZ=-Z*WH                                                          DASO 160
      E=EXP(WHZ)                                                         DASO 170
      P=W*RZ                                                             DASO 180
      SRZ=SN/RZ                                                          DASO 190
      W2H=W2*H                                                           DASO 200
      W3H=2.*W*W2H                                                       DASO 210
      C1=E*(CS+Z*SRZ)                                                    DASO 220
      C2=E*SRZ/W                                                         DASO 230
      C3=-(1.-C1)/W2                                                     DASO 240
      C4=-(1.-2.*Z*(1.-E*CS)/WH-(1.-2.*Z2)*E*SN/PH)/W2                   DASO 250
      C5=-(-4.*Z-((2.-8.*Z2)/WH-2.*Z)*(1.-E*CS)+((1.-2.*Z2)+2.*Z*(3.-4.*DASO 260
     1Z2)/WH)*E*SRZ)/W3H                                                 DASO 270
      D1=-E*SRZ*W                                                        DASO 280
      D2=E*(CS-Z*SRZ)                                                    DASO 290
      D3=-SN/P                                                           DASO 300
      D4=-(1.-C1)/W2H                                                    DASO 310
      D5=-(2.-(1.+4.*Z/WH)*(1.-E*CS)-((2.-4.*Z2)/WH-Z)*E*SRZ)/W2H        DASO 320
      R=0                                                                DASO 330
      RD=RDO                                                             DASO 340
      A0=A(1)                                                            DASO 350
      A1=A(2)-A(1)                                                       DASO 360
      A2=A(3)-A(2)-A1                                                    DASO 370
      RS=0.                                                              DASO 380
      R=R*C1+RD*C2+A0*C3+A1*C4+A2*C5                                     DASO 390
      SS=ABS(R)                                                          DASO 400
      RD=RS*D1+RD*D2+A0*D3+A1*D4+A2*D5                                   DASO 410
      DO 2 I=3,N                                                         DASO 420
      RS=R                                                               DASO 430
      A0=A(I-1)                                                          DASO 440
      A1=A(I)-A0                                                         DASO 450
      A2=A1-A0+A(I-2)                                                    DASO 460
      R=R*C1+RD*C2+A0*C3+A1*C4+A2*C5                                     DASO 470
      AR=ABS(R)                                                          DASO 480
      IF(AR.GT.SS)SS=AR                                                  DASO 490
      RD=RS*D1+RD*D2+A0*D3+A1*D4+A2*D5                                   DASO 500
    2 CONTINUE                                                           DASO 510
      PHM=RD*RZ/(R*W+RD*Z)                                               DASO 520
      PHP=ATAN(PHM)                                                      DASO 530
      EPP=-Z*PHP/RZ                                                      DASO 540
      RMAX=EXP(EPP)*(R*COS(PHP)+(W*Z*R+RD)*SIN(PHP)/P)                   DASO 550
      RMAX=ABS(RMAX)                                                     DASO 560
      IF(RMAX.GT.SS)SS=RMAX                                              DASO 570
      SS=W*SS                                                            DASO 580
      RETURN                                                             DASO 590
      END                                                                DASO 600
```

```
      SUBROUTINE DVVSOH(V,N,H,W,SS,Z,RDO)                                DVSO  20
C     THIS ROUTINE COMPUTES THE DAMPED VELOCITY SHOCK SPECTRUM FROM THE  DVSO  30
C     SAMPLED VELOCITY INPUT USING THE METHOD OF O'HARA.                 DVSO  40
      DIMENSION V(1)                                                     DVSO  50
      W2=W*W                                                             DVSO  60
      WH=W*H                                                             DVSO  70
      Z2=Z*Z                                                             DVSO  80
      RZ=SQRT(1.-Z2)                                                     DVSO  90
      WH2=WH*WH                                                          DVSO 100
      PH=RZ*WH                                                           DVSO 110
      H2=H*H                                                             DVSO 120
      CS=COS(PH)                                                         DVSO 130
      SN=SIN(PH)                                                         DVSO 140
      WHZ=-Z*WH                                                          DVSO 150
      E=EXP(WHZ)                                                         DVSO 160
      P=W*RZ                                                             DVSO 170
      SRZ=SN/RZ                                                          DVSO 180
      W2H=W2*H                                                           DVSO 190
      W3H=2.*W*W2H                                                       DVSO 200
      Z2WH=2.*Z/WH                                                       DVSO 210
      C1=E*(CS+Z*SRZ)                                                    DVSO 220
      C2=E*SRZ/W                                                         DVSO 230
      C4=-(1.-C1)/W2H                                                    DVSO 240
      C5=-(.5-Z2WH+E*((.5+Z2WH)*C1-.5*SRZ))/W2H                          DVSO 250
      D1=-FMSRZ*W                                                        DVSO 260
      D2=E*(CS-Z*SRZ)                                                    DVSO 270
      D4=D1/W2H                                                          DVSO 280
      D5=-((1.-C1)/WH-E*SRZ/2.)/WH                                       DVSO 290
      R=0                                                                DVSO 300
      RD=RDO                                                             DVSO 310
      V1=V(2)-V(1)                                                       DVSO 320
      V2=V(3)-V(2)-V1                                                    DVSO 330
      RS=0.                                                              DVSO 340
      R=R*C1+RD*C2+V1*C4+V2*C5                                           DVSO 350
      SS=ABS(R)                                                          DVSO 360
      RD=RS*D1+RD*D2+V1*D4+V2*D5                                         DVSO 370
      DO 2 I=3,N                                                         DVSO 380
      RS=R                                                               DVSO 390
      V1=V(I)-V(I-1)                                                     DVSO 400
      V2=V1-V(I-1)+V(I-2)                                                DVSO 410
      R=R*C1+RD*C2+V1*C4+V2*C5                                           DVSO 420
      AR=ABS(R)                                                          DVSO 430
      IF(AR.GT.SS)SS=AR                                                  DVSO 440
      RD=RS*D1+RD*D2+V1*D4+V2*D5                                         DVSO 450
    2 CONTINUE                                                           DVSO 460
      PHM=RD*RZ/(R*W+RD*Z)                                               DVSO 470
      PHP=ATAN(PHM)                                                      DVSO 480
      EPP=-Z*PHP/RZ                                                      DVSO 490
      RMAX=EXP(EPP)*(R*COS(PHP)+(W*Z*R+RD)*SIN(PHP)/P)                   DVSO 500
      RMAX=ABS(RMAX)                                                     DVSO 510
      IF(RMAX.GT.SS)SS=RMAX                                              DVSO 520
      SS=W*SS                                                            DVSO 530
      RETURN                                                             DVSO 540
      END                                                                DVSO 550
```

```
C     FINITE DISCRETE FOURIER TRANSFORM                                  FRXF  20
C     IT REPLACES THE VECTOR Z=X+IY BY ITS FOURIER TRANSFORM             FRXF  30
C     THE LENGTH OF THE VECTOR IS NTHPOW=2**N2POW                        FRXF  40
C     THE FINITE DISCRETE FOURIER TRANSFORM IS THE PRODUCT WITH          FRXF  50
C     THE MATRIX WHOSE I,J ELEMENT IS W**(I*J), WHERE                    FRXF  60
C     W=CEXP(2.*PI*I/NTHPOW), THE NTHPOW PRINCIPLE ROOT OF UNITY         FRXF  70
C     I,J=0,,NTHPOW-1                                                    FRXF  80
C     NOTE ZERO SUBSCRIPTS HERE REFER TO FORTRAN SUBSCRIPTS=1 IN THE     FRXF  90
C     CODE. I.E. THE FORTRAN SUBCRIPTS RUN FROM 1 TO NTHPOW.             FRXF 100
C     DEVELOPED BY B. LANGDON AND G. SANDE FROM THE ARPROACH OF          FRXF 110
C     J.W. TUKEY AND J. COOLEY.                                          FRXF 120
C     PRINCETON UNIVERSITY, NOVEMBER 1965.                               FRXF 130
C     THIS WORK MADE USE OF COMPUTING FACILITIES SUPPORTED IN PART       FRXF 140
C     BY NSF GRANT NSF-GP579.                                            FRXF 150
      SUBROUTINE FRXFM(N2POW,X,Y)                                        FRXF 160
      REAL X(2), Y(2), I, I1, I2, I3, I4                                 FRXF 170
      INTEGER PASS, SEQLOC, L(13)                                        FRXF 180
      EQUIVALENCE (NTHPOW,IJ), (J,JI), (N4POW,J5), (PASS,J6),            FRXF 190
     1    (NXTLTH,J7), (LENGTH,J8), (SEQLOC,J9), (SCALE,J10),           FRXF 200
     2    (ARG,J11), (A1,J12), (C2,L2), (C3,L2), (S1,L3),               FRXF 210
     3    (S2,L4), (S3,L5), (R1,L6), (R2,L7), (R3,L8), (R4,L9),         FRXF 220
     4    (I1,L10), (I2,L11), (I3,L12), (I4,L13), (R,I)                 FRXF 230
      EQUIVALENCE (L13,L(1)),(L12,L(2)),(L11,L(3)),(L10,L(4)),           FRXF 240
     1    (L9,L(5)),(L8,L(6)),(L7,L(7)),(L6,L(8)),(L5,L(9)),            FRXF 250
     2    (L4,L(10)),(L3,L(11)),(L2,L(12)),(L1,L(13))                   FRXF 260
      NTHPOW=2**N2POW                                                    FRXF 270
      N4POW=N2POW/2                                                      FRXF 280
      IF(N4POW.EQ.0) GO TO 6                                             FRXF 290
C     RADIX 4 PASSES, IF ANY.                                            FRXF 300
      DO 4 PASS=1,N4POW                                                  FRXF 310
      NXTLTH=2**(N2POW-2*PASS)                                           FRXF 320
      LENGTH=4*NXTLTH                                                    FRXF 330
      SCALE=6.283185307/FLOAT(LENGTH)                                    FRXF 340
      DO 4 J=1,NXTLTH                                                    FRXF 350
      ARG=FLOAT(J-1)*SCALE                                               FRXF 360
      C1=COS(ARG)                                                        FRXF 370
      S1=SIN(ARG)                                                        FRXF 380
      C2=C1*C1-S1*S1                                                     FRXF 390
      S2=C1*S1+C1*S1                                                     FRXF 400
      C3=C1*C2-S1*S2                                                     FRXF 410
      S3=C2*S1+S2*C1                                                     FRXF 420
      DO 4 SEQLOC=LENGTH,NTHPOW,LENGTH                                   FRXF 430
      J1=SEQLOC-LENGTH+                                                  FRXF 440
      J2=J1+NXTLTH                                                       FRXF 450
      J3=J2+NXTLTH                                                       FRXF 460
      J4=J3+NXTLTH                                                       FRXF 470
      R1=X(J1)+X(J3)                                                     FRXF 480
      R2=X(J1)-X(J3)                                                     FRXF 490
      R3=X(J2)+X(J4)                                                     FRXF 500
      R4=X(J2)-X(J4)                                                     FRXF 510
      I1=Y(J1)+Y(J3)                                                     FRXF 520
      I2=Y(J1)-Y(J3)                                                     FRXF 530
      I3=Y(J2)+Y(J4)                                                     FRXF 540
      I4=Y(J2)-Y(J4)                                                     FRXF 550
      X(J1)=R1+R3                                                        FRXF 560
      Y(J1)=I1+I3                                                        FRXF 570
```

```
      IF(J.EQ.1) GO TO 2                                                FRXF 580
      X(J3)=C1*(R2-I4)-S1*(I2+R4)                                       FRXF 590
      Y(J3)=S1*(R2-I4)+C1*(I2+R4)                                       FRXF 600
      X(J2)=C2*(R1-R3)-S2*(I1-I3)                                       FRXF 610
      Y(J2)=S2*(R1-R3)+C2*(I1-I3)                                       FRXF 620
      X(J4)=C3*(R2+I4)-S3*(I2-R4)                                       FRXF 630
      Y(J4)=S3*(R2+I4)+C3*(I2-R4)                                       FRXF 640
      GO TO 4                                                           FRXF 650
    2 X(J3)=R2-I4                                                       FRXF 660
      Y(J3)=I2+R4                                                       FRXF 670
      X(J2)=R1-R3                                                       FRXF 680
      Y(J2)=I1-I3                                                       FRXF 690
      X(J4)=R2+I4                                                       FRXF 700
      Y(J4)=I2-R4                                                       FRXF 710
    4 CONTINUE                                                          FRXF 720
C     END OF RADIX 4                                                    FRXF 730
      IF(N2POW.EQ.2*N4POW) GO TO 10                                     FRXF 740
C     RADIX 2 PASS, IF ANY.                                             FRXF 750
      DO 8 J=1,NTHPOW,2                                                 FRXF 760
      R=X(J)+X(J+1)                                                     FRXF 770
      X(J+1)=X(J)-X(J+1)                                                FRXF 780
      X(J)=R                                                            FRXF 790
      I=Y(J)+Y(J+1)                                                     FRXF 800
      Y(J+1)=Y(J)-Y(J+1)                                                FRXF 810
    8 Y(J)=I                                                            FRXF 820
C     SET UP PARAMETERS FOR SORT                                        FRXF 830
   10 DO 12 J=1,13                                                      FRXF 840
      L(J)=1                                                            FRXF 850
   12 IF(J.LE.N2POW) L(J)=2**(N2POW+1-J)                                FRXF 860
C     NOTE EQUIVALENCE OF L1 AND L(14-1)                                FRXF 870
C     BINARY SORT                                                       FRXF 880
      IJ=1                                                              FRXF 890
      DO 14 J1=1,L1                                                     FRXF 900
      DO 14 J2=J1,L2,L1                                                 FRXF 910
      DO 14 J3=J2,L3,L2                                                 FRXF 920
      DO 14 J4=J3,L4,L3                                                 FRXF 930
      DO 14 J5=J4,L5,L4                                                 FRXF 940
      DO 14 J6=J5,L6,L5                                                 FRXF 950
      DO 14 J7=J6,L7,L6                                                 FRXF 960
      DO 14 J8=J7,L8,L7                                                 FRXF 970
      DO 14 J9=J8,L9,L8                                                 FRXF 980
      DO 14 J10=J9,L10,L9                                               FRXF 990
      DO 14 J11=J10,L11,L10                                             FRXF1000
      DO 14 J12=J11,L12,L11                                             FRXF1010
      DO 14 JI=J12,L13,L12                                              FRXF1020
      IF(IJ.GE.JI) GO TO 14                                             FRXF1030
      R=X(IJ)                                                           FRXF1040
      X(IJ)=X(JI)                                                       FRXF1050
      X(JI)=R                                                           FRXF1060
      I=Y(IJ)                                                           FRXF1070
      Y(IJ)=Y(JI)                                                       FRXF1080
      Y(JI)=I                                                           FRXF1090
   14 IJ=IJ+1                                                           FRXF1100
      RETURN                                                            FRXF1110
      END                                                               FRXF1120
```